UNIVERSIDAD NACIONAL AUTÓNOMA DE MÉXICO

Programa de Doctorado en Ciencias Biomédicas
Instituto de Investigaciones Biomédicas

"CONTROL OF ENERGY HOMEOSTASIS:

A ROLE FOR THE ARCUATE NUCLEUS,

WITH SPECIAL EMPHASIS ON VGF".

T E S I S

QUE PARA OPTAR POR EL GRADO DE

Doctor en Ciencias

PRESENTA

Nadia Saderi

Director de tesis: Dr. Rudolf M. Buijs
Instituto de Investigaciones Biomédicas

Ciudad Universitaria   **abril 2014**

BIOMÉDICAS

ACKNOWLEDGMENTS

INDEX

Chapter 2: *NPY and VGF are upregulated in the Arcuate nucleus, but downregulated in the Nucleus of the Tractus Solitarius, of type-II diabetic patients.*

Chapter 3: *A role for VGF in the hypothalamic Arcuate and Paraventricular nuclei in the control of energy homeostasis*

ABSTRACT

Nutrients supply is an essential aspect of life for all the living organisms, and evolution provided them of redundant systems to defend the energy status of the body and to keep constant the body weight during or in anticipation of food scarcity. In mammalians, energy for long term utilization can be stored in form of adipose tissue, but this capacity has become one of the main risks for humans' health. In fact, the malfunctioning of the energy homeostatic mechanisms, or to their failure to adapt to changes in the environment, is thought to base the predisposition to obesity. Very often, challenges for the energy homeostasis consist in the increased availability of high caloric food, associated with a sedentary style of life. The result is a pandemic diffusion of obesity, together with insulin resistance and type-II diabetes, as well as cardiovascular diseases.

Energy balance is regulated by a complex of neural and neuroendocrine systems, which assure the correct correspondence between food consumption and energy expenditure for a given organism. Such systems inform the brain about food intake and its composition, communicate the levels of fuel stored in the body, and then generate appropriate endocrine, autonomic and behavioral responses. These reactions are the result of the integration of hormonal and neural of cues, all leading to the regulation of feeding behavior and energy expenditure.

The hypothalamus is the brain division that most integrates food-related input and determinates feeding behavior, as well as other homeostatic functions related to drinking, sexual and defensive behaviors, and to the control of body temperature and the immune response.

In the present work we focused on the Arcuate nucleus of the hypothalamus, a unique area for its anatomical and biochemical characteristics, where metabolic cues are received from periphery, integrated and sent to other hypothalamic nuclei to modulate neuroendrocine and autonomic functions. Our results demonstrate that a delicate balance of three neuropeptides, NPY, α-MSH and

4

VGF exists in the Arcuate nucleus of rats in response to changes in food availability, and that neurons expressing these substances transmit their information directly to pre-autonomic neurons within the hypothalamic Paraventricular nucleus. In addition, we found that the same neuropeptides are expressed in the human Arcuate nucleus and, by comparing the hypothalamus of type-2 diabetic and non-diabetic patients, that the Arcuate nucleus of the former showed an expression pattern of NPY, α-MSH and VGF similar to the Arcuate nucleus of fasted animals. Finally, we explored the hypothesis of the Arcuate nucleus as an essential relay of metabolic information in route to the circadian system. Surprisingly, the Arcuate nucleus showed weak connections with the master circadian clock, the Suprachiasmatic nucleus. Nevertheless, and extra-hypothalamic nucleus turned out as the metabolic messenger to the circadian system: the thalamic Intergeniculate Leaflet.

ABBREVIATIONS

α-MSH:	α- Melanocyte-Stimulating Hormone
AH:	Anterior Hypothalamus
AP:	Area Postrema
AVPV:	Anteroventral Periventricular nucleus
AgRP:	Agouti-Related Peptide
AH:	Anterior Hypothalamus
AP:	Area Postrema
ARC:	Arcuate Nucleus (*Infundibular Nucleus in the human brain*)
CART:	Cocaine Amphetamine –Related Transcipt
DMH:	Dorsomedial Hypothalamus (Dorsomedial Nucleus)
DVC:	Dorsal Vagal Complex
PFA	Perifornical Area
GABA:	γ-Amino-Butyric Acid
GAD:	Glutamate Decarboxylase
GLP-1:	Glucagon-Like Peptide 1
Inf:	Infundibular stem
IGL:	Intergeniculate Leaflet
IML:	Intermediolateral Column
LH:	Lateral Hypothalamus
LM:	Lateral Mammillaty nucleus
LPo:	Lateral Preoptic area
MC3-R:	Melanocortin-3 Receptor
MC4-R:	Melanocortin-4 Receptor
MCPO:	Magnocellular Preoptic nucleus

me:	Median Eminence
MM:	Medial Mammillary nucleus
MnPO:	Median Preoptic nucleus
MPO:	Medial Preoptic nucleus
NA:	Noradrenaline
NPY:	Neuropeptide Y
NTS:	Nucleus of the Tractus Solitarius
PBN:	Parabrachial Nucleus
PFA:	Perifornical area
PMD:	Dorsal Premammillaty nucleus
PMV:	Ventral Premammillaty nucleus
POMC:	Pro-Opiomelanocortin
PVN:	Paraventricular Nucleus
SCN:	Suprachiasmatic Nucleus
SuM	Dorsal Premammillaty nucleus
TDM:	Supramammillary nucleus
TH:	Tyrosine Hydroxylase
TVM:	Dorsal Premammillaty nucleus
VMH:	Ventromedial Hypothalamus (Ventromedial Nucleus)

INTRODUCTION

1. Feeding Behavior and Energy Homeostasis

Feeding behavior is the result of the interaction of a multitude of systems that accounts for the complexity of the processes behind the decision of having food (or not).

The three main systems that influence the brain to make the decision about the start and the termination of food ingestion are:

a) The *metabolic system*, that monitors the amount of fuel stored in the body by sensing nutrients circulating in blood, available to satisfy immediate metabolic needs, and information from the gastrointestinal tract (about nutrients ready to be digested) and the adipose tissue (about the amount of fat depots) that account for energy available over longer time periods.

b) The *circadian system*, which determines the phase of the day that, for a given species, is more convenient and safe to look for food.

c) The *immune system* that may signal the brain whether an infection has occurred and whether rest is needed.

As consequence of this complexity is that a large parts of the Central Nervous System are dedicated this decision making process. For instance the hypothalamus is the center for the integration and execution of most homeostatic functions, including tracking peripheral energy status, the time organization of body physiology and motor functions associated with food intake. In addition, the cortex and the limbic system provide extensive networks that also process food-related cues from the environment and generate food-related experience for example associated with taste that organizes and motivates feeding behavior to guarantee energy supply. The coordination of these three domains is thought to be of evolutionary advantage allowing mammals to survive successfully. In fact, feeding

8

has been a very stressful activity for millions of years, and only organisms that could resist famine, and remember when and where to look for food, could also survive and reproduce.

XXI century humans living in developed countries no longer need to carry out a daily fight against a hostile environment. Danger is not represented anymore by seasons and predators, but by the modern life-style that continuously challenges the coordination between the homeostatic systems and elicits conflicts between the "homeostatic" and the "emotional brain", resulting in an expanding epidemic of metabolic diseases.

How does modern life affect human energy homeostasis?

Currently, three kinds of body-environment conflicts are thought to trigger pathological conditions: first, the alterations in the relationship between the physiologic rhythms imposed by the circadian system and the actual consumption of the meals (*Buijs and Kreier 2006, Kreier et al 2003, Knutsson et al, 2004; Salgado-Delgado et al, 2008*), like it occurs in shift-workers and night-workers.;for second, the increasing availability of very rewarding and cheap food and drinks (*Prentice et al, 2005; Wells JC, 2006*); finally, sedentariness, which is favored by mechanized transport and the use of electronic devices during the work- and the free-time. This situation has been taken place in most western countries and in many developing countries, where rapid changes in centuries-old alimentary traditions and in life-style are thought to have disclosed the genetic predisposition to a series of chronic metabolic diseases, with important consequences on public health (*Boutin & Frougel, 2001; Ravussin & Bogardus, 2000; Mokdad et al, 2003; Prentice et al, 2005*). In these circumstances, at the basis of the metabolic impairment is the energy state of the homeostatic system, which working beyond its pre-settled organization, fails to adjust to this environmental mutation.

2. Analysis of the internal energy state

Nutrient ingestion, breakdown and absorption takes place in the digestive tract, whereas the sensation of hunger or satiety is generated in the Central Nervous System (CNS). Thus, in order to

regulate the internal energy state and to promote consequent adaptive responses, the homeostatic brain has a constant and reciprocal cross-talk with the periphery. To understand the mechanisms by which the brain responds to the presence or absence of nutrients in the periphery, we briefly describe the two main brain areas that directly receive peripheral information, which are the Dorso-Vagal Complex (DVC) of the brainstem and the Arcuate Nucleus of the hypothalamus (ARC), and review the neural and endocrine pathways that constitute feed-back circuitry between the periphery and the CNS.

The Dorso-Vagal Complex, which comprises the Nucleus of the Solitary Tract (NTS), Area Postrema (AP) and Dorsal Motor Nucleus of the Vagus Nerve (DMV) is a crucial area for the processing of food-related cues for several reasons. First of all, the NTS is the gateway of sensory information from mouth, stomach and intestines. Second, the neural circumventricular organ AP, which is highly sensitive to blood borne metabolic signals but also receives vagal afferents, projects to the NTS, so that circulating cues may modify the information carried by neural afferents. Third, NTS projections to the DMV generate autonomic reflexes that convey parasympathetic impulses to the viscera. Finally, the NTS provides this metabolic information to the forebrain (***Figure 1***).

2.1 Pre-absorptive Processes

Sensing food in the oral cavity is the first source of metabolic information to the CNS. In the mouth nutrients interact with taste receptors and this information is conveyed by glossopharyngeal, facial and vagal primary afferents to the NTS. In addition, trigeminal afferents bring to the NTS information about texture and temperature of food via 2nd order afferents. This sensory information is complemented by olfactory and visual 3rd order afferents (*Berthoud & Morrison, 2008*). Tasting and smelling food is perhaps the most important step for the continuation of the meal because central processing of these sensations may either stop feeding behavior immediately, or generate rewarding feelings that positively affect the size of the meal. Processing sensory information in the NTS may

generate parasympathetic motor reflexes in the DMV, which for example may results either in increased salivation in response to a grateful sensation, or in vomiting in response to a distasteful one. Mouth - Vagal reflexes are responsible also of the cephalic phase of digestion, including the secretion of insulin after the activation of sweet taste receptors in the tongue (*Ahren B, 2000*).

Once food is recognized as palatable and safe, it is swallowed and processed first in the stomach and in then in the intestine. The gastrointestinal tract, far from being a passive container in which food digestion and nutrient absorption occur, is the protagonist of an intense cross-talk with the brain. In the stomach and intestine, vagal afferents directed to the NTS have poly-modal properties: they are sensitive both to the gastric mechanical distension following food ingestion (*Phillips & Powley, 2000; Berthoud HR, 2004*) and to chemical messages released before and after a meal by the gastrointestinal mucosa.
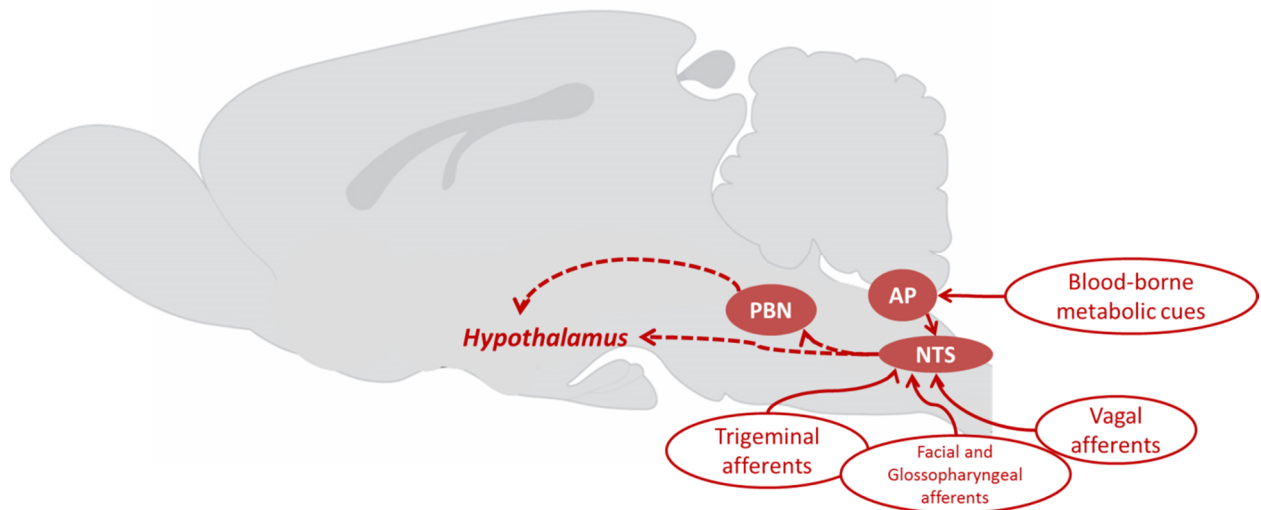
FIGURE 1. Sagittal diagram of the rat brain showing the gut-brain axis. *The Nucleus of the Tractus Solitarius (NTS) receives circulating metabolic information via the Area Postrema (AP), a neural circumventricular organ located down of the floor of the Fourth Ventricle (4V), expressing receptors and transporters for hormones and metabolites. Glossopharyngeal, facial, trigeminal and vagal afferents convey to the NTS peripheral information about food chemical composition and taste, and gut distension and digestion. The NTS transmits visceral input to the hypothalamus, mainly via large projections to the Parabrachial Nucleus (PBN). [Adapted from: Paxinos & Watson, The Rat Brain in Stereotaxic Coordinates, IV Edition, Academic Press, 1998.]*

These so-called "metabolic hormones" are a group of small peptides including: ghrelin, which is released by the P and X/A cells of the gastric oxyntic mucosa; cholecystokinin (CCK), secreted by the I cells of the small intestine; peptide YY and glucagon-like peptide 1 (GLP-1), which are both secreted by L-cell of the lower gut (*Smith et al, 1985; Moriarty et al, 1997; Patterson et al, 2007*). Most of these signals are released after a meal and represent a negative feedback that relay the necessity to suppress feeding behavior. The only exception is the gastric hormone ghrelin, which is the only peptide released by a peripheral organ known to stimulate hunger and food seeking (*Asakawa et al, 2001; Cummings et al, 2001; Date et al, 2002; Holsen et al, 2012*). It is worth to stress that secretion of gastric and intestinal hormones is a consequence of the chemosensory properties of the luminal mucosa, which displays a set of G-coupled receptors similar to those expressed in the tongue mucosa and responds to nutrient stimuli with the release of an appropriate set of hormones (*Janssen & Depoortere, 2013*). For example, P and X/A cells, which release ghrelin, express sweet/umami and medium/long fatty acid receptors (*Hass et al, 2010; Janssen et al, 2012*); CCK-releasing I cells express medium/long fatty acid receptors (*Edfalk et al, 2008), as well as* Calcium-sensing receptors, which are activated by peptides and aromatic aminoacids (*Feng et al, 2010*); L cells, which release PYY and GLP-1 express a wide range of receptors, including sweet/umami (*Steinert et al, 2011*), short, medium and long chain fatty acids (*Karaki et al, 2006; Edfalk et al, 2008;)*, and bitter taste receptors (*Rozengurt E, 2006*). After secretion, hormones diffuse beyond the basal lamina, where they activate specific receptors on vagal terminals and reach the systemic circulation.

2.2 Post-absorptive Processes

Additional information is sent to the NTS after food digestion and micronutrients are released in the circulation. For instance: glucose receptors present in both the portal vein and on the liver vagal (*Adachi et al, 1984*) afferents are thought to trigger autonomic response that adjust glucose levels in

blood, such as the inhibition of the counter regulatory response after a meal (*Thorens & Larsen, 2004; Matveyenko & Donovan, 2006*). Analogously, GLP-1 released by the intestinal mucosa provides additional stimulation for the pancreatic secretion of insulin and amylin via stimulation of the Vagus nerve via the AP (*D'Alessio et al, 1995*). Nevertheless, satiety and energy-related information reach the brain not only through the Vagus nerve. For example, glucose itself, acts on both the periphery [i.e. in the liver to inhibit glycogen phosphorylation (*Carabaza et al, 1992*) and on the endocrine pancreas to stimulate insulin secretion], and directly on the glucoreceptors located in the DVC and the ventromedial hypothalamus (*Anand et al, 1964; Dallaporta et al, 1999*). Similarly, the activity of gut hormones is not only paracrine and conveyed to the central nervous system by vagal feedback; ghrelin, PPY and GLP-1 act also in an endocrine fashion and interact with specific receptor localized at different levels of the brain (*Larsen et al, 1997; Batterham et al, 2002; Kojima & Kangawa, 2005*).

2.3. Endocrine Properties of Adipose Tissue

As the gastrointestinal tract accomplishes more functions than food digestion and nutrient absorption, adipose tissue is not only a long-term energy depot with active function in thermogenesis but it can also be considered the mammalians largest endocrine organ. Endocrine cells within adipose tissue release a family of hormones called cytokines, most of them characterized by promoting inflammatory and immune responses when secreted in high amounts (*Fonseca et al, 2004*). Among the different cytokines, leptin and adiponectin have the role to communicate to the brain the amount of fat stored in the body (*Trayhurn and Bing, 2006*). Leptin is an adipocytes-derived factor released into the circulation in proportion to the amount of white adipose tissue. A transient increase in leptin after a meal indicates to the brain a positive energy status, and persistent high levels of circulating leptin are associated with obesity. Leptin receptors are widespread throughout the brain, including many hypothalamic nuclei which regulate energy homeostasis and the DVC.

In contrast to leptin and to most of the cytokines, adiponectin is the only cytokine whose levels in the circulation are inverse proportional to white adipose fat tissue. Adiponectin improves insulin sensitivity, promotes energy utilization by peripheral tissue, has anti-inflammatory and anti-atherogenic effects, and is decreased in obese subjects. (*Arita et al, 1999*).

In conclusion we have seen that the brain needs signals from the body in order to be able to initiate or to cease food ingestive behavior. These signals can be direct neuronal information about the feeding state of the body or hormonal signals released by the gastrointestinal tract that inform the brain about food ingestion and gut distension. These effects are almost immediate and consequently these signals are also known as "satiety and adiposity signals" at the one hand and "hunger" signals at the other hand.

3. The hypothalamic control of energy homeostasis

The hypothalamus has a crucial role in the regulation of body homeostasis, since it is the area where endocrine messages from the periphery and neural information from the brainstem are integrated and sent to the "decision-making" brain centers, and where complex autonomic and endocrine responses are generated and returned to the periphery.

3.1 Basic organization of the Hypothalamus

The hypothalamus is the most ventral part of the diencephalon (***Figure 2-A***). It is located at both sides of the third ventricle, above the optic chiasm rostrally and the pituitary gland caudally. On the rostro-caudal extent, the hypothalamus can be divided in four regions: the preoptic, the anterior, the tuberal and the mammillary regions and, with respect to the midline sagittal plane, all these regions can be divided in three main areas: the periventricular area, which along the walls of the Third Ventricle (3V); and medial area and a lateral area.

The periventricular zone of the hypothalamus organizes the final output for neuro-endocrine pathways controlling pituitary and autonomic functions while it is also essential for the execution of

14

behavior such as food or water intake, and comprises the Suprachiasmatic, Paraventricular and Arcuate Nuclei (***Figure 2-B***).
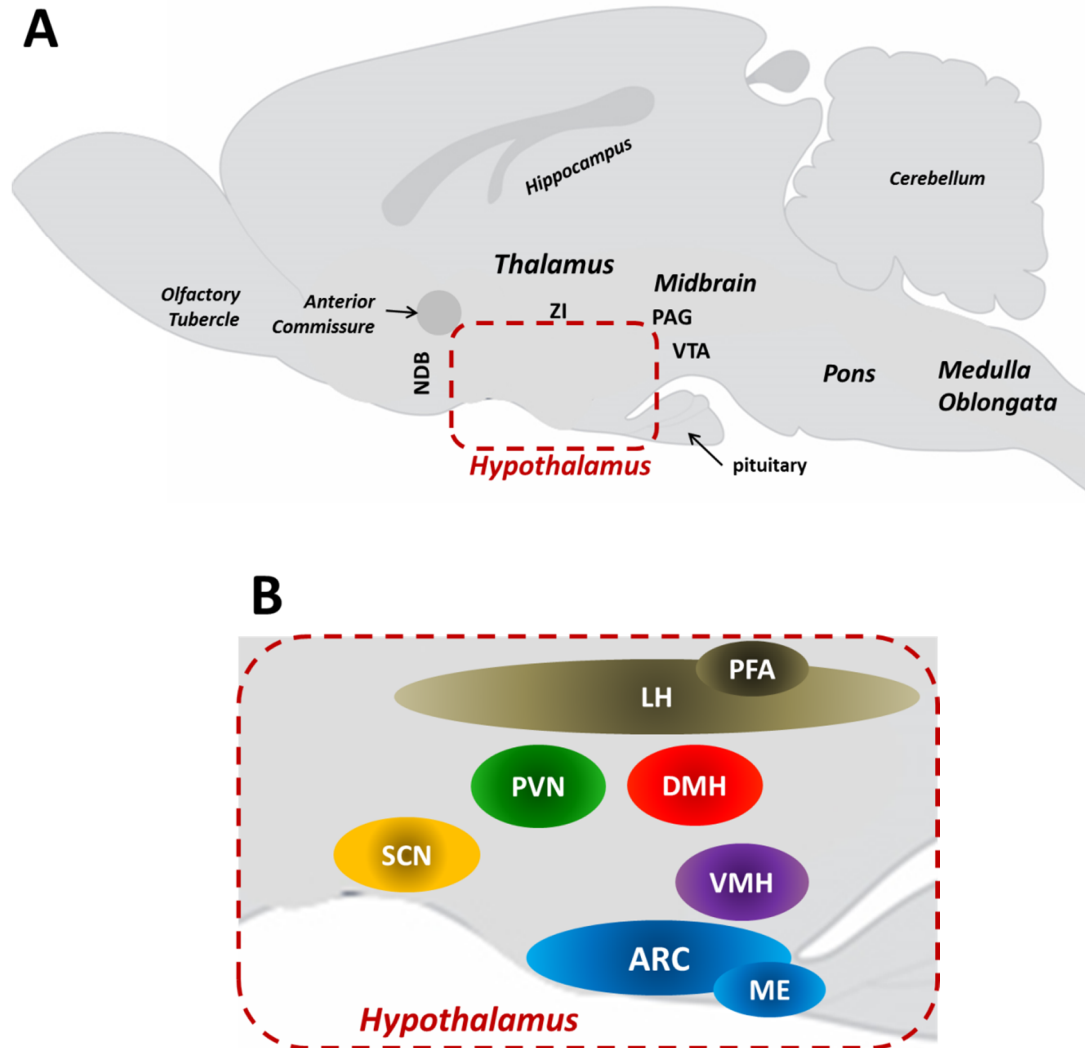
FIGURE 2. Sagittal diagram of the rat brain indicating the hypothalamic boundaries and nuclei. **(A)** *The hypothalamus abuts on: rostrally, the anterior commissure and the nuclei of the Diagonal Band (NDB); dorsally, the thalamic Zona Incerta (ZI); caudally, the Periaqueductal Grey (PAG) and the Ventral Tegmental Area (VTA) of the Midbrain.* **(B)** *Hypothalamic nuclei involved in the regulation of energy homeostasis: the Arcuate Nucleus (ARC) and the contiguous Median Eminence (ME, which are involved in the detection of peripheral metabolic cues; Suprachiasmatic Nucleus (SCN), which organizes daily fluctuations of body physiology; the Periventricular Nucleus (PVN), which provides a neuroendocrine output for the Arc and the SCN; the Dorsomedial Nucleus (DMH) and Ventromedial Nucleus (VMH), which are both involved in the control of food intake and body weight. Laterally and dorsally from these nuclei, lie the Lateral Hypothalamus (LH) and Perifornical Area (PFA), which interconnect the homeostatic aspect of feeding to arousal and motivated behavior.*

In the base of the periventricular hypothalamus, just above the optic chiasm, is the location of the Suprachiasmatic Nucleus (SCN) which sends its timing signals to many areas within and outside the hypothalamus in order to synchronize all our physiological functions according to the time of the day. This nucleus is known as the "master circadian clock" because it synchronizes the body physiology and behavior with the changes in environment, such as the light-dark cycle. For instance, the SCN is responsible for the daily variation in glucose and insulin tolerance (*Kalsbeek & Strubbe, 1998; Kalsbeek et al, 2008*), as well as to the increase in glucocorticoids and locomotor activity at the beginning of the active phase in mammalians (*Buijs & Kalsbeek, 2001*).

A bit more caudal the Paraventricular Nucleus (PVN) is a heterogeneous mosaic of neuronal sub-populations, broadly divided in the magnocellular and parvocellular groups. Magnocellular neurons contain either Vasopressin or Oxytocin, which are released at the level of the posterior pituitary, via projections passing through the inner (dorsal) layer of the Median Eminence (ME). The parvocellular sub-population of the PVN is composed by neuroendocrine and pre-autonomic neurons. The former produces hypophysiotrophic releasing factors that are secreted in the pituitary portal system via projections passing through the outer (ventral) layer of the ME. The pre-autonomic neurons project to autonomic nuclei in the midbrain, the hindbrain and the spinal intermediolaterial column (IML) (*Luiten et al, 1997; Cechetto et al, 1998; Hosoya et al, 1991*) (**Figure 3**). PVN neuroendocrine and autonomic neurons receive direct and indirect information from the SCN that serves to time the hormonal and autonomic output of the PVN. In addition, the PVN is involved in the organization of neuro-endocrine responses to metabolic changes detected by the Arcuate Nucleus (ARC) (***See Paragraph 3.2***) (**Figure 4**).

In addition to the SCN and PVN the medial zone of the hypothalamus comprises several large nuclei, such as the Dorsomedial Nucleus (DMH), the Ventromedial Nucleus (VMH) (**Figure 2-B**), which both receive various sensory inputs, interconnect with the rest of the hypothalamic nuclei and are involved

in adaptive behaviors and energy homeostasis (*Canteras et al, 1994; Thomson & Swanson, 1998; Bartness & Bamshad, 1998; Elmquist et al, 1998*). The VMH was the first hypothalamic nucleus recognized as essential for energy balance. In particular, the VMH was identified as a "satiety center" because lesioning this nucleus led to obesity (*Brobeck JR, 1946*). In time, it was demonstrated that the dramatic effect of the VMH ablation depended on the disruption of descending pathways crossing the mediobasal hypothalamus (*Devemport & Balagura, 1971*). Nevertheless, the VMH is currently recognized a crucial area for the control of body weight and glucose homeostasis, mainly through the regulation of the autonomic system (*Amir S, 1990; Minokoshi et al, 1999; Bingham et al, 2008).*
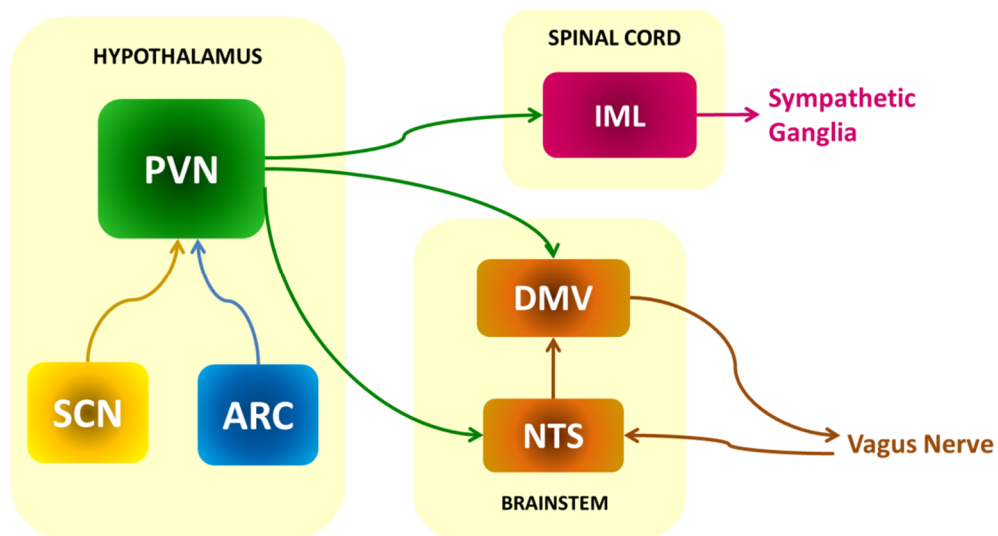
FIGURE 3. **Autonomic feedback loops across the PVN.** *The Vagus nerve conveys chemical and mechanical information about food ingestion to the Nucleus of the Tractus Solitarius (NTS), which in turn transmits it to the Paraventricular Nucleus (PVN). In addition, the NTS relays this information to the Arcuate Nucleus (ARC), where it is integrated and then transmitted to the PVN as well. Circadian rhythms imposed by the SCN are also mediated through the PVN pre-autonomic output. PVN Pre-sympathetic and pre-parasympathetic neurons project to the autonomic nuclei in the Intermediate Lateral Column (IML) of the spinal cord and Dorsal Motor nucleus of the Vagus nerve (DMV) in the brainstem, respectively. Note that a parasympathetic reflex exists between the vagal afferents to the NTS and the vagal efferents from the DMV.*

17

As for the VMH, the lesion of the DMH revealed the importance of this nucleus for energy balance (*Bernardis et al, 1963*), in particular for the feeding-inducing activity of DMH neurons (*Bellinger et al, 1986*). More recently, the DMH was demonstrated to regulate a number of homeostatic mechanisms, including glucocorticoid secretion (*Horst & Luiten, 1986*); arousal and circadian control of locomotor activity (*Chou et al, 2003*); fat mobilization, thermogenesis and thermoregulation by mean of the activation of the sympathetic system (*Dimicco & Zaretsky, 2007*).

Finally, the most lateral zone of the hypothalamus is characterized by the presence of wide undefined areas, such as the Lateral hypothalamic area (LH) and the Perifornical area (PFA) (**Figure 2-B**), with a broad net of contacts within and outside of the hypothalamus. The LH/PFA area contains at least two neuronal families: the Orexins (ORX) and the Melanocorting Concentrating Hormone (MCH)-expressing cells. Both ORX and MCH neurons activity increases food intake, although with different mechanisms (*Qu et al, 1998; Sakurai et al, 1998*). In particular, ORX are involved in the activation of the arousal circuitries, including those that control feeding behavior. In view of the neural connections and the neuropeptides activity, the LH and PFA are thought to be the interface between the medial hypothalamus and prefrontal cortical and limbic areas associated with reward, motivation and learning, which translates food-related experience into a somatic and autonomic motor output (*Ceccheto & Saper, 1995; Saper CB, 2000*).

3.2 The Arcuate Nucleus and metabolism

Among the many hypothalamic nuclei involved in the control of metabolism, the ARC has a crucial place, for its anatomical and physiological features. The ARC is located in the ventromedial hypothalamus, laterally from wall of the third ventricle (3V) and in continuity with circumventricular organ Median Eminence (ME). Several studies indicate that at least the ventromedial part of the ARC itself can be seen as a circumventricular organ, where the blood brain barrier is less dense (*Brightman & Broadwell, 1976; Peruzzo et al, 2000; Fry & Ferguson, 2007*) and circulating metabolic

18

factors can be sensed in their actual concentration than if sensitivity would depend on the saturable transport systems of the brain blood barrier. Metabolic neural inputs that are signaled via the Vagus nerve to the NTS reach the ARC either directly from the NTS or with the interposition of the Parabrachial nucleus (PBN) (**Figure 1** and **4**).

Within the cellular elements of the ARC, there are at least two neuronal populations that are differentially sensitive to circulating metabolic cues: the POMC/CART and the NPY/AgRP neurons, which exert opposite effect on energy balance (*Glaum et al, 1996; Mercer et al, 1996; Baskin et al, 1999; Muroya et al, 1999*).

POMC (propiomelanocortin) is the precursor of α-MSH (α-melanocyte stimulating hormone), an anorexigenic peptide that inhibits food intake and promotes energy expenditure. These effects are mediated by the melanocortin receptors, MC3 and MC4, which are expressed in brain areas profoundly involved in energy balance and the control of autonomic activity, such as the PVN and the DMH (reviewed in: *Cone RD, 2005*). On the contrary, NPY and AgRP are orexigenic peptides, because the infusion of these neuropeptides in the central nervous system powerfully stimulates food intake (reviewed in: *Schwartz, 2006*). These NPY/ AgRP cells, where the two peptides are almost completely co-localized (*Hahn et al, 1999*), are inhibited by signals of increased fuel availability in the body and are activated by a negative energy status (*Baskin et al, 1999; Elias et al, 1999*).

Arcuate metabolic neurons are sensitive to a wide range of satiety and adiposity signals, including circulating nutrients, ghrelin, insulin and leptin. Energy depletion cues, such as hypoglycemia and ghrelin, activate NPY/AgRP neurons, whereas satiety and adiposity signals, such as glucose, insulin and leptin inhibit NPY/AgRP cells and simultaneously activate POMC neurons.

Within the CNS, the balance between the anorexigenic and orexigenic signals is achieved by mean of two levels of integration. Initially, this occurs in the ARC, where POMC neurons receive inhibiting GABA collaterals from NPY/AgRP neighboring cells, thus they are inhibited when orexigenic neurons

19

are active (*Cowley et al, 2001*). This implies that satiety/adiposity signals activate the anorexigenic pathways directly via the receptors expressed on POMC neurons, and indirectly by suppressing the inhibitory control from the NPY/AgRP neighbors. The second level integration occurs on 2nd-order hypothalamic targets of ARC projections, in particular in the PVN, where NPY and melanocortin receptors are expressed on the same neurons, and AgRP and α-MSH compete for binding to the MC3/4 receptors (*Cowley et al, 1999*) (**Figure 5**). In addition to the PVN, second-order neurons for α-MSH and NPY/AgRP projections are located in other areas of the hypothalamus that participate in the regulation of energy balance: LH, VMH and the DMH.

Bidirectional connections between ARC-NPY neurons to ORX and MCH cells are thought to activate reciprocally the orexigenic-arousal circuitries. MCH neurons also receive inhibitory α-MSH projections, which are thought to suppress the melanocortin-dependent activation of the hypothalamus-pituitary-adrenal axis and food intake (*Ludwig et al, 1998; Tritos et al, 1998*).
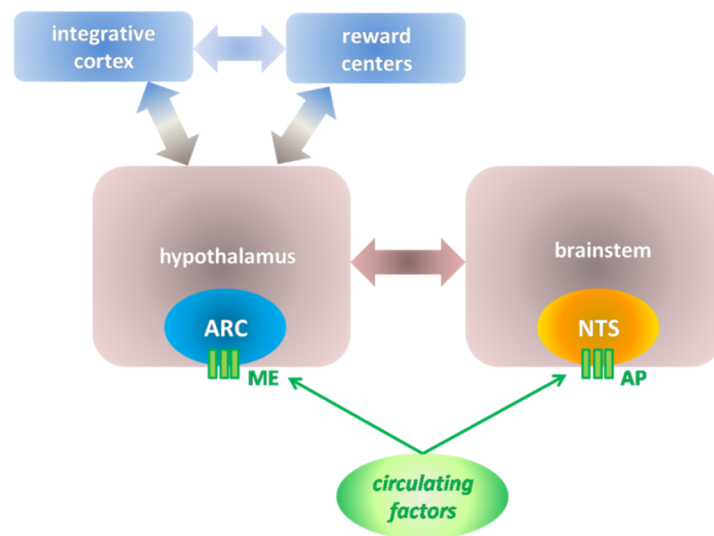
FIGURE 4. The ARC has a crucial role in the central nervous system control of energy homeostasis and feeding behavior. *The peripheral metabolic state is transmitted to the Arcuate Nucleus (ARC) by metabolic cues directly, via the Median Eminence (ME), and indirectly, via the Nucleus of the Solitary Tract (NTS).The information collected and integrated by the ARC is then conveyed to intra-hypothalamic second-order neurons, which in turn generate neuroendocrine/autonomic adjustments and modulate feeding behavior.*

ARC communication with the brainstem and the spinal cord is also possible, both with direct and indirect (via the PVN and the LH) projections from the ARC. These projections are supposed to influence the frequency of the meals. The integrity of direct ARC-brainstem connections is essential not only for the autonomic adjustments in response to changes in the internal energy status, but also for feeding behavior. Recently, Wu and Colleagues showed that the ablation of the AgRP/GABA projections to the pontine PBN leads to starvation (*Wu et al, 2009; Wu & Palmitter, 2011*), suggesting that the sensing of the energy status by the ARC and the sensory input from the mouth and the viscera are integrated in the PBN.
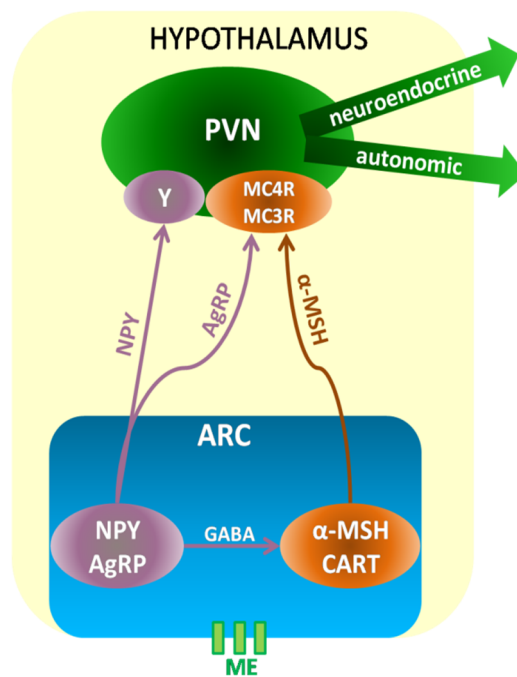
FIGURE 5. **Orexigenic and anorexigenic crosstalk in the ARC and the PVN**. *NPY/AgRP orexigenic neurons activation promotes feeding behavior, whereas anorexigenic α-MSH/CART transmission suppresses feeding and enhances the utilization of excess of energy stored in the periphery. During negative energy status, NPY/AgRP inhibit α-MSH/CART locally, by mean of GABA-ergic projections, and in the PVN, where sensitive cells to metabolic peptides co-express NPY receptors (Y) and melanocortin receptors 9MC3/4-R).*

4. The brainstem and hypothalamus participation in the control of glucose homeostasis

For decades the study of glucose metabolism was restricted to the peripheral organs (endocrine pancreas, liver, skeletal muscle), where insulin was thought to exert its effect. However, the discovery of the neural and endocrine circuits that we have just described showed also the importance of the central *"glucose and insulin sensing"* for the maintenance of glucose homeostasis. In particular, both brainstem and the ventromedial hypothalamus are able to detect changes of glucose and insulin levels, and to trigger counter regulatory responses that attenuate the effects of hypo- and hyper-glycaemia.

Plasma glucose levels of a healthy individual are in a narrow range between 5 and the 7mM.This is achieved by balanced autonomic and endocrine adjustments mainly determined by the levels of glucose present in the glucosensory areas of the gastrointestinal tract, pancreas, circulatory system and brain.

Briefly, the process of glucosensing starts in the mouth, where glucose stimulates nervous reflexes directed to the DVC and the PBN (*Berhoud et al, 1981*), which in turn gives start to the cephalic phase of insulin secretion (2). In the intestine, glucose stimulates the secretion of the several hormones, including *incretins* (GLP-1 and GIP) by the K-cells, and activates the enteric and the parasympathetic nervous systems (*Thorens & Larsen, 2004*). Incretins promote glucose uptake by peripheral tissue, mainly by enhancing the β-cells activity (*Preitner et al, 2004).* In the hepato-portal system, glucose activates vagal reflexes that inhibit the autonomic stimulation of hepatic glucose production (HPG, see below) and feeding behavior*; Burcelin et al, 2004; Fukaya et al, 2007)* , and increase insulin secretion. The glucose absorbed after a meal is taken up by: 1. the liver, which stores it as glycogen and will release it as soon as necessary to maintain normal glycaemia; 2. by muscular and adipose tissues, which depend on insulin to transport glucose into their cells; 3. by tissues that do not require insulin to internalize glucose, including the brain. The systemic effect of

the post-prandial increased glycaemia (glucose levels > 5-5.6mM) is particularly evident in the pancreas, where glucose directly promotes insulin release. On the contrary, when glycaemia decreases in the time between two meals, the endocrine pancreas responds first by decreasing insulin secretion (glucose levels ≈ 4.5mM) and then by increasing glucagon release (glucose levels ≈ 3.9mM). Maybe most important the brain exerts an essential control on all this processes by acting directly on the main protagonists of glucose homeostasis: liver, pancreas and skeletal muscle (*Cryer et al, 2003*).

The best characterized central counterregulation is the response to hypoglycemia. Since the 1960s in the brainstem and in the ventromedial hypothalamus neuronal populations were identified that were sensitive to a drop in blood glucose (*Anand et al, 1964; Oomura et al, 1969; Ritter el al, 1981*). These were the same circuitries that we have previously described for the control of energy homeostasis. Glucosensing neurons are distributed in the AP, NTS, ARC, VMH, LH and PVN, where this information is integrated with sensory afferents carried from the mouth, carotid body, gastrointestinal epithelia and portal/mesenteric veins by cranial parasympathetic nerves. As results, short- and long term adaptation in the autonomic/endocrine activities and in feeding behavior allow the individual to deal with low energy availability. In particular, a primary response is a reactive decrease in insulin secretion and in glucagon and adrenaline/noradrenaline secretion, which results in reduced glucose uptake by cells and an increase in HPG (i.e. glycogen breakdown and gluconeogenesis). In addition, an adaptive increase in glucocorticoids and growth hormone occurs, which allows the individual to reset metabolism according to the new energy state. Finally, hypoglycemia stimulates food search and consumption. It will be clear from figures 3 and 5 of the close relationship between input-integration and output pathways that contribute to HGP in conditions of low circulating glucose. Glucose sensors within the hindbrain and the hypothalamus increase their firing rate in response to hypoglycemia. This information is then conveyed to integrative centers that generate the appropriate

output. For instance, the NTS projects directly on the DMV, which represents the parasympathetic output to the pancreas and liver, but also to the sympathetic network within the reticular formation. In addition, the NTS sends cathecholaminergic/NPY projections to the hypothalamus, in particular to the ARC and the PVN. A sub-population of ARC-NPY neurons is also able to detect a drop in glucose levels (*Akabayashi et al, 1991*), and NPY projections from the ARC to the PVN are essential for the onset of the counterregulatory response (*Menendez et al, 1990*). Because of the presence of both pre-autonomic and neuroendocrine cells, the PVN has a crucial role in the generation of the output in response corresponding to the information received by the ARC and the NTS. Descending autonomic projections from the PVN activate pre-ganglionic nuclei that directly increase the sympathetic tone on the liver, the pancreas and the adrenal medulla, which results in adrenaline secretion and HPG. Intracellular cascades activated by adrenalin in the hepatocytes catalyze glycogen breakdown and the production of gluconeogenetic precursors. Releasing factors-synthetizing neurons of the PVN activate somatotropes and corticotropes in the anterior pituitary, which results in secretion of growth hormone (GH) and Adrenocortical Releasing Hormone (ACTH). Both ACTH and glucocorticoids have counterregulatory properties, and act in the hindbrain and the hypothalamus to raise glycaemia. The activation of the neuroendrocrine pathways occurs at lower level of glucose ($\approx$ 3.2 mM) than the activation of the autonomic reflexes (3.6-3.9 mM) (*Cryer et al, 2003*).

The functional anatomy of the central pathways that counteract an increase in plasma glucose is less clear. For a long time, the existence of glucoresponsive neurons was matter of controversies and the counter regulation to hypoglycemia was considered the only contribution of the CNS to glucose homeostasis. Currently we know that glucoresponsive neurons are present in all the brain areas that control the energy balance, and especially in the ventromedial hypothalamus (*Wang et al, 2004*). Also, a subset of the ARC-POMC cells are excited by glucose, an effect that is in part driven by the

closure of ATP-dependent K$^+$-channels (a mechanism described also for pancreatic β-cells) (*Ashford et al, 1990; Ibrahim et al, 2003; Ashcroft et al, 1984*).

More information about the effect of a positive glucose balance on the brain is provided by insulin. As we already mentioned, brain does not depend on insulin for glucose up-take, but insulin signaling in the ARC represents an adiposity signal. In rodents, insulin signaling on ARC-AgRP neurons is essential for the suppression of HGP (*Pocai et al, 2005a*). This effect is mediated by the Vagus nerve and results in the inhibition of gluconeogenic enzyme expression: the glucose-6-phosphatase and phosphoenolpyruvate carboxy-kinase. In addition, central insulin signaling regulates the sympathetic output to the white adipose tissue to inhibit lipolysis, which reduces the availability of gluconeogenic substrates to the liver, such as glycerol (*Obici et al, 2002; Inohue et al, 2006; Scherer et al, 2011*).

5. Framing the problem

Although early studies support the hypothesis that energy balance is a state of equilibrium between systems that enhance fuel accumulation in the body or its dissipation, like NPY/AgRP and α-MSH do, a number of following studies showed that the alteration of one of the components very seldom is able to alter significantly the overall energy homeostasis. For example, neither the prenatal deletion of the NPY gene, nor of the NPY receptors, induces lean and hypophagic phenotypes (*Beck, 2001*). Conversely, MC4 receptors deficiency causes severe obesity in experimental animals and humans. However such condition is responsible for obesity in only a small percentage of overweight humans (*Cone R, 2005; Butler et al, 2006*). These observations indicate that ***a correct energy balance is the result of the integration of multiple systems***, some of them apparently redundant but all essential for the maintenance of energy homeostasis.

In addition, the hypothalamus alone can hardly account for the ultimate decision for having food or not, it is clear that different kinds of information (chemical and neural), originating from inside the body and/or triggered by stimuli coming from the environment, converge in the hypothalamus, where

they are integrated and produce a more or less adequate feeding behavior. Nevertheless, recent evidence indicates that the coordination by the hypothalamus of all functions relevant to homeostasis, including metabolism, wake-sleep cycles and temperature settings, is essential for a healthy life. Hence single or multiple alterations in the above coordinated functions may lead to dysfunction or overt disease. Thus, the physiology (and pathology) of the feeding control systems may be affected by many factors at multiple levels, which may be related or not to the simple signaling of metabolic cues to the brain, ***but all these signals are integrated at different levels, inside and outside of the hypothalamus***.

6. Aim of the Project

In the present project, we have developed three different sub-projects to investigate specific items within the hypothalamic integrative network regulating energy balance, with particular emphasis on the role of the ARC in the hypothalamic integration of metabolic cues.

First, we focused on the ventromedial ARC, where in addition to NPY and α-MSH, a third neuropeptide is co-expressed: VGF. This is a polypeptide synthesized in response to different kind of stimuli in a variety of (neuro)endrocrine cells, which has an essential, although not well characterized, role in the control of energy homeostasis. Therefore in order to get a better insight in the possible functions of this peptide we investigated in the present study changes in the expression and synthesis of this polypeptide VGF in relationship with two main categories of ARC neurons: NPY neurons and α-MSH expressing neurons (***Chapter 1***).

Next we hypothesized that changes present in the ARC of rodents under different metabolic conditions might be reflected in a similar way in the diabetic human. Therefore we performed a post-mortem analysis in the ARC of people who had suffered of type-II diabetes in their lives and compare with the ARC of patients who died in consequence of other pathologies, in order to compare the NPY, α-MSH and VGF immunoreactivity. In fact, ample animal studies demonstrate that neuropeptides

26

NPY and α-MSH expressed in ARC and NTS modulate glucose homeostasis and food intake. In contrast, there exisit no relating these observations for human disease. Here we compare the post mortem immunoreactivity of the metabolic neuropeptides NPY, α-MSH, Tyrosine Hidroxylase (TH) and VGF in the infundibular nucleus (ARC), and brainstem of 11 type-2 diabetic and 11 non-diabetic individuals (*Chapter 2*).

Finally, in view of observations made in study 1 we hypothesized that the NPY neurons of the Intergeniculate Leaflet (IGL) projecting to the SCN could signal the nutritional state to the biological clock. (*Chapter 3*).

Chapter 1

A role for VGF in the hypothalamic Arcuate and Paraventricular nuclei in the control of energy homeostasis

INTRODUCTION

Vgf (non-acronymic) is a neurotrophin-induced gene that is expressed in neuronal and neuroendocrine cells (*Levi et al, 1985; Salton et al, 1991)*. The *vgf* gene encodes for a precursor polypeptide that is stored in dense core vesicles, cleaved by prohormone convertases typical of neuronal/endocrine tissues and then released after depolarizing stimuli (*Possenti et al, 1989; Trani et al, 1995*). *VGF* mRNA is widely expressed throughout the nervous system, both in embryonic and adult tissues (*Snyder et al, 1998; Snyder and Salton, 1998*). The highest expression of *vgf* has been detected in the ventromedial hypothalamus, especially in the Arcuate Nucleus (ARC) and in the Suprachiasmatic Nucleus (SCN) (*Van den Pol et al, 1989; Van den Pol et al, 1994).*

The participation of VGF in metabolism was discovered after development of *vgf* knock-out mice: these animals are smaller than their control littermates (both heterozygous and normal mice) and are lean throughout their lives. At birth, however, they weigh the same as the controls and, in proportion to their size, they eat more food than the controls (*Hahm et al, 1999*); they also show a high level of oxygen consumption and locomotor activity, indicating that an inappropriate increase in energy expenditure could be the cause of the lean phenotype.

Interestingly, *vgf* is required for the development of several forms of obesity (*Hahm et al, 2002; Watson et al, 2005*). For instance, Agouti mice (A^y/a) over-express the agouti polypeptide, thus have a decreased α-MSH satiety-signaling and develop obesity; in addition, they also show a typical yellow-colored coat. When inbred with *vgf-/-* mice, A^y/a animals fail to become obese, but they still have a yellow coat, suggesting that *vgf* may be a key component of the metabolic melanocortin signaling specifically in the brain (*Hahm* et al, 2002; *Watson et al, 2005*). The chemical lesion of the ARC also indicates that *vgf* is essential for energy balance. In particular, gold thioglucose (GTG) is a substance that produces the loss of glucosensitivity in the ARC resulting in obesity (*Bergen et al, 1998*); the latter is totally prevented by *vgf* ablation (*Hahm et al, 2002; Watson et al, 2005*). Monosodium glutamate (MSG) is another neurotoxic agent that causes extensive injuries to the hypothalamus, including the removal of NPY and melanocortin signaling and the impairment of the sympathetic output (*Pizzi and Barnhart, 1976*). Conversely to GTG lesion, *vgf* gene inactivation in knock-out mice does not prevent MSG-induced obesity, suggesting that *vgf* acts on the hypothalamic autonomic outflow, and that this action of *vgf* is necessary for the development of the hypermetabolic phenotype (*Hahm et al, 2002*). More recently, Watson et al (2009) demonstrated that the *vgf* knock-out mice display hyperactivation of the sympathetic system that can be responsible for the reduced accumulation of fat, together with an up-regulation of uncoupling proteins in brown adipose tissue.

Additional data indicate that in the fed state, *VGF* mRNA co-localizes with *POMC* mRNA in the lateral ARC, whereas, in the fasted state, the co-localization between *VGF* mRNA and POMC decreases, and *VGF* is expressed in NPY/AgRP cells (*Hahm et al, 2002*).

AIM & HYPOTHESIS

In the present work, we aimed to study two aspects of VGF's participation in the hypothalamic regulation of metabolism: we investigated the dynamic of VGF synthesis in α-MSH and NPY cells of

the ARC according to the metabolic state, and we studied the neural pathways through which VGF of the ARC may exert a control on energy expenditure.

We first compared *VGF* mRNA expression and VGF protein synthesis with NPY and POMC or α-MSH in response to different feeding conditions, with the hypothesis that VGF distribution shifts from NPY to α-MSH according to a negative or positive metabolic state, respectively. In particular, we compared the changes of: (a) *VGF*, *NPY* and *POMC* mRNA; (b) VGF, NPY and α-MSH immunoreactivity (IR); (c) VGF immuno-co-localization in NPY and α-MSH neurons, in response to 48 hours fasting; 48 hours fasting followed by 3 hours re-feeding; 48 hours fasting followed by 6 hours re-feeding.

Next we explored the possibility that pre-autonomic neurons within the hypothalamic PVN might be a target of VGF neurons of the ARC, by injecting an anterograde tracer in the ARC and a retrograde tracer in the Dorsovagal complex (DVC) of the brainstem, and observing the VGF projection by triple fluorescent immunohistochemistry.

Results showed that VGF provides an anabolic signal, which might be necessary to reach a state of positive energy balance that is missing in *VGF -/-* animals, and that it could exert this effect on metabolism through pre-autonomic neurons in the PVN.

MATERIALS & METHODS

Male Wistar rats, weighting 250-300g, were used for all experiments; they were housed in individual cages, for one week at 22°C, under a 12:12 light-dark cycle, with free access to food (*Teklad Global Diet 2018S, Harlan, Madison, WI, USA*) and water, before each one of the following experiments. All the procedures were approved by the committee for ethical evaluation at the Universidad Nacional Autónoma de México, in strict accordance with the Mexican norms for animal handling (Norma Oficial Mexicana NOM-062-ZOO-1999).

Experimental design

Male Wistar rats were randomly divided in 4 groups (N=5 animals/group): the control group was fed ad libitum for all the time of the experiments (CTR); the fasted group was food-deprived for 48h (FST); the 3-hours re-fed group was fasted for 48h and then re-fed for 3 hours (3h-RF); the 6-hours re-fed group was fasted for 48h and then re-fed for 6 hours (6h-RF). Fasting and re-feeding procedures were performed in the way that all the animals were sacrificed at the same time of the day (ZT10). On the day of the sacrifice, animals were deeply anesthetized with an overdosed of sodium pentobarbital (*Sedalpharma, Pet's Pharma, Mexico*; 50mg/kg) and perfused transcardially with 0.01M phosphate buffered saline (PBS; ph=7.4) and 4% Paraformaldheyde(*Sigma-Aldrich Corp., St. Luis, MO, USA*) in 0.01M phosphate buffer.

In situ hybridization

Brains were rapidly removed, additionally post-fixed overnight by immersion in the same fixative at 4°C, followed by cryoprotection in 30% diethyl pyrocarbonate-treated sucrose in PBS at 4 °C, cut in series of 16 μm-thick coronal sections throughout the rostrocaudal extent of the hypothalamus. Alternate sections were collected on Superfrost/Plus glass slides (*Fisher Scientific Co., Pittsburgh, PA, USA*) and stored at -80°C. Sections were dried at room temperature for 2 h before overnight incubation at 65 °C in hybridization buffer [1 × diethyl pyrocarbonate-treated 'salts' (200 mmNaCl, 5 mm EDTA, 10 mmTris, pH 7.5, 5 mm $NaH_2PO_4.2H_2O$, 5 mm Na_2HPO_4); 50% deionized formamide; 1 × Denhardts (RNase/DNase-free; *Invitrogen Corporation, Carlsbad, CA, USA*); 10% dextran sulphate (Sigma–Aldrich)] containing 400 ng/mL digoxigenin-labelled RNA probes purified in Sephadex G-50 columns. Sense and antisense probes were generated by linearization or excision of plasmids with appropriate enzymes, and purified using QIAquick PCR Purification Kit (*QIAGEN Inc., Valencia, CA, USA*). Primers were synthesized by Sigma: sense 5´ TATCCCTGCTCGTGTGTTTG 3´ and antisense

31

5´ AGGCAGACTGGTTTCACAGG 3' for NPY; sense 5´ GACTGAAAATCCCCGGAAGT 3´ and antisense 5´ TCTTGATGATGGCGTTCTTG 3' for POMC; sense 5´ ATGAAAACCTTCACGTTGCC 3´ and antisense 5´ GCGCTTAGCATTACTCGGAC 3' for VGF.

The hybridization solution consisted of 50% formamide, 2 × sodium phosphate, sodium chloride and EDTA (SSPE), 1 µg/µl bovine serum albumin (BSA), 1 µg/µl poly A, 2 µg/µl tRNA in diethyl pyrocarbonate (DEPC)-treated water). Following hybridization, sections were washed three times in wash solution (50% formamide, 1 × saline citrate, 0.1% Tween-20) at 65 °C and twice at room temperature in 1 × MABT (20 mM maleic acid, 30 mMNaCl, 0.1% Tween-20) before being incubated in blocking solution [1% blocking reagent (*Roche Applied Science, Burgess Hill, UK*)] and then overnight in alkaline phosphatase-conjugated anti-digoxigenin antibody (1: 1500; Roche). BM purple AP substrate precipitating (*Roche*) with 1 mMLevamisole (*Roche*) was used for colorimetric detection at 37 °C for 8–20 h. Sections were mounted with Glycerol (*Sigma*).

Immunohistochemistry

After anesthesia, perfusion and post-fixation, rat brains were cryoprotected in 30% sucrose, 0.04% NaN_3 in PBS at 4°C until sectioning. Serial 40 µm-thick coronal sections of the ARC and the PVN were used for immunohistochemical procedures. For immunostaining quantification, each sixth section was pre-incubated for 1 hour at room temperature and then incubated overnight at 4°C with either rabbit anti-VGF C-terminus (see *Brancia et al, 2005*; 1:10.000), rabbit anti-NPY (see *Buijs et al 1989*; 1:4.000) or sheep anti-α-MSH (*Chemicon International, Millipore Corporation, Billerica, MA, USA*; 1:8000) antisera. After rinsing, sections were incubated in either biotinylated donkey anti-rabbit or biotinylated donkey anti-sheep IgG (*Jackson Immunoresearch, West grove, PO, USA*) for 1.5 hours, and then in the avidin-biotin complex (*Vector Elite, Burlingame, CA, USA*; 1:500) for further 1.5 hours. For all the incubation steps, antibodies were diluted 0.01M Tris Buffered Saline (TBS),

containing 0.5% Triton X-100 (*Sigma-Aldrich Corp., St. Luis, MO, USA*) and 0.25% gelatin (*Merck KGaA, Damstadt, Germany*). Sections were rinsed in PBS 3 times for 5′ before each incubation step. The final reaction was performed with a solution of 3,3′-diaminobenzidine 0.25% and H_2O_2 0.01% (both provided by *Sigma-Aldrich Corp., St. Luis, MO, USA*) in TBS for 10′. Sections were the rinsed and mounted on gelatinized slides, dehydrated with graded solutions of ethanol (70°, 96° and 100°) and xylene, and coverslipped with Entellan embedding agent (*Merck KGaA, Damstadt, Germany*).

For immunofluorescence studies, two series of section for each brain were incubated with guinea-pig anti-NPY (*Abcam, Cambridge, MA, USA*), sheep anti- α-MSH (*Santa Cruz Biotechnology, Santa Cruz, CA, USA*) and rabbit-VGF antisera as indicated before. After rinsing, sections were incubated with a mixture of Cy2™-conjugated donkey anti-sheep and Cy3™-conjugated donkey anti-rabbit antibodies. (*Jackson Immunoresearch, West Grove, PO, USA*) for 1.5 hours.Finally, sections were mounted on gelatinized slides, coverslipped with 30% glycerol in PBS.

Tracing studies from the ARC to the PVN

The anterograde tracer Phaseulus Vulgaris Leucoagglutinin (Pha-L) (*Vector Elite, Burlingame, CA, USA*) was unilaterally injected, by iontophoresis, in the mediobasal hypothalamus of 12 rats at the coordinates: 3.3 caudal from the bregma; 1.0 lateral from the midline; 9.8 deep from the surface of the brain, with an angle of 4º degrees. After a week from the surgery, animals were perfused and the brains processed as above. A first DAB/peroxydeimmunohistochemisty with a rabbit anti-Pha-L (*Vector Elite, Burlingame, CA, USA*) was performed to test the accuracy of the injection. Six samples were considered useful for the further steps of the experiment.

Then, a double fluorescent immunohistochmistry was carried out to confirm the origin of VGF projection to the PVN. A series of section was incubated in a mixture of goat anti-Pha-L (*Vector Elite, Burlingame, CA, USA*) and rabbit anti-VGF antisera. Primary antibody binding was visualized by

mean of a mix of donkey anti-goat donkey anti-rabbit antibodies conjugated with Cy2™, DyLight™-649 and Cy3™, respectively (*Jackson Immunoresearch, West Grove, PO, USA*).

Tracing studies from the Dorso-Vagal Complex

The Cholera Toxin Subunit B (CTB), conjugated with the Alexa Fluor® fluorescent dye (*Molecular Probes, Eugene, OR, USA*), was injected in the DVC of 8 rats. Surgical experiments were done on a stereotact (*Stoelting Co, Wood Dale, IL, USA*) with the head of rats flexed at 45°.The stereotact was kept at a 10° angle so that the micropipette could be placed at a 90% angle onto the medulla oblongata. The dura mater and arachnoid membranes were dissected to expose the dorsal surface of medulla at the level of the Area Postrema (AP). Injections of 0.1 μl, 1% CTB were made using a micropipette with a 20- to 40-μm tip diameter. The tip of micropipette was placed 0.3-0.4 mm rostral and 0.5 mm lateral of the Obex. Injections were made 0.5 mm below the surface of the brainstem. Rats were allowed to survive for 14 days before sacrifice.

The resulting section were incubated with a sheep anti-NPY and rabbit anti-VGF antisera, followed by an incubation with a mix of Cy2™-conjugated donkey anti-sheep and DyLight™-649-conjugated donkey anti-rabbit (*Jackson Immunoresearch, West Grove, PO, USA*).

Histochemical Analysis

Digital pictures of the ARC were taken by using an Axioplan microscope (*Zeiss, Jena, Germany*) equipped with a digital color photocamera (*Olympus DP25, Olympus, Japan*). Both mRNA and immunoreactivity analyzed bilaterally and were quantified as integrated optical density with the program ImageJ. Results are expressed as mean ± the standard error from the mean (SEM). They were analyzed with a one-way ANOVA followed by a Turkey multiple comparison post-hoc test. p-Values <0.0.5 were considered statistically significant.

Sections stained with fluorescent markers were analyzed with the LSM 5 Pascal confocal microscope (*Zeiss, Jena, Germany*).

RESULTS

Fasting and refeeding induced changes in NPY, POMC and VGF mRNAs in the ARC

The analysis of NPY, POMC/α-MSH and VGF expression and synthesis under the different feeding conditions tested demonstrated that except of POMC in the mid ARC, the rostral, mid and caudal levels of the ARC showed a similar direction of changes under the different metabolic conditions for all three peptides. Detailed results are shown in **Table 1.1** and **1.2**.

As expected from an orexigenic neuropeptide, *NPY* mRNA is strongly increased after 48hours fasting ($F_{(3,16)}$=14.39; p<0.001), and returned to basal level rapidly already after 3 hours of refeeding (**Figure 1.1-A**).

POMC mRNA was expressed in big-sized neurons in the ventrolateral ARC. Somewhat unexpectedly for an anorexigenic neuropeptide, *POMC* only showed a tendency to decrease in the fasted group (**Figure 1.1-B**), but the difference with the controls was never significant. Surprisingly except for the mid portion of the ARC, *POMC* was significantly down-regulated after 3-hours refeeding ($F_{(3,16)}$=3.89; p=0.02) (Figure 1-B), whereas it returned to basal levels after 6 hours refeeding (**Table 1.1**).

In control *ad libitum* fed animals we observed that *VGF* was expressed in the whole ARC, but most strongly in large-size cells the lateral part, in which POMC neurons predominate. Smaller and less intensely labeled VGF neurons were present in the medial ARC (NPY area) (**Figure 1.1-C**). Fasting was associated with an up-regulation of *VGF* mRNA ($F_{(3,16)}$=19.98; p<0.001) and the distribution shifted to the NPY area where now most of the *VGF* was expressed in very few *VGF* cells remaining in the ventrolateral ARC (**Figure1.1-C**). Also here, re-feeding rapidly decreased *VGF* expression to

control levels whereby *VGF* mRNA disappeared from the medial ARC (NPY area) and reappeared in the lateral ARC (POMC area).

Fasting and refeeding induced changes in NPY, α-MSH and VGF immunoreactivity in the ARC

Consistent with the results of *in situ* hybridization, NPY-IR in the ARC was significantly augmented in fasted animals. This increase persisted in 3h re-fed animals and NPY levels returned only to basal levels 6h after refeeding ($F_{(3,16)}$=12.63; p<0.001) (**Fig. 1.2-A**). On the contrary, the levels of α-MSH-IR were constant in all feeding conditions (**Fig. 1.2-B**) the apparent increased staining density in the fasted ARC was not statistically significant ($F_{(3,16)}$=0.96; p=0.43).

The results concerning VGF-IR presented important similarities and differences with the results of *in situ* hybridization. As compared to control ARC, we noticed again many VGF big neurons in the ventrolateral ARC and less numerous smaller VGF neurons along the medial ARC, including near the ME (**Figure 1.2-C**). In addition similar to the change in the mRNA VGF expression, fasting displaced the visualization of VGF positive cells from the lateral ARC to medial ARC. Nevertheless, different from both NPY and α-MSH, VGF-IR was increased only in the re-fed groups ($F_{(3,16)}$=8.10; p=0.001) (**Figure 1.2-C**) the increase in immunoreactivity was especially apparent in the nerve fibers as also can be seen by the increase in staining in the median eminence.

VGF co-localization with NPY and α-MSH in the ARC and the PVN

Fluorescent immunohistochemistry indicated that VGF and NPY co-localize in fibers in the mid and posterior ARC and in the PVN. No NPY and VGF co-expressing neurons are visible in the medial ARC (**Figure 1.3**) VGF and α-MSH co-localized in cell bodies where their mRNAs dominated: in the lateral ARC over the whole rostro-causal extent, big-sized α-MSH-VGF co-expressing neurons are observed in the ventro-lateral ARC (**Figure 1.3**). Fasting alters these patterns: NPY-VGF containing fibers became denser, whereas α-MSH decreased its VGF content (**Figure 1.3**).

36

Examining the possibility that VGF from the ARC may influence PVN output we examined the co-localization between VGF and NPY or α-MSH in terminals in the PVN area. Most of VGF terminals in the PVN co-express either NPY or α-MSH (**Figure 1.4-A** and **1.4-B**) suggesting that most of the VGF terminals in the PVN may arise from the ARC. In order to confirm this possibility we injected the anterograde tracer Pha-L into the ARC and investigated the co-localization between Pha-L and VGF in the projections from the ARC to the ventromedial area of the PVN (**Figure 1.5**).

Furthermore, in order to identify the neural pathway by which VGF might exert its effect on metabolism, we investigated whether the PVN pre-autonomic cell populations are a possible target for ARC-VGF projections. The retrograde tracing from the DVC shows that many of VGF fibers, also containing NPY, contact pre-autonomic neurons in the ventromedial PVN (**Figure 1.5**).

DISCUSSION

Fasting induces opposite changes in NPY neurons as compared to POMC neurons

In the present study, we refer to two well characterized metabolic genes expressed in the ARC; *NPY* and *POMC*, to understand the response to changing metabolic conditions of a third gene *VGF*, expressed in the same brain area. The *VGF* gene presents the remarkable characteristic of being expressed in both *NPY* and *POMC*, which are activated during negative and positive metabolic conditions, respectively. By comparing *NPY* and *POMC* distribution and expression levels when animals were free fed, fasted and re-fed, we determined which one of the two neuronal populations also responds by expressing *VGF* to a particular energy status.

The in situ hybridization shows that, in agreement with the literature, food deprivation is a very strong stimulus for *NPY* expression in the *ARC (Hahm et al, 1999)*. Access to food for 3 hours after fasting suppresses the *NPY* anabolic signal and triggers the *POMC* catabolic one. Interestingly, *POMC* mRNAs reaches the minimum levels in 3-hours re-fed and not in fasted animals. A possible

explanation for this *POMC* expression profile is that 3 hours access to food after 2 days of fasting is not sufficient for the organism to recover from such anabolic challenge. *POMC* expression peaks in the 6h-refed group and, at this time, circulating leptin has already reached the plasma peak (*Maffei et al, 1995; Saladin et al, 1995*), suggesting this hormone as the booster of the anorexigenic *POMC* response.

As *NPY*, *VGF* is significantly up-regulated in the *ARC* after a period of fasting but, beside this quantitative measurement, is important to observe how the feeding condition determines which population expresses more *VGF*. In fact, the detailed analysis of the distribution of *VGF* under the different experimental conditions revealed that the *VGF* response is strongly dependent on its medial-lateral distribution in the *ARC*. The highest increase of *VGF* to fasting occurs in the *NPY* area, whereas in free-fed and re-fed animals *VGF* mRNA can be mainly detected in the *POMC* areas. Thus, the switch from a positive to negative metabolic state and *vice versa*, induces in one of the two antagonist population the same response: *NPY* neurons, which are challenged by energy depletion, express *VGF* during fasting; *POMC* neurons, which are active when the energy balance is positive, express *VGF* in free-fed and re-fed animals. This suggests that *VGF* is expressed either in *NPY* or *POMC* neurons in the metabolic condition in which the respective neurons are required to be more active. Analogous observations concerning the *VGF* induction in the hypothalamus in response to a stimulus with relevance for that particular structure was already reported by demonstrating that *VGF* expression is induced in the PVN the Supraoptic nucleus and the Subfornical Organ after salt-loading (*Mahata et al, 1993*) or that a light pulse induces *VGF* expression in the caudal SCN of hamsters (*Wisor and Takahashi, 1997*).

The VGF shift from NPY to α-MSH according to the energy status was confirmed by fluorescent immunohistochemistry showing that indeed VGF co-localizes with α-MSH in both soma and fibers, whereas the co-localization between VGF and NPY was visible only in fibers. This result is in contrast

38

to what was reported by Hahm and Colleagues in 2002, who reported that NPY and VGF are co-expressed in the same ARC neurons after food deprivation. This can be explained by the fact that the rats used in their protocol were previously treated with colchicine in order to enhance the NPY content in the cell bodies (*Hahm et al, 2002*).

Interestingly, none of the observed neuropeptide IR followed the same time course as their mRNAs. In fact, NPY-IR continued to be increased in the 3h-refed group; α-MSH –IR did not change significantly in any of the experimental groups and the VGF peptide is increased in both the re-fed groups. These differences might be explained by the turnover rate of each neuropeptide in response the changing metabolic state. For example, refeeding might block the NPY release while fasting might block α-MSH secretion from the terminals thus promoting the accumulation of these neuropeptides in soma and fibers of the corresponding neurons. In addition to changes in the dynamic of the peptide utilization by the cells, the changes observed in the VGF peptide levels might be also due to modifications that the VGF-precursor might undergo in each cellular sub-type and/or due to the modulation of VGF turnover in every particular metabolic situation.

The PVN is target for VGF neurons of the ARC

In the PVN, NPY and α-MSH interact with both pre-autonomic and neuro-endocrine cellular groups (*Legrádi and Lechan, 1998; Cowley et al, 1999; Balthasar et al, 2005; Kalsbeek et al, 2008*).

The role of VGF in nerve terminals is still unclear. Previous studies *in vitro* reported that pro-VGF is stored in dense core vesicles, cleaved while transported to the synaptic boutons, where it is released after depolarization (*Possenti et al, 1989; Van den Pol et al, 1989; Trani et al, 1995; Trani et al, 2002*). All these cues, together with structural and secretion similarities with chromogranins/secretogranins, suggested VGF as a secreted polypeptide (*Salton et al, 2000; Taupenot et al, 2003*). On the other hand, VGF has been associated with the modulation of synaptic

activity of neurotrophins and proposed as a modulator of synaptic transmission of other neuropeptides (*Salton, 2003*). In support to this model, there is the evidence that VGF in the hippocampus is the precursor of a bioactive peptide which is a positive modulator of synaptic plasticity in the learning process (*Alder et al, 2003*).

In 2009, Toshinai and Nakazato proposed a negative feedback model for the regulation of vasopressin (AVP) secretion by magnocellular hypothalamic neurons in which the VGF cleavage products NERPs, in which these peptides exert a pre-synaptic inhibition of glutamatergic neurons via GABAergic interneurons (*Toshinai and Nakazato, 2009*). In view of this, Cowley and Cols. (*1999*) suggested GABAergic interneurons within the medial parvocellular subdivision of the PVN as a key site where NPY and α-MSH information is integrated; thus VGF derivatives released by VGF projections from the ARC might take part in this integrative model. However, the viability of this proposal is absolutely dependent on the identification of VGF receptors and VGF derivatives active in this context.

VGF fibers target pre-autonomic neurons of the PVN

In the PVN there are two anatomically distinct populations of pre-autonomic neurons: pre-sympathetic and pre-parasympathetic (*Buijs et al, 2001; Buijs et al, 2003*). These neuronal groups belong to one of the two branches of the autonomic nervous system projecting to the pre-ganglionic autonomic nuclei of the brainstem and the spinal cord. We observed that VGF containing terminals, either alone or co-expressing with NPY, end on pre-autonomic neurons of the medial PVN projecting to the dorsal motor complex. This evidence provides the anatomical basis for previous studies that proposed VGF as essential for the activity of the sympathetic autonomic output to the periphery (*Jethwa et al, 2007; Bartolomucci el al, 2009; Watson et al, 2009*). For instance, the intracerebroventricular administration of the VGF-derivative TLQP-21 enhances catabolism in

adipocytes and it increases the adrenaline/noradrenalin ratio, indicating that this VGF product acts centrally to increase the sympathetic tone on WAT and induces adrenaline release from adrenals (*Bartolomucci et al, 2009*).

The NTS is also widely interconnected with sympathetic nuclei, such as the rostral ventrolateral medulla and the intermediolateral column (*Luiten et al,1985; Cechetto and Saper, 1998; Hosoya et al, 1991*). The present observation of VGF contacting PVN preautonomic neurons indicates that VGF may modulate both the sympathetic and the parasympathetic output of the brain.

CONCLUSIONS

VGF expression and synthesis is stimulated or inhibited depending on food availability in both NPY and POMC neurons. We speculate that VGF may be used to signal the metabolic condition sensed by ARC to the PVN acting, at least in part, on the NTS projecting neurons within this nucleus. The mechanism by which VGF acts are still obscure but it might be by modulating the efficiency of the peptidergic transmission thus amplifying the functional antagonism between NPY and melanocortins in the PVN. In addition, it cannot be excluded that VGF cleavage products might act independently from NPY and melanocortins, as is suggested by functional studies that report VGF is involved in the regulation of feeding behavior and autonomic balance, as well as by our present observation that VGF terminals on NTS projecting neurons of the hypothalamus.

Table 1.1. Quantification of the Integrated Optical Density of NPY, POMC and VGF mRNAs in the rostral, mid and caudal levels of the ARC. Data statistical significant for p<0.05; NS=no statistically significant.]

	rostral ARC			
	control	48h fasted	3h re-fed	6h re-fed
NPY	11.39 ± 1.19	20.71 ± 1.14, p<0.001	9.9 ± 1.48, NS	12.33 ± 0.7, NS
POMC	12.08 ± 1.11	9.90 ± 0.84, NS	7.33 ± 0.90, p=0.01	8.73 ± 0.41, NS
VGF	8.15 ± 0.91	15.35 ± 1.15, p=0.001	8.26 ± 1.02, NS	7.02 ± 0.48, NS

	mid ARC			
	control	48h fasted	3h re-fed	6h re-fed
NPY	12.01 ± 1.33	25.25 ± 1.64, p<0.01	15.20 ± 1.86, NS	11.19 ± 0.95, NS
POMC	11.10 ± 1.00	8.45 ± 1.12, NS	9.01 ± 0.89, NS	10.99 ± 0.33, NS
VGF	9.24 ± 0.83	18.35 ± 0.70, p<0.001	9.67 ± 0.98, NS	9.52 ± 0.63, NS

	caudal ARC			
	control	48h fasted	3h re-fed	6h re-fed
NPY	14.93 ± 1.51	22.93 ± 1.63, p<0.01	14.67 ± 1.21, NS	12.32 ± 1.10, NS
POMC	12.94 ± 0.98	9.53 ± 1.15, NS	7.87 ± 0.71, p<0.005	12.21 ± 0.61, NS
VGF	9.49 ± 0.95	19.67 ± 1.49, P<0.001	8.77 ± 1.07, NS	8.11 ± 0.68, NS

TABLE 1.2. Integrated Optical Density quantification of NPY, α-MSH and VGF neuropeptides immunoreactivity in the rostral, mid and caudal levels of the ARC. [Data statistical significant for p<0.05; NS=no statistically significant.]

	rostral ARC			
	control	48h fasted	3h re-fed	6h re-fed
NPY	23.88 ± 1.44	46.71 ± 1.13, p<0.001	47.11 ± 1.56, p<0.001	26.33 ± 0.8, NS
α-MSH	36.48 ± 2.40	41.91 ± 3.35, NS	40.71 ± 3.45, NS	35.93 ± 1.67, NS
VGF	22.69 ± 1.22	24.10 ± 1.08, NS	27.86 ± 1.24, p=0.01	28.78 ± 1.23, p<0.01

	mid ARC			
	control	48h fasted	3h re-fed	6h re-fed
NPY	30.90 ± 0.97	43.25 ± 1.50, p<0.001	38.80 ± 1.68, p<0.001	35.19 ± 10.1, NS
α-MSH	36.05 ± 1.86	42.05 ± 1.54, NS	35.40 ± 2.51, NS	34.79 ± 0.79, NS
VGF	24.69 ± 1.32	26.22 ± 1.42, NS	29.86 ± 0.84, p=0.01	31.78 ± p<0.01

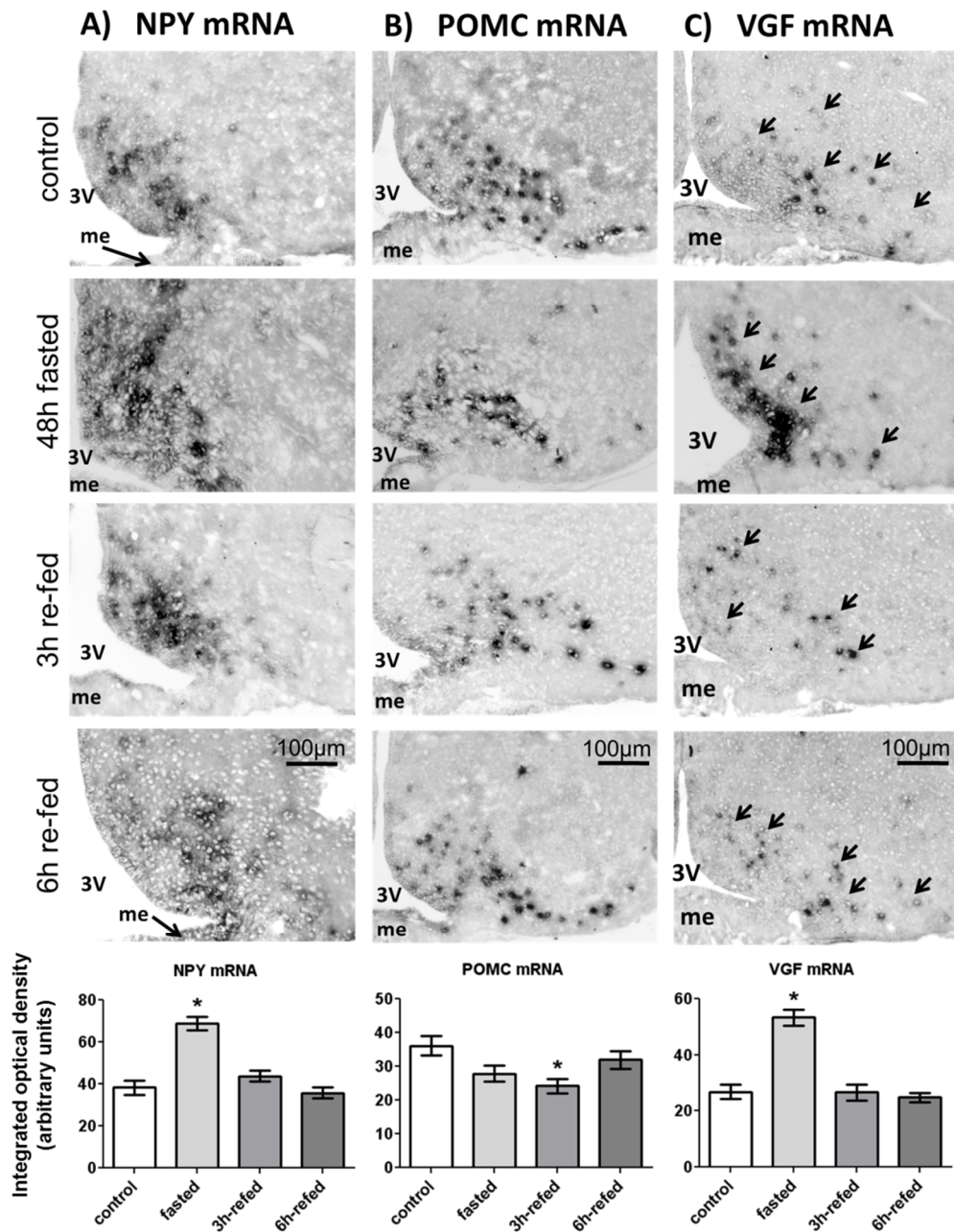|	caudal ARC			
	control	48h fasted	3h re-fed	6h re-fed
NPY	32.93 ± 1.21	41.33 ± 1.04, p<0.001	40.67 ± 1.93, p=0.005	32.32 ± 0.62, NS
α-MSH	36.52 ± 2.34	38.13 ± 2.41, NS	41.47 ± 2.43, NS	32.41 ± 0.98, NS
VGF	23.66 ± 1.71	28.35 ± 1.77, NS	32.95 ± 0,97, p=0.001	30.95 ± 1.40, p=0.01

FIGURE 1.1: *VGF expression is up-regulated by food deprivation.*

The mRNA of the orexigenic peptide NPY (**panel A**) is up-regulated after a 48h of fasting ($F_{(3,16)}$=14.39; p<0.001), and returns to basal level after 3h of refeeding. Note that NPY neurons are concentrated in the medial area of the ARC. The anorexigenic precursor POMC (**panel B**) tends to decrease after fasting and it is significantly down regulated still after 3h of refeeding ($F_{(3,16)}$=3.89; p=0.02). POMC is expressed in big neurons within the ventrolateral ARC. In the animals fed *ad libitum* (control), VGF (**panel C**) is expressed mainly in big sized neurons in the POMC area of the ARC. Fasting triggers a significant increase of VGF mRNA ($F_{(3,16)}$=19.98; p<0.001) in the NPY area of the ARC, whereas refeeding brings VGF expression back to basal levels. Scale bar=100μm. 3V: Third Ventricle; me= Median Eminence.
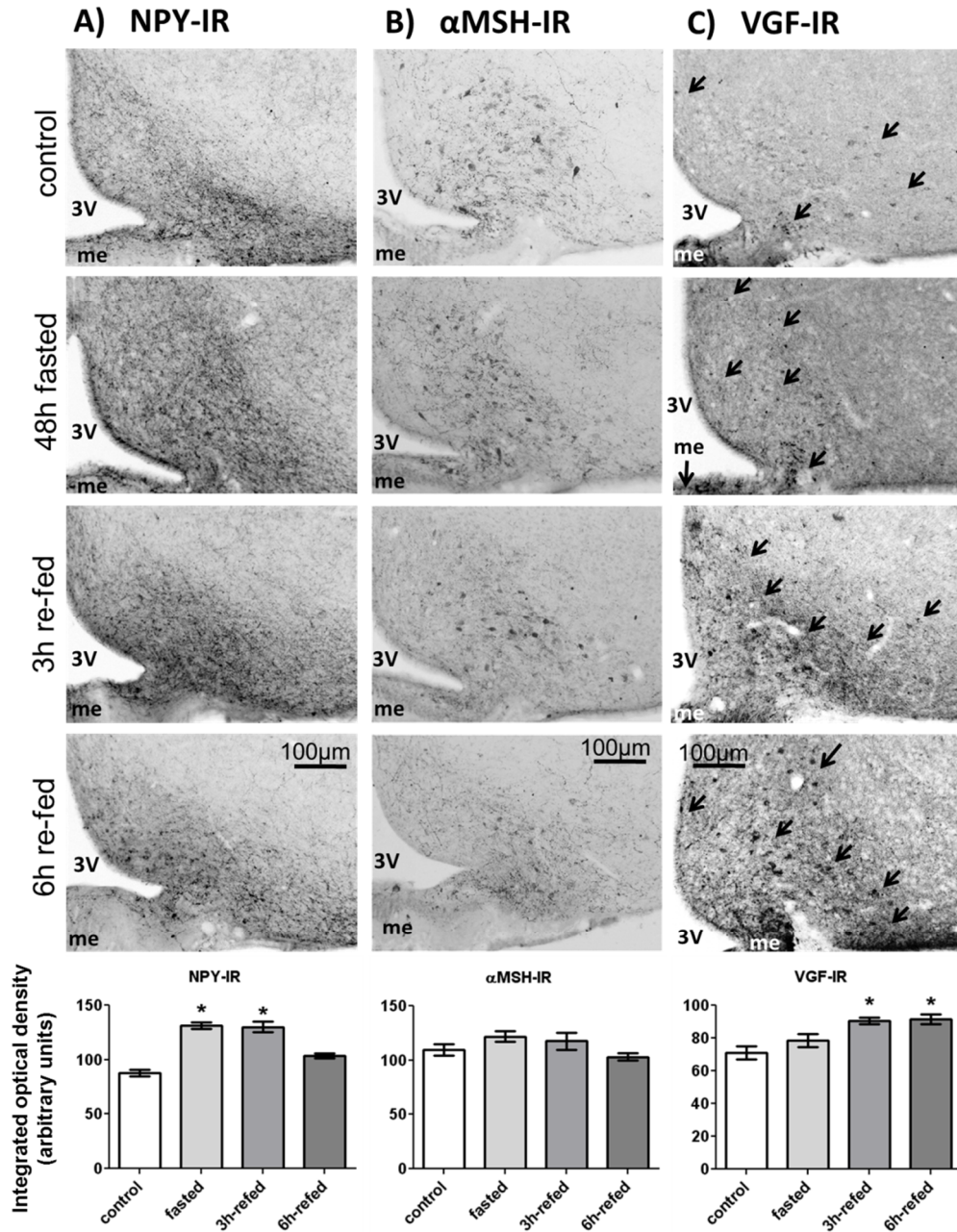
FIGURE 1.2: *VGF peptide is up-regulated by refeeding after food deprivation.*

The orexigenic peptide NPY (**panel A**) is up-regulated after a 48h of fasting, and the increase persists after 3h of refeeding ($F_{(3,16)}$=22.39; p<0.001) .The density of the anorexigenic peptide α-MSH (**panel B**) is not significantly affected by any of the metabolic conditions. In the animals fed *ad libitum* (control),VGF (**panel C**) is expressed mainly in big sized neurons in the α-MSH area of the ARC, but small VGF immunoreactive cells are present in the NPY area, especially near the Median Eminence (me). Fasting shifts VGF immunoreactivity from the lateral ARC to smaller cells within the medial part. With refeeding, VGF gradually reappears in the lateral ARC. Note that fasting does not increase VGF density in the ARC, and a significant up-regulation occurs only after refeeding ($F_{(3,16)}$=8.10; p=0.001). Scale bar=100μm. 3V: Third Ventricle; me= Median Eminence.

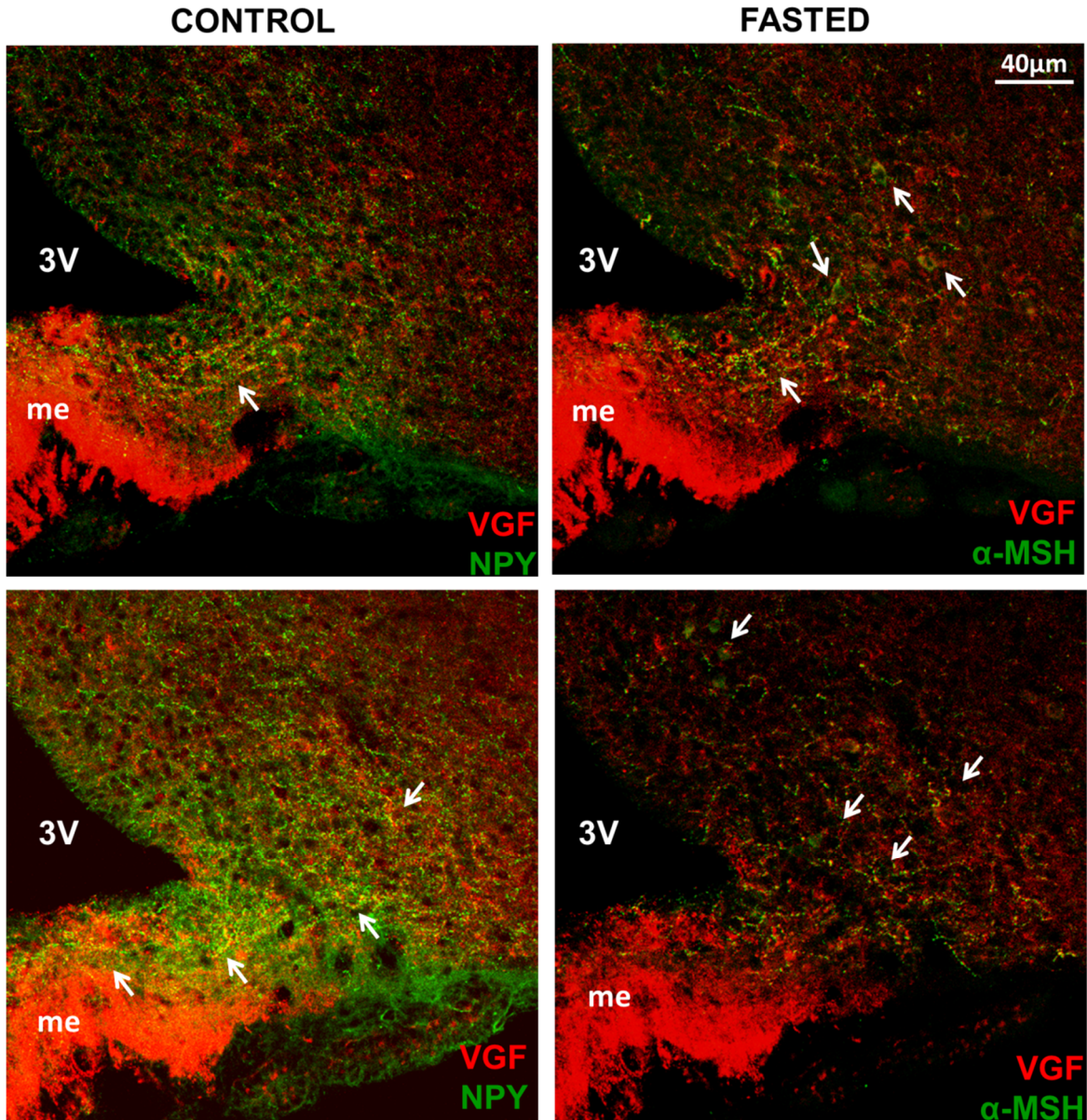**FIGURE 1.3**: *VGF co-localizes with both NPY and α-MSH in the ARC.*
Confocal fluorescent images of the ARC of free-fed and fasted animals showing cellular elements immunoreactive for VGF (*red*) and NPY or α-MSH (*green*). Left column: in control animals, VGF co-localizes with α-MSH in both neurons in fibers (*yellow* cells and fibers; white arrows), whereas the co-localization with NPY is limited to fibers in the ventromedial ARC (*yellow*; white arrow). Right column: fasting ARC is characterized by an increase in NPY-IR cell bodies. VGF-NPY containing fibers are visible in the whole ventral ARC (white arrows), while α-MSH neurons seem to decrease their VGF content (white arrows). Scale bar: 40μm. 3V: Third Ventricle; me: Median Eminence
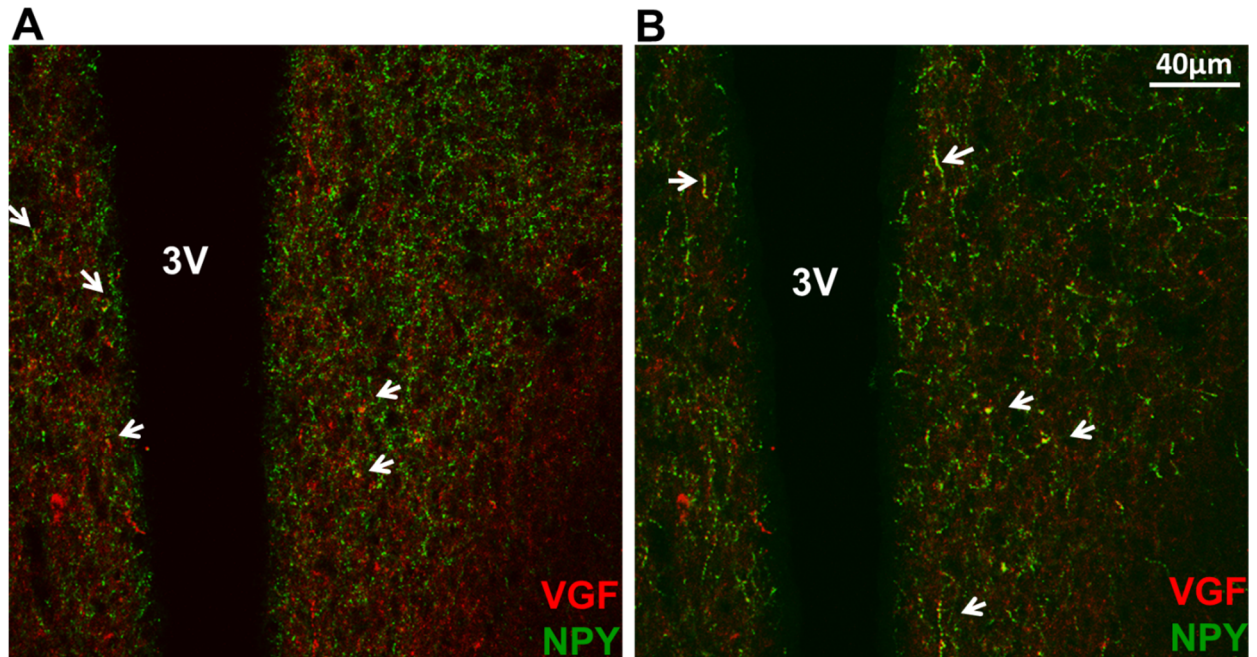
FIGURE1. 4*: VGF in the PVN co-localizes with either NPY or α-MSH*.
VGF fibers, either containing NPY or α-MSH are localized in the ventral PVN, along the wall of the Third Ventricle (3V). In the Panel A, yellow arrows show that VGF (*red*) and NPY (*green*) are co-expressed in tiny fibers (*yellow*). In the Panel B, the arrows indicate that VGF (*red*) and α-MSH (*green*) are co-localized in big-sized fibers (*yellow*). Scale bar: 40μm.
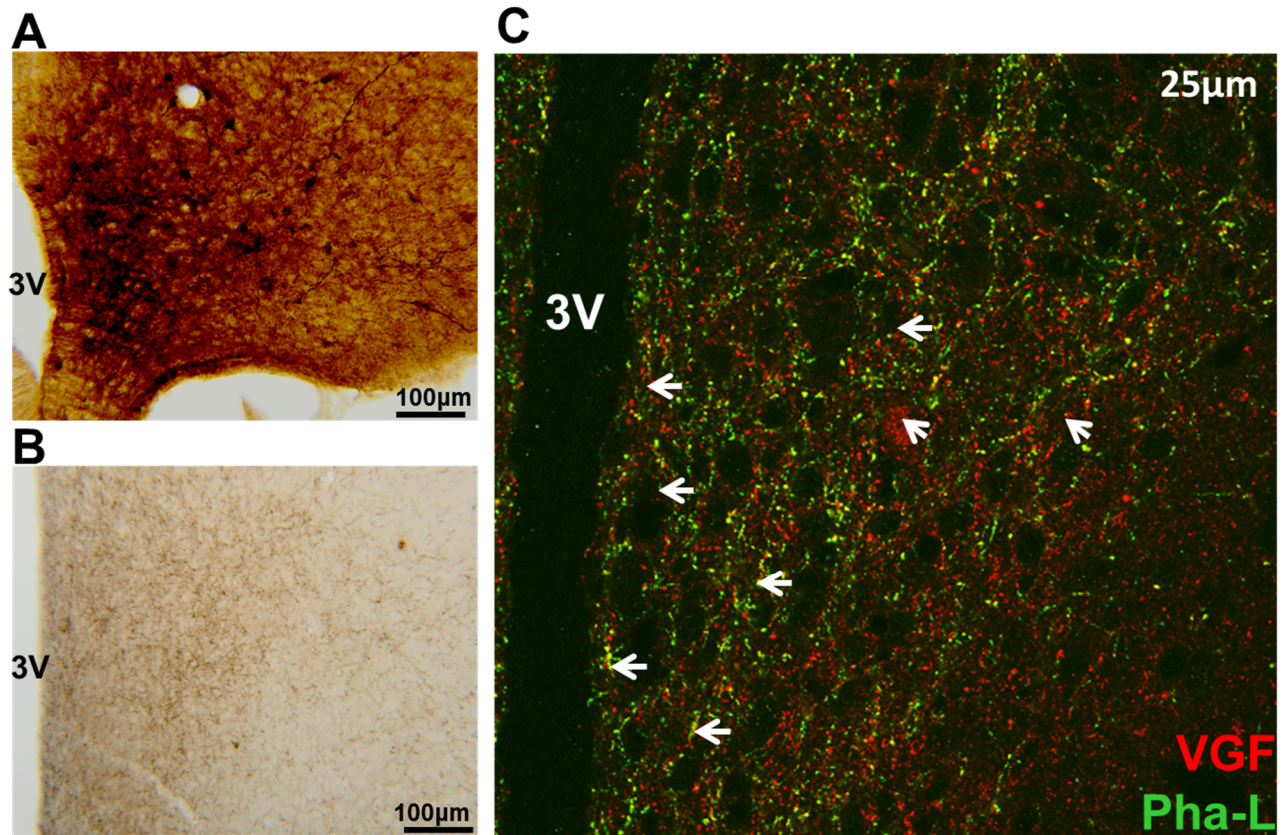
FIGURE 5: *VGF neurons of the ARC project to the PVN.*
Panel A: immunoreactive neurons for Pha-L in the ARC after the injection of the tracer. Scale bar: 100 μm.
Panel B: Pha-L containing fibers in the PVN. Scale bar: 100 μm. **Panel C:** confocal image of the PVN showing projection from the ARC containing the tracer (*green*), VGF (*red*) or both co-localized in the same fiber (*yellow*). Some of the fibers containing both VGF and Pha-L are indicated by the white arrows. Scale bar: 25 μm. 3V: Third Ventricle
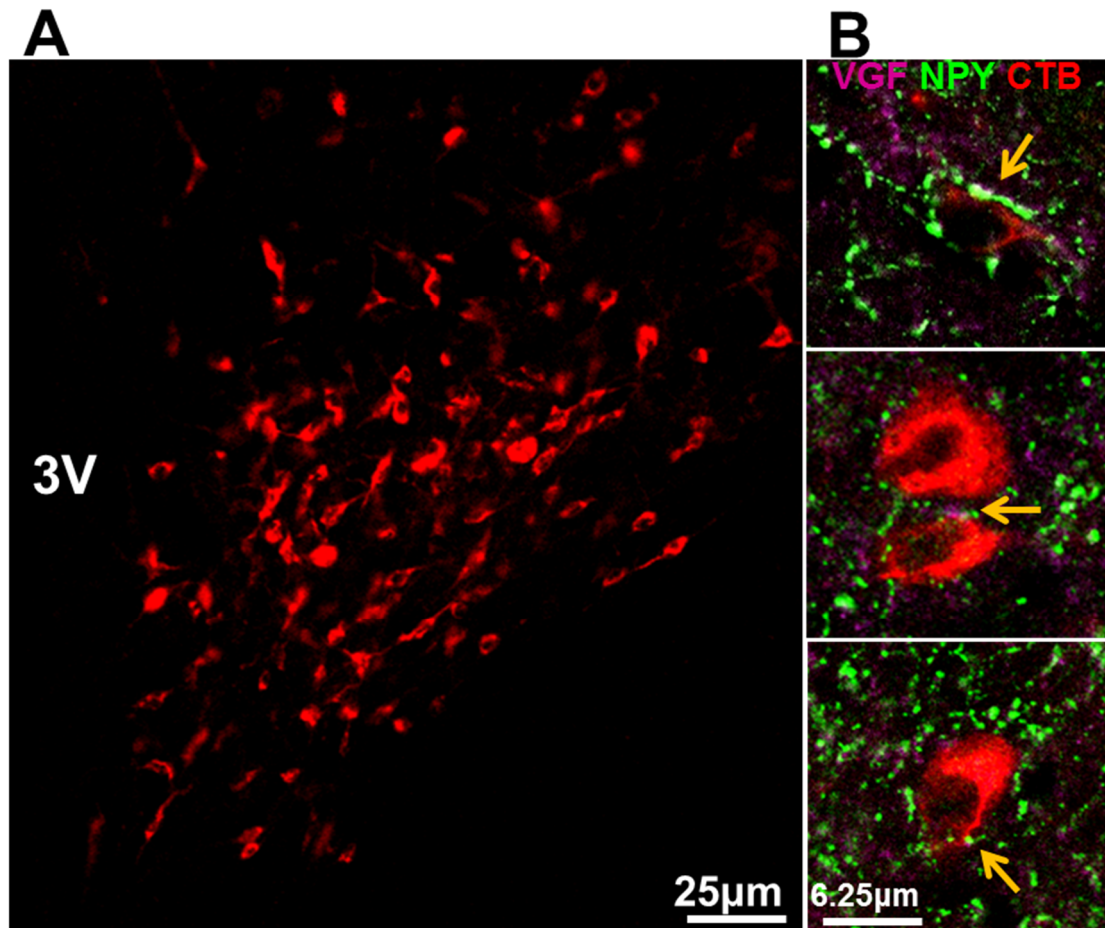
FIGURE 6: *VGF and NPY-containing fibers in the PVN appose onto pre-autonomic neurons.* **Panel A**: the retrograde tracer CTB-Cy3 (*red*), injected in the dorsovagal-complex, shows the presence of pre-autonomic neurons in the hypothalamic PVN. Scale bar: 25µm. **Panel B**: yellow arrows indicate VGF (*magenta*) and NPY (*green*) containing fibers apposing onto the pre-autonomic CTB containing neurons. Scale bar: 6.25µm. 3V: Third Ventricle.

Chapter 2

NPY and VGF are upregulated in the Arcuate nucleus, but downregulated in the Nucleus of the Tractus Solitarius, of type-II diabetic patients.

INTRODUCTION

Animal studies have shown that the levels of circulating insulin and glucose are monitored in the hypothalamic ARC and the caudal brainstem. The ARC is also referred to as Infundibular nucleus in the human brain. Changing concentrations of insulin and glucose modify the activity of several neuronal populations within these areas. These nutrient/hormone sensitive neurons project to pre-autonomic neurons located in the hypothalamus and brainstem and modulate the autonomic output to liver and pancreas. In both areas, neurons were identified that are either activated or inhibited by changes in glucose availability [*Anand et al, 1964; Oomura et al, 1969; Ritter et al, 1981; Balfour et al, 2006*]. At present, the ARC is mainly characterized by two antagonistic neuronal groups: the Neuropeptide Y (NPY) and proopiomelanocortin (POMC) expressing cells. In experimental animals, NPY neurons in the ARC are activated by negative metabolic challenges, such as fasting and hypoglycemia [*White & Kershaw, 1990; Akabayashi et al, 1993*] and NPY signaling is required to stimulate hepatic glucose production in response to a decrease in plasma glucose levels [*Menendez*

49

et al, 1990; Van den Hoek, 2004]. POMC neurons, in contrast, are activated by positive energy conditions and satiety factors, and promote catabolism and energy expenditure. POMC is the precursor of several neuropeptides of which α-MSH is the cleavage product that mediates the effects on metabolism [*Cone RD, 2006*]. VGF is a neuropeptide precursor co-expressed in NPY and POMC neurons of the rat ARC. The ablation of the VGF gene produces a hyper-phagic and hyper metabolic phenotype, and results in increased NPY and diminished POMC expression, typical of prolonged fasting [*Hahm et al, 1999*]. Notwithstanding the wealth of data present in experimental animals nearly nothing is known about the response and changes of these peptide containing-neurons in the human brain. Except for a study that examined the changes of NPY neurons in the ARC in obese humans [*Goldstone et al, 2002*] no information is available about the possible changes in NPY, α-MSH and VGF neurons in the ARC and NTS in the human ARC.

AIM & HYPOTHESIS

We hypothesized that if animal studies have a predictive value for what may happen in the human, the metabolic alterations caused by, or causing diabetic illness may modify the expression of the metabolic neuropeptides in the brain and thus indicate the disturbance of insulin and glucose detection in the brain of the diabetic. Hereto, we investigated the expression of NPY, α-MSH and VGF in the post-mortem brain of type-2 diabetic individuals which was compared with their expression in brains obtained from age and sex matched non-diabetic patients. Moreover, we investigated the co-expression of VGF in human NPY and POMC neurons. Finally, because noradrenalin (NA) is proposed to play an important role in glucose homeostasis [*Ritter et al, 1991*], we verified the relationship of catecholaminergic neurons with NPY neurons in the brainstem of diabetic and non-diabetic individuals.

50

MATERIALS AND METHOD

Human Brains

For this study, 22 human brains were examined, 11 brains from patients (age mean ±SEM: 60.1±4.3, 6 males; 52±5.1, 5 females) who died of complications of type II-diabetes (DBT group) and 11brains of non-diabetic individuals (52.2±4.3, 6 males; 54.2±5.7, 5 females), who died of conditions not related with a chronic metabolic impairment, considered as controls (CTR group) (Table 2.1 and 2.2). Diabetic and control cases were age and sex matched, post mortem time due to hospital practice was always between 8 and 12 hours and brains of controls and diabetics were always stained in pairs to avoid staining intensity differences due to procedure. Brains were collected by a team of Neuropathologists at the Hospital General de Mexico in Mexico City from January 2004 to 2008. The protocol was revised and approved by the Ethical Committees of the Hospital General de Mexico and the Faculty of Medicine at Universidad Nacional Autonoma de Mexico, in according with the Mexican law Reglamento de la Ley General de Salud, Diario Oficial de la Federacion: D.O.F. 20-II-1985; D.O.F. 26-XI-1987; D.O.F. 06-1-1987. During hospitalization, Patients subscribed a written informed consent for the post-mortem utilization of organs, tissues and cells for Investigation at University, as it is required by the Mexican statute (Ley General de Salud, Titulo Decimo Quarto, Capitulo II, Articulo 321, Articulo 322). We should mention that most of the brains in the present study were obtained of patients of humble social origin and consequently the medication received was very limited or nil.Patients were admitted to the public hospital when their health was already seriously compromised and moreover most did not receive any long-term drug treatment for their pathologies andtheir complications. With the exception of three diabetic patients, from whom we don't know how long they suffered type-2 diabetes, the rest of the individuals were diagnosed and affected by the diabetic disease for at least 10 years. The causes of death of the persons included in both the diabetic and control groups are mostly acute renal failure and severe infections, with some cases of respiratory

51

insufficiency, gastrointestinal hemorrhages and myocardial infarction. Diabetic and control individuals were affectedby similar complications elicited by a series of chronic pathologies, such as Cardiovascular, renal and hepatic dysfunctions, sometimes associated with pneumonia or cancer.

Tissue Processing and Immunohistochemistry

Brains were removed during routine autopsy always within 8–12 hours after the death. Brains were fixed by immersion in phosphate buffer (0.01M, ph7.2) 4% Paraformaldehyde (Sigma-Aldrich Corp., St. Luis, MO, USA) for two weeks. Dissected

hypothalami and brainstems were stored in 4% paraformaldehyde for additional 30 days and then transferred to 30% sucrose- 0.04% NaN3 in Phosphate Buffer Saline (PBS, 0.01M, ph7.6) at 4°C until sectioning. At 22°C the medio-basal hypothalamus and the caudal brainstem were cut in slices of 50 mm such to obtain alternate sections of the ARC and the NTS. Sections were collected in 6 series and then stored in 30% sucrose- 0.04% NaN3in PBS for immunohistochemical procedures.

For each antibody, one series of 10 sections was used for immunohistochemical analysis, each section 300 mm apart, thus covering an area of 3 mm of the hypothalamus including the ARC or the Dorsal-Vagus complex (Figure 1). Sections of controls and diabetic brains were always incubated together in order to avoid differences in staining intensities. Sections were incubated with either NPY, α-MSH or VGF antibodies. For this, a rabbit anti-NPY 1:4000 (see for details on antibody specificity [*Buijs et al, 1989*]) and a sheep anti-α-MSH, 1:5000 (Chemicon International, Millipore Corporation, Billerica, MA, USA) were used. A rabbit antibody was raised against the human VGF C-terminal sequence VGF609-615, 1:10000. [*Brancia et al, 2005*]. A series of sections from the brainstem was incubated also with a Tyrosine Hydroxylase (TH), 1:4000 (Millipore Corporation, Billerica, MA, USA) antibody. Dilution series of all antibodies were made and the optimal dilution wasselected in such a way that never a saturation of the staining was obtained.Antibodies were diluted 0.01M Tris Buffered

Saline (TBS), added with Triton X-100 0.5% (Sigma-Aldrich Corp., St. Luis, MO, USA) and gelatin 0.25% (Merck KGaA, Darmstadt, Germany), at room temperature for 1h and then transferred at 4°C for 48h. After rinsing, sections were incubated in biotinylated donkey-second antibodies,1:400 (Jackson Immuno research, West Grove, PO, USA) for 1.5 h, and then after extensive rinsing in PBS in avidin-biotin complex, 1:500 (Vector Elite, Burlingame, CA, USA) for further 1.5h. The final reaction was performed with a solution of 3,3′-diaminobenzidine 0.25% and H_2O_2 0.01% (both Sigma-Aldrich Corp., St. Luis, MO, USA) in TBS, for 10′. Sections were mounted on gelatinized slides, dried and cover slipped with Entellan embedding agent (Merck KGaA, Darmstadt, Germany).

Staining Quantification

To quantify the immunoreactivity, 10 sections of the ARC and 10 sections of the NTS were photographed at 40X and 63X magnifications respectively and analyzed unilaterally for each neuropeptide. Digital pictures were taken using an Axioplan (Zeiss, Jena, Germany) microscope equipped with a digital color photo camera (Olympus DP25, Olympus, Japan). In order of identify the nuclei of interest the several bibliographic sources [*Pearson et al, 1983; Swaab DF, 2003; Kitahama et al, 2009*] were consulted and the areas delineated accordingly (Figure 2.1). The total optical density in cells and fibers as well as the total number of positive cells for each neuropeptide were counted with the program ImageJ. Data are represented as mean 6 standard error of the mean (S.E.M.), analyzed with a one-way ANOVA analysis results were considered statistically different when they deviated from each other with a $p < 0.05$.

Fluorescent Immunohistochemistry

To investigate the co-localization of VGF with NPY and α-MSH, sections of the ARC and the NTS from at least three controls and three form the diabetic group were incubated for 48 h with rabbit anti-VGF antibody with either sheep anti-NPY or sheep anti-α-MSH (from Santa Cruz Biotechnology,

Santa Cruz, CA, USA and Chemicon International, Millipore Corporation, Billerica, MA, USA, respectively). Sections from the brainstem of both groups were also incubated with rabbit anti-TH and sheep anti-NPY. Sections were then incubated with a mix of donkey anti-rabbit and donkey anti-sheep antibodies conjugated with fluorescent dyes (Cy3TM- anc Cy2TM-conjugated, respectively), allprovided by Jackson Immunoresearch, West Grove, PO, USA. At the end of the reaction, sections were processed with 10% solution of Sudan Black (Sigma-Aldrich Corp., St. Luis, MO, USA) in ethanol, for 109, to prevent autofluorescence. Finally, sections weremounted on gelatinized slides, cover slipped with 30% glycerol in PBS and analyzed with the LSM 5 Pascal confocal microscope (Zeiss, Jena, Germany).

RESULTS

Ante Mortem Data

Unfortunately little or no ante mortem data such as glucose levels were available; for a part because 6 controls and one diabetic died from cardiovascular problems before they could reach the hospital. At the other hand blood glucose levels at admission were of special interest because they were less influenced by medication. In the controls glucose levels were in the range of 76–145 mg/dl with a mean of 100 mg/dl. The diabetics showed much more variation 72–1058 mg/dl with a mean of 228.1 mg/dl of which the low values were obtained after treatment with oral hypoglycemic drugs before hospitalization. Because of the missing values no statistical analysis could be done. Unfortunately also no data on body weight were available since such measurement is not routinely performed during hospitalization in this hospital.

NPY, α-MSH and VGF in ARC and NTS of the Human Brain

The expression of NPY and POMC mRNAs, as well as the presence of NPY, a-MSH and TH peptides, in the human brain has been extensively described, and our results essentially concur with

these descriptions [*Pelletier et al, 1984; Ciofi et al, 1990; Dudás, 2000; Goldstone et al, 2002*]. NPY cellular elements can be encountered throughout the whole diencephalon, but the ARC is one of the areas with the highest number of NPY-expressing neurons. In the ARC of both diabetic and non-diabetic patients, NPY positive neurons were scattered in the whole area of the nucleus (Figure 2.2-A). The distribution of NPY and TH neurons in the medulla oblongata also corresponds to what previously has been reported for the human brain [*Halliday et al, 1988(a); Halliday et al, 1988(b); Pilcher et al, 1988; Swaab DF, 2003; Van den Hoek et al, 2004*]. In the brainstem, the majority of NPY and TH immuno reactive cells are found in the NTS and the ventro lateral medulla, whereby NPY is often co-expressed in catecholaminergic neurons (Figures 2.3, 2.4, 2.5, 2.6, and 2.7). In the hypothalamus, POMC expression has been reported to be restricted to the medio-lateral ARC [*Desy & Pelletier, 1978; Pilcher et al, 1988; Sukhov et al, 1995*].

However, our results indicate that a-MSH neurons, in addition to the ARC, are also present in the human ventromedial hypothalamus and in the adjacent ventro lateral area (Figure 2.8). α-MSH, immunoreactivity was hardly detectable in the NTS ofboth diabetic and control groups. Indeed, no references about POMC expression in human brainstem are available in literature. In humans, VGF mRNA has been observed in neural and endocrine cells [*Ferri et al, 2011*]. We observed VGF-containing neurons in both ARC and NTS, as well as in the catecholaminergic areas of the brainstem (Figure 2.2-B, 2.5, 2.9). In our present study following the NPY, a-MSH and VGF immunohistochemical procedure, we have never seen any indication for a staining in glial cells, and as is also clear from the figures, only cells clearly identifiable as neurons were stained.

NPY and VGF Show Higher Immunoreactivity in the ARC of type-2 Diabetic Subjects

The ARC of diabetic patients displayed a significant increase in the number and intensity of immunoreactive NPY cells as well as in the total NPY optical density (cells and fibers) ($p < 0.03$ and

p<0.02, respectively) and for VGF (p<0.003 for both parameters),when compared with non-diabetic controls (Figure 2.2, 2.10). For a-MSH, in contrast, no-significant changes were found. Both diabetics and non-diabetics showed a large variation in the number of positive cells (p =0.430589), as well as in the opticaldensity (p =0.412148) (Figure 2.8, 2.10-A).

As can be seen in figure 2 in the hypothalamic target areas of the ARC also an increased staining for NPY can be observed reflecting the higher amount of peptide present in the fibers. In contrast to this increase in ARC staining is the observation in the NTS where a diminishment of NPY and VGF staining was observed. This result shows that the changes in NPY and VGF staining are not due to a general change in fixation or procedural artifact but is due to local peptide changes.

NPY and VGF Show Lower Immunoreactivity in the NTS of Type-2 Diabetic Subjects

The NTS of the diabetic group shows a reduction in both the number of immuno reactive cells and as well as in the optical density of NPY (p<0.005 and p<0.001, respectively) and VGF (p<0.005 and p<0.001, respectively) (Figure 2.3, 2.9, 2.10-B). Although there was a considerable variation of these two parameters in the diabetic group, the difference with the controls was highly significant. In contrast to NPY, TH showed a tendency to decrease in the NTS of diabetic individuals, but the difference with the controls did not reach significance (p =0.06 and p = 0.51 for the difference in cell number and optical density, respectively).(Figure 2.4, 2.10-B).

VGF co-localizes with NPY and a-MSH in the Human ARC

We examined the co-localization of VGF with both NPY and α-MSH in the human ARC and examined possible differences between controls and diabetics. VGF and NPY co-localize both in soma and fibers, especially in the medial (ventral and periventricular) zone of the nucleus (Figure 2.11). In the controls, VGF and α-MSH co-localize only sporadically in fibers and cell bodies within the ARC. However, in diabetics, (almost) all α-MSH neurons along the ventro-lateral portion of the nucleus also

contain VGF (Figure 2.12). VGF and α-MSH did not co-localize in the immunoreactive neurons clustered in the most ventro-lateral part of the ARC, neither in controls nor in diabetics.

NPY Co-localizes with VGF and TH in the Human Brainstem

The distribution of NPY, VGF and TH in the brainstem at the level of the dorso-vagal complex was quite similar: neurons and fibers stained for these neuropeptides were found not only within the NTS and the surrounding area, but also along the trajectory of the Vagus nerve and the A1/C1 area (Figure 2.5). Because the TH cells showed a tendency to be diminished in diabetic brains we investigated whether there could be a difference in co-localization of TH with VGF or NPY. In the NTS, NPY co-localizes with VGF and TH (Figure 2.6 and 2.13). NPY was found to be present in the majority of the TH cell bodies in the A1 area (Figure 2.7). No differences were observed in the co-localization pattern of NPY, VGF and TH in diabetic brain as compared to the control brain.

DISCUSSION

NPY Changes in the ARC, Related to Diabetes?

The increase in NPY immunoreactivity in the ARC of diabetic subjects is comparable to the increase of NPY under negative energy status as observed in rodent studies [*Menendez et al, 1990; White & Kershaw, 1990; Akabayashi et al, 1993; Van den Hoek et al, 2004*]. This suggests that in diabetic persons the NPY neurons react as if glucose levels are lower than normal. In rodents it has been shown that a variation in glucose and insulin signaling to NPY neurons of the ARC results in the generation of physiological responses that culminate in the regulation of hepatic glucose production and lipid metabolism via the autonomic system [*Desy & Pelletier, 1978; Marks & White, 1996; Van den Hoek, 2004; Pocai et al, 2005*]. Specifically, an increase in plasma glucose and insulin levels is followed by suppression of sympathetic activity to the liver resulting in lower glucose production [*Pocai et al, 2005*]. Type-2 diabetes patients, instead, display inappropriately high hepatic glucose

57

production, in spite of their hyperglycemic, hyperinsulinemic condition. This high hepatic glucose production is shown to be caused by increased sympathetic tone, which stimulates both glycogenolysis and gluconeogenesis [*Boden et al, 2001; Basu et al, 2004*]. All in all, the present data suggest that the ARC of diabetic patients perceives a negative metabolic state which may result in enhanced hepatic glucose production mediated by the sympathetic system.

Technical Considerations

Animal experimental studies have indicated the ARC as a major site for the control of metabolism and have suggested its importance for the development of diabetes. However one of the limitations of animal studies is the question whether these findings can be of relevance for human disease. The aim of the present study was to answer at least in part that question. However, also the present analysis of human brain material has several limitations that need to be taken into consideration for the interpretation of the data. First the conditions before and during death vary considerably and cannot be controlled as in animal experiments, in addition no information about body weight was available. Second, medication between the individuals, especially in the last phase of life may have varied enormously. Third, all measurements are done with immunohistochemical techniques and are therefore semi-quantitative and only reflect relative differences between the groups. Yet, in spite of all these differences and putative problems, the diabetic group reacted quite distinct with respect to staining intensity and number of NPY and VGF neurons in the ARC as well as in the NTS. Moreover, this is not due to a general change in NPY of VGF immunoreactivity or change in neuron number, as can be concluded from the fact that in the NTS the opposite changes were noted as compared to the ARC. Self-evidently more research will be needed to substantiate these findings but they indicate that indeed also in the human diabetic brain similar changes can be observed as in the diabetic rodent brain.

Brain-liver Interplay

In rodents, inactivation of the insulin receptor, specifically in the periventricular area of the ARC causes an increase of NPY expression of about 50% and, at the same time, produces insulin resistance in the liver and increased hepatic glucose production, even in presence of high levels of insulin in plasma [*Brüning et al, 2000; Obici et al, 2002*].According to the present data, the increase of NPY in the ARC in the human diabetic brain, suggests in addition to the peripheral insulin resistance as defined by the diabetic state, the presence hypothalamic insensivity to circulating insulin and/or glucose. At the other hand changes in leptin or other adipokines as occur in diabetes may also play a role in the observed *changes in the ARC.*

NPY in the NTS

In the NTS of diabetic patients, NPY was decreased indicating a different mechanism of regulation between brainstem and hypothalamus. A comparable observation was made by Goncharuket al, in 2007 [*Goncharuk et al, 2007*] who reported that CRH neurons are activated in the hypothalamus of hypertensive patients, but not inthe brainstem. The present observation suggests that in the NTS ofdiabetic subjects the proper inhibition of NPY neurons may take place by glucose and insulin suggesting that the gluco-sensing elements within the brainstem of diabetic subjects are functioning properly.

At the other hand our present results may indicate that the brainstem NPY neurons have a different role than those of the ARC. It seems logical to assume that both the NTS and ARC are able to sense and process the same information, i.e. glucose and insulin in the circulation, but will control glucose homeostasis using different mechanisms. Thus, the different NPY signaling as we observed in the NTS of diabetic patients might be the basis for a disruption in one of the multiple components of the homeostatic systems upstream of the NPY neurons.

The POMC System

The contribution of POMC neurons in the control of glucose homeostasis has been a matter of controversy since a long time[*Rossetti et al, 1997; Wang et al, 2004; Fioramonti et al, 2007; Könner et al, 2007; Lin et al, 2010*]. Thus the wide variation in α-MSH content observed in the ARC of both diabetic and control groups may be due to other factors, as mentioned in technical considerations above. These other effects may influence α-MSH synthesis, making it difficult to distinguish from the changes eventually triggered by hyperglycemiaand/or hyperinsulinemia. At the other hand the present observation may suggest that in the human brain the POMC neurons may be less important for the inhibition of glucose production than in the rodent.

VGF – Comparison with NPY and a-MSH

VGF, like NPY, is increased in the ARC of diabetic patients. This result agrees with the observation in mice that lack *vgf*, suggesting an anabolic role for VGF. VGF KO mice are lean and hyper-metabolic, show increased energy consumption, and are resistant to several forms of obesity, hyperglycemia and hyperinsulinemia [*Hahm et al, 1999; Watson et al, 2005*]. Animal studies, suggest that both NPY and VGF are upregulated by negative metabolic state and are in volvedin sympathetic control of hepatic glucose production [*Hahm et al, 1999*]. The present study also shows that the increase in VGF immunoreactivity coincides with an increase in NPY.

Remarkably, α-MSH neurons in the ARC of diabetic patients increase their VGF content. Also in animals, VGF has been shown to be present in α-MSH neurons [*Hahm et al, 2002*]. The increased colocalization of VGF and a-MSH indicate that, contrarily to whatα-MSH immunoreactivity suggests, at least a portion of the POMC neurons is affected in the diabetic group.

VGF in the NTS

For the first time, we report here not only the presence of VGF in the human brain but also that VGF and NPY are co-localized in a subset of neurons within the NTS. In addition, as in the ARC, both peptides follow a similar, though opposite pattern of immunoreactivity in the NTS.

The wide distribution of VGF in the brain, the large number of *vgf*-inducing factors, the complexity of the *vgf*-ko phenotype and the co-expression of *vgf* in neuronal populations with opposite effects on metabolism do not allow a conclusion about the involvement of VGF in diabetes. However, we demonstrated that VGF, just as in rodents, is also present in the human brain in neurons that control energy balance and react to metabolic changes similar as NPY.

CONCLUSIONS

In the present study we demonstrated that type-2 diabetic patients, in spite of the hyperglycemia that characterizes this pathology, show an increased NPY content in the ARC, suggesting that the diabetic brain sensed a negative metabolic state. In view of the fact that many features of the NPY cells in the human ARC and NTS show similarities to the rodent NPY cells in these areas, we would like to propose that the changed perception of the metabolic condition in the ARC of diabetic persons might be the basis for these changes in NPY neurons. Hence, increased NPY signaling to second order neurons that control the activity of the sympathetic system may contribute to the anomalous, unbalanced hepatic glucose production.

TABLE 2.1. Clinical-pathological details of control individuals

Matching Nr	Sex	Age	Cause of the death	Other clinical problems
1	M	55	Pneumonia	Multiple myeloma
2	M	58	Acute renal failure	Hypertension Renal insufficiency Prostatic carcinoma
3	M	41	Acute renal failure	Obesity Hypertension Nephrosclerosis Coronal and aortic atherosclerosis Hemorrhagic gastritis
4	M	59	Septic shock from perforated gastric ulcers and peritonitis	Hepatic cirrhosis Pulmonary emphysema Coronal atherosclerosis
5	M	76	Pneumonia	Prostatic hyperplasia Nephosclerosis Thrombosis at left femoral artery
6	M	60	Gastric hemorrhage	Alcoholic liver cirrhosis Hypertension
7	F	51	Pneumonia	Hypertension Renal insufficiency Unilateral nephoectomy
8	F	53	Metastasis from ovary cancer	Hysterectomy (2 years before)
9	F	41	Hypovolemic shock from gastric hemorrhage	Non-Hodgkin lymphoma
10	F	54	Acute renal failure	-
11	F	69	Pulmonary congestion	Hepatic cirrhosis Nephrosclerosis Coronal and aortic atherosclerosis Ovary cancer

TABLE 2.2. Clinical-pathological details of type-2 diabetic individuals

| Matching Nr	Sex	Age	Illness duration (years)	Cause of the death	Other clinical problems
1	M	57	22	Pneumonia	Hypertension Renal insufficiency
2	M	60	15	Cardiovascular failure post-surgery for the amputation of the left leg	Hypertension Nephrosclerosis Renal insufficiency
3	M	41	15	Acute renal failure	Hypertension Nephrosclerosis Coronal and aortic atherosclerosis Necrosis at right foot
4	M	65	12	Pulmonary Thromboebolism	Pulmonary tuberculosis Peritonitis Hypertension
5	M	72	10	Septic shock from perforated gastric ulcers	Liver insufficiency Chronic pneumonia from nicotinism Chronic alcohol abuse
6	M	66	20	Coma	Hypertension Atherosclerosis Nephrosclerosis Gangrene at left hand
7	F	45	23	Septic shock after pyelonephritis	Renal insufficiency
8	F	48	-	Myocardial infarction	Hypertension Coronal and aortic atherosclerosis Lymphoid spleen hyperplasia
9	F	45	45	Hypovolemic shock from gastric hemorrhage	Non-Hodgkin lymphoma
10	F	50	18	Respiratory failure	Thoracic lymphoma
11	F	72	-	Myocardial infarction	Aortic atherosclerosis Hypertension Pulmonary emphysemas Perforated gastric ulcers Hysterectomy
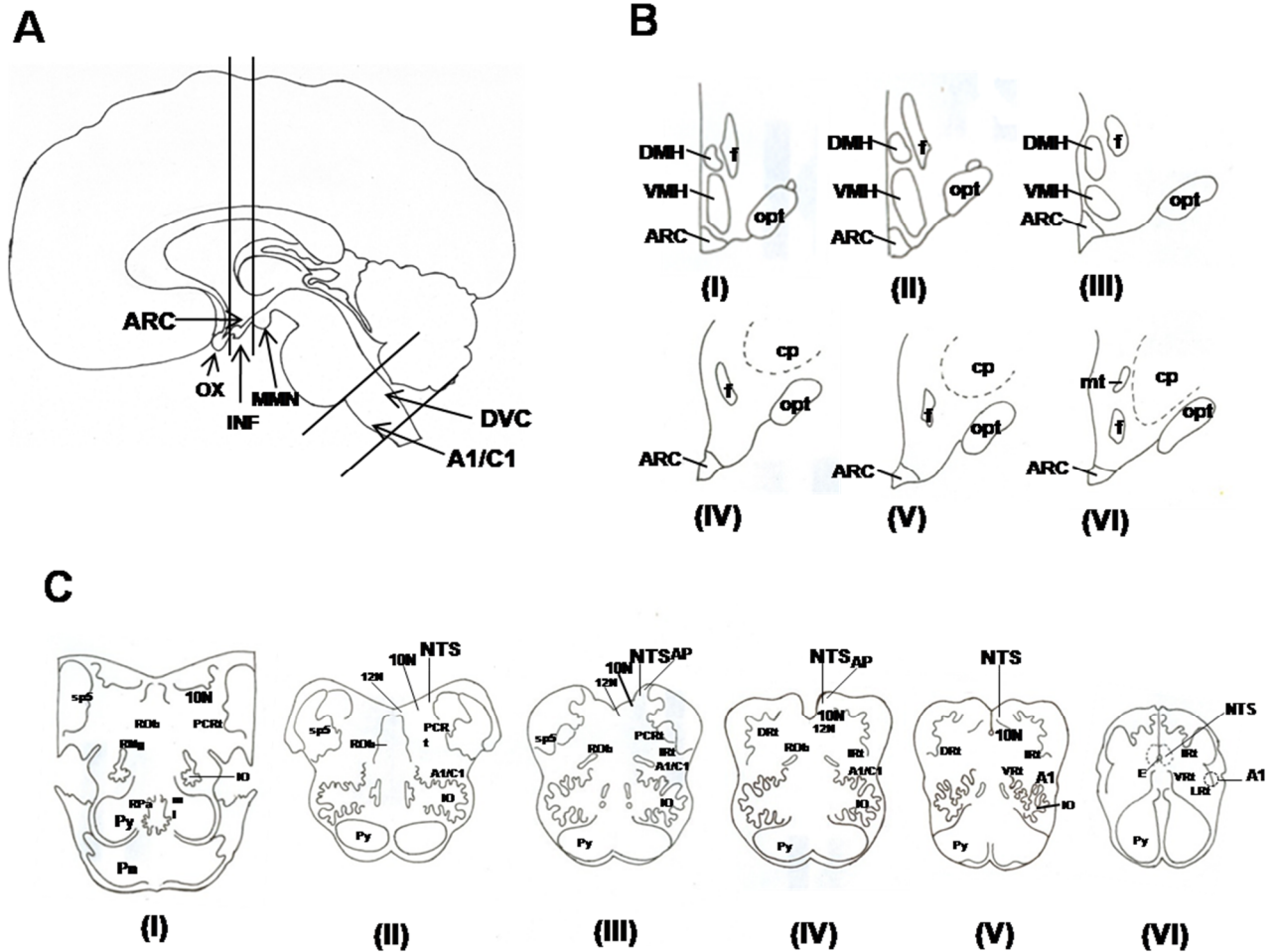
FIGURE 2.1: *Schematic illustration of the human brain*: a) sagittal view: areas included in the black lines were analyzed; b) semi-coronal illustration of the hypothalamus; c) coronal illustration of the medulla oblongata, all displayed in rostrocaudal order as indicated by the levels from I to VI (from Pearson *et* al, 1983; Kitahama *et al*, 2009; Swaab, 2003). The stained area of the ARC was identified by: 1) the third ventricle at the midline; 2) the external layer of the median eminence and the ventral hypothalamic border; 3) the ventromedial hypothalamus clearly visible as having no NPY fibers. In the brainstem, the NTS region was delimited by: 1) dorsomedially, the fourth ventricle; 2) ventrolaterally, by the vagus nerve; 3) non-immuno positive areas in the other bordering areas.

Abbreviations: 10N = Dorsal motor nucleus of the Vagus nerve; 12N = Hypoglossal nucleus; A1/C1 = Noradrenergic/adrenergic cell groups; AP = area postrema; ARC = Arcuate nucleus; cp = Cerebral peduncle; DMH = Dorsomedial hypothalamic nucleus; DRt = Dorsal reticular nucleus; DVC = Dorso-vagal complex; E = Sub-ependymal layer; f = fornix; Inf = Infundibulum; IO = Inferior Olive; IRt = Intermediate reticular nucleus; LRt = Lateral reticular nucleus; α-MSH = Melanocyte Stimulating Hormone α; MMN = Mammillary nucleus; ;ml = Medial lemniscus; mlf = Medial longitudinal fasciculus; mt = Mammillo-thalamic tract; NTS = Nucleus of the Tractus Solitarius; NPY = Neuropeptide Y; opt = Optic tract; och = Optic chiasm; PCRt = Parvocellular reticular nucleus; pn = Pontine nucleus; py = Pyramidal tract; RMg = raphe magnus nucleus; ROb = Raphe obscurus nucleus; RPa = Raphe pallidus nucleus; sp5 = Spino-thalamic tract; TH =Tyrosine Hydroxylase; VMH = Ventromedial hypothalamic nucleus; VRt = Ventral reticular nucleus.
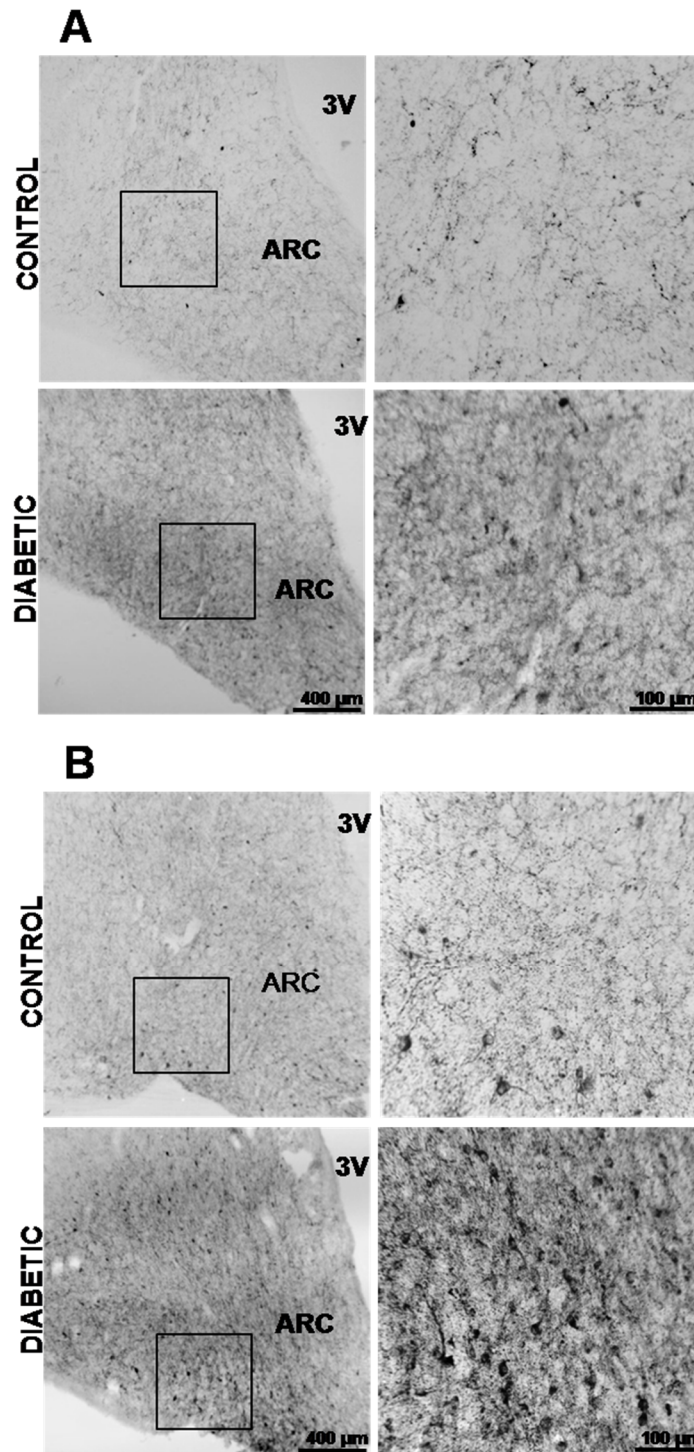
FIGURE 2.2: NPY and VGF immunoreactivityis upregulated in the diabetic ARC*.*
Panel A demonstrates NPY and **panel B** VGF immunoreactivity in the ARC of control and diabetic patients, at level II and III respectively. Boxed areas are reproduced at higher magnification in the right columns. Scale bar = 400 μm in the left columns; =100 μm in the right columns.
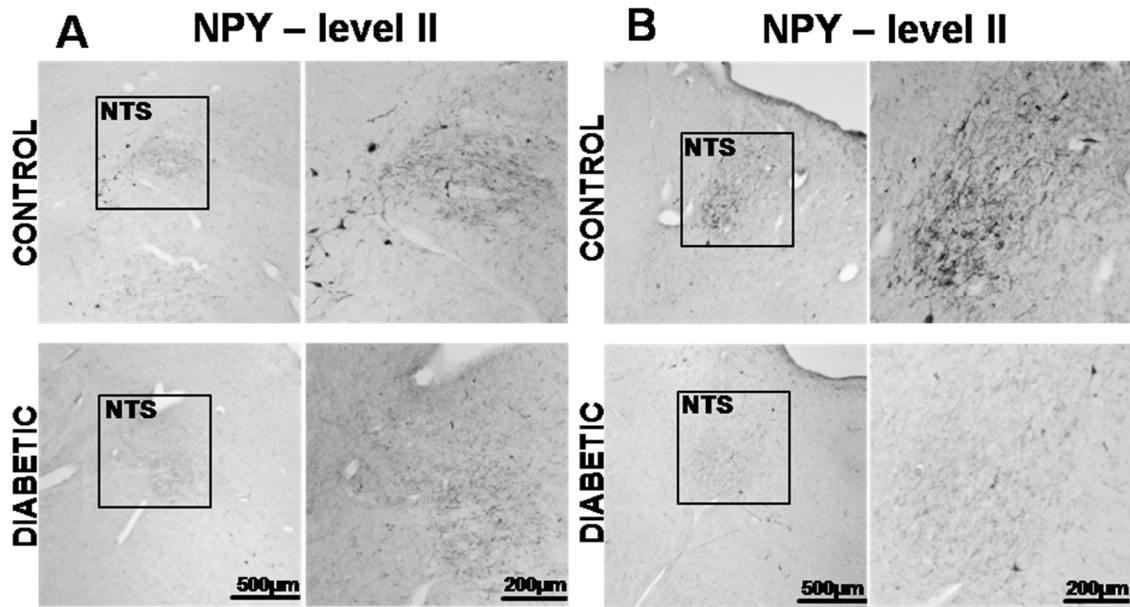
FIGURE 2.3: *Diabetic NTS shows a weakened NPY immunoreactivity in comparison to the control NTS.*
Panels A and **B** represent the levels II and III of the brainstem, respectively. Boxed areas are reproduced at higher magnification in the correspondent right columns of each panel. Note that these results are in contrast to what has been observed in the ARC. Scale bar=500µm in the left columns; =200µm in the right columns.
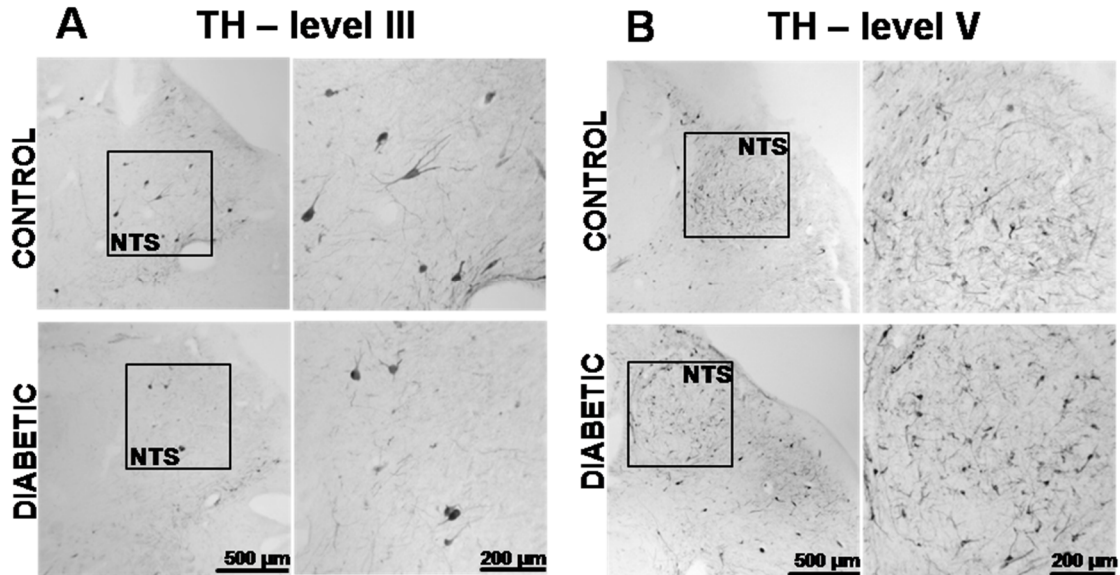

FIGURE 2.4: *TH immunoreactivity in the diabetic NTS displays a tendency to decrease, but it does not differ significantly from the control.*
The series of pictures represents the levels III and V. Boxed areas are reproduced in the right columns at higher magnification. Note that big-sized TH-neurons are present at higher levels of the NTS and the surrounding area, whereas smaller TH-positive cellas are scattered in the whole area of the most caudal NTS. Scale bar = 400µ in the column A; = 150µm in the column B.
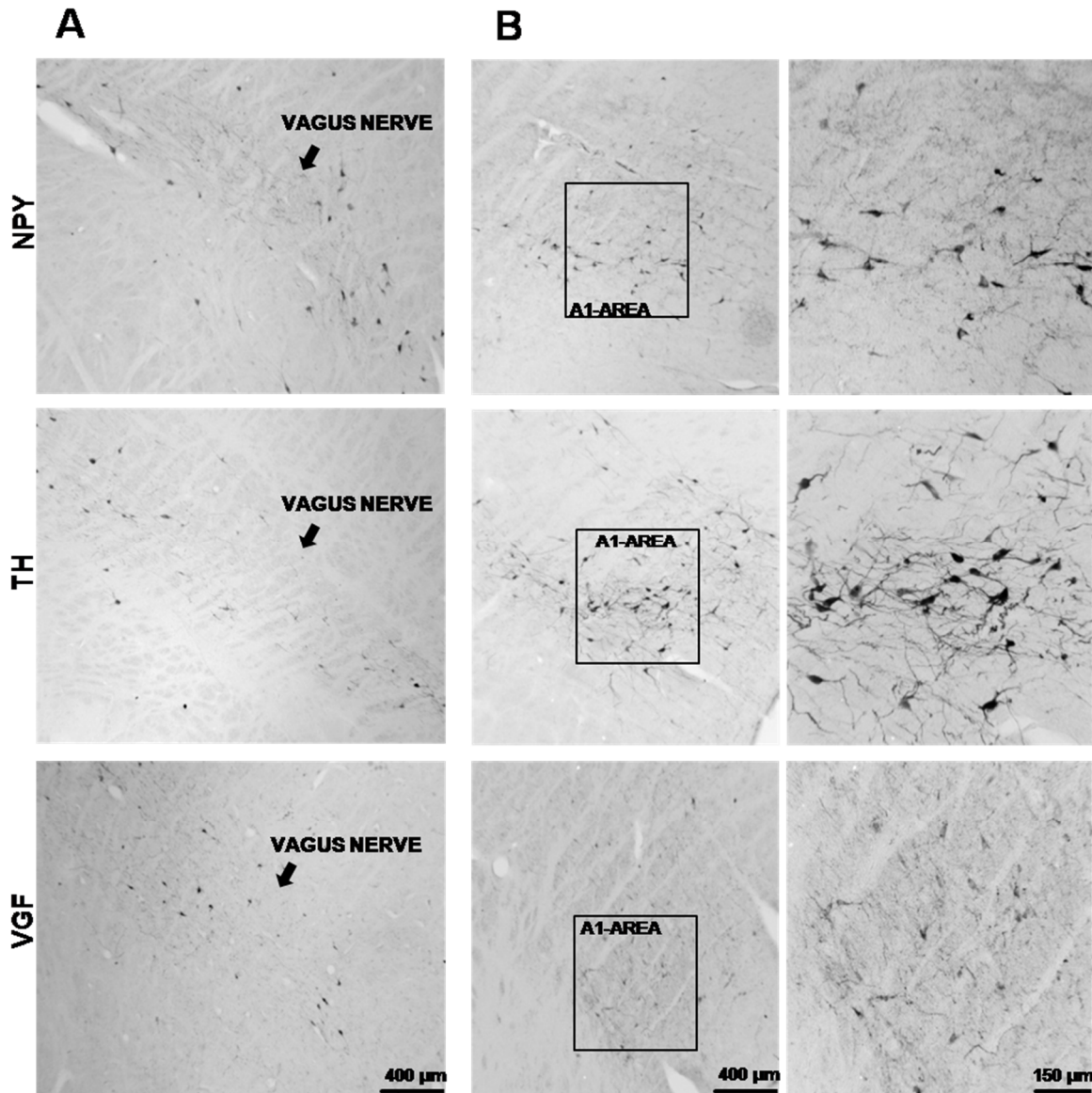
FIGURE 2.5: *NPY, TH and VGF immunostained neurons and fibers are observable along the pathway of the Vagus nerve and the A1/C1-area in the human medulla oblongata.*
Panel A: Vagus nerve; scale bar=400µm. **Panel B**: A-1 area, scale bar =400µm; **Panel B′**: higher magnification of the boxed areas in the left column of the panel B; scale bar = 150µm.
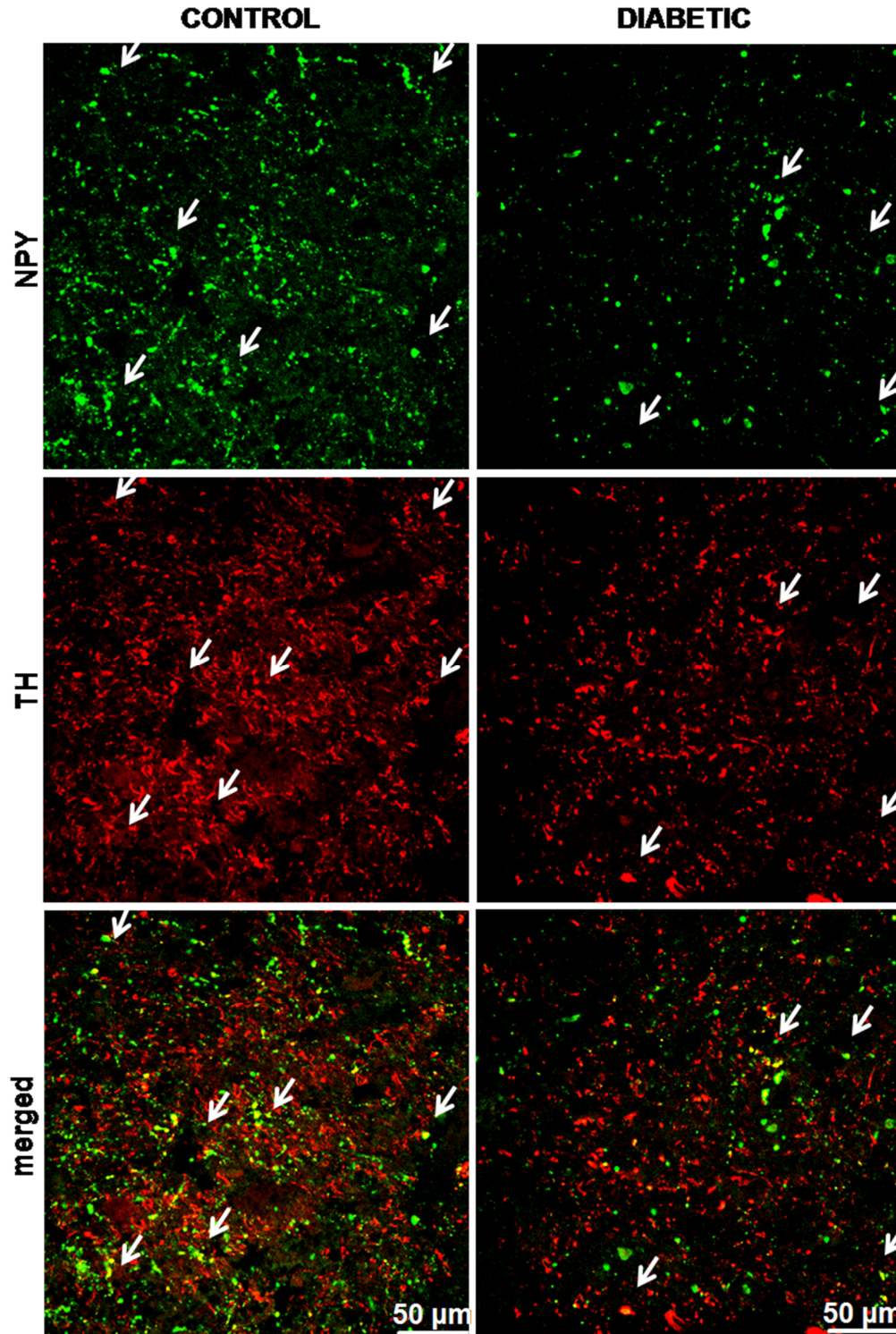
Figure 2.6: NPY and TH co-localizes in the human control and diabetic NTS.
Confocal image of the NTS at level III: NPY and Th are visualized in green-Cy2 and red-Cy3, respectively. The white arrows indicate yellow co-localizing cellular elements. The co-localization of NPY and TH was already reported in both rodent and human studies. Scale bar = 50µm.
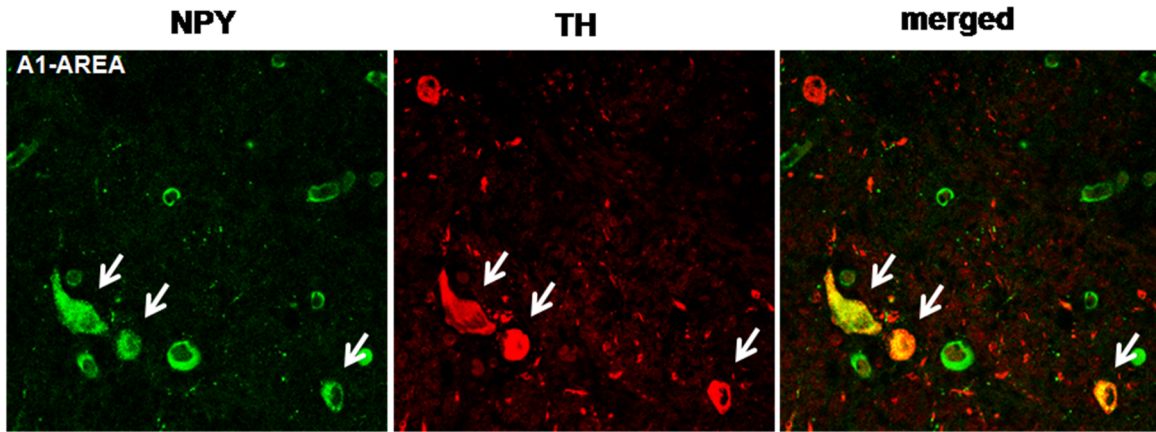
FIGURE 2.7: *NPY and TH co-localize in the human A1 area.*
Confocal image of the A1 area level IV: NPY and TH are visualized in green-Cy2 and red-Cy3, respectively. The white arrows indicate yellow co-localizing cell bodies. The main part of TH neurons within the catecholaminergic areas of the ventrolateral medulla is glucosensitive, and NPY expression in this A1/C1 cellular cluster   is essential for glucoprivation-induced food intake [*Ritter et al, 1981*]. Scale bar = 50μM.
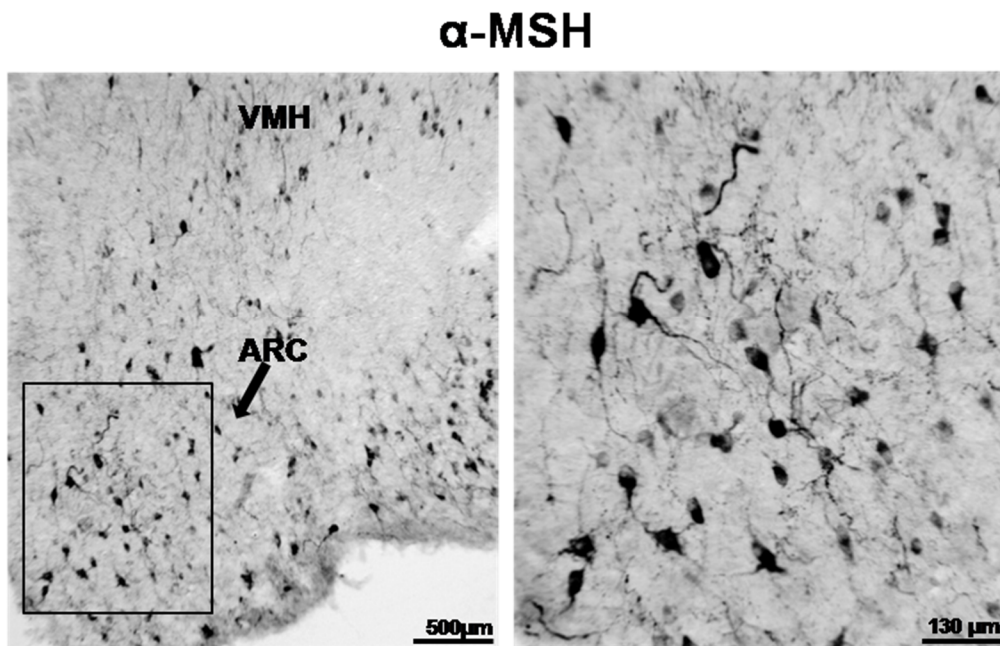
α-MSH

FIGURE 2.8: *α-MSH big-sized neurons are present in the medio-lateral portion of the ARC.*
Remarkably, α-MSH positive neurons are detectable also in the VMH and in a ventral area lateral to the ARC. Boxed area is reproduced right column. Scale bar = 500μm and 130μm respectively.
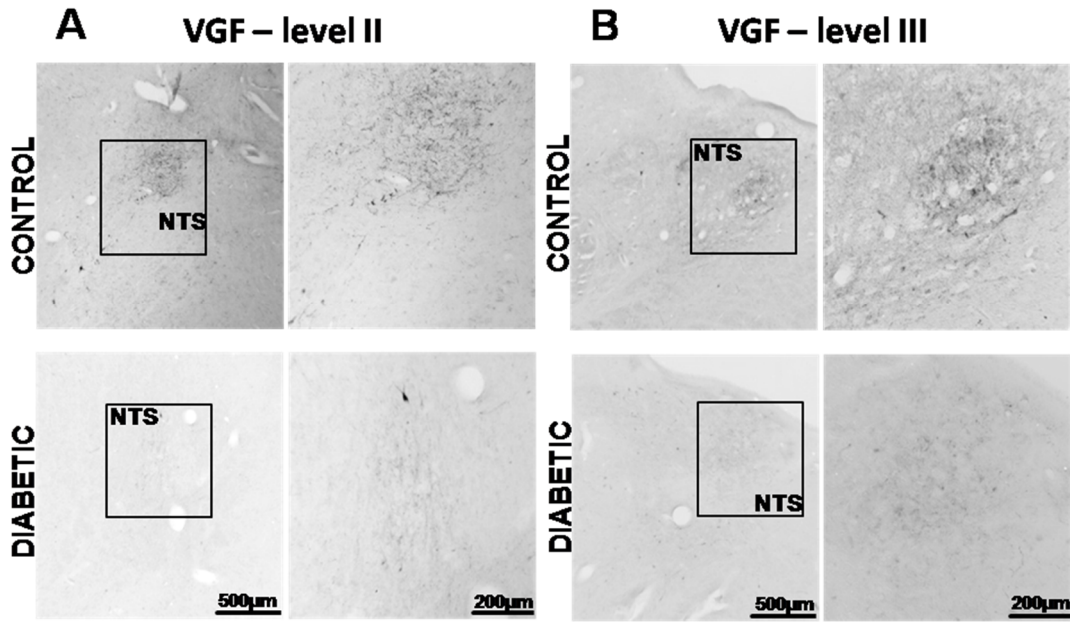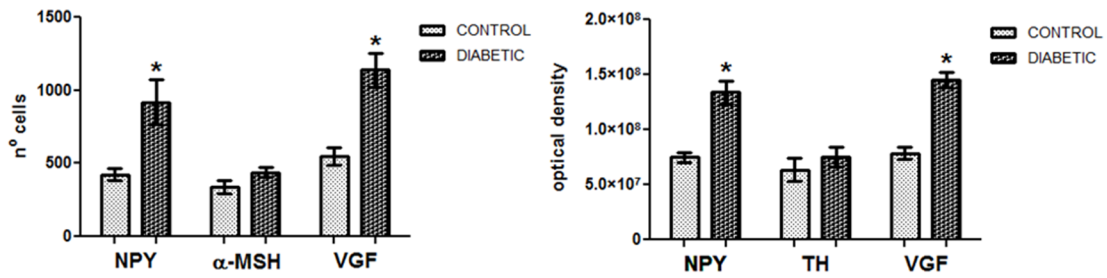
FIGURE 2.9: *VGF immunoreactivity in the diabetic and control NTS.*

Panels A and **B** represent the levels II and III of the brainstem, respectively. Boxed areas are reproduced at higher magnification in the correspondent right columns of each panel. Note that these results are similar to what has been reported for NPY in both the observed areas (see Figure 3). Scale bar=500µ in the left columns; =200µm in the right columns.
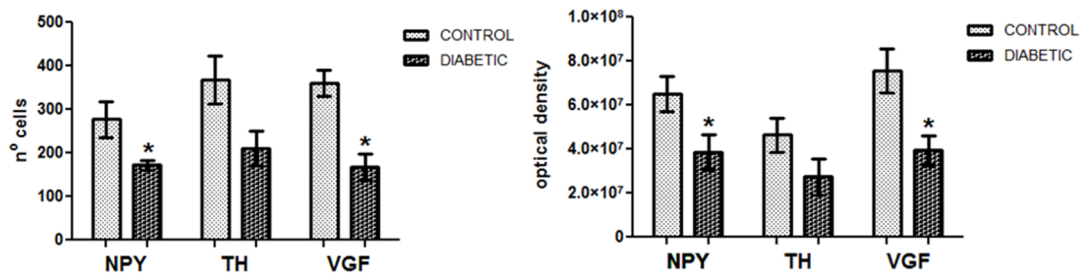
FIGURE 2.10: *Quantification of the immunohistochemical staining.*
ARC NPY and VGF increases in the diabetic ARC, but decreases in the diabetic NTS. **Panel A**: the number of cells (right) containing NPY and VGF and the optical density (left) are higher in the ARC of diabetic individual, whereas α-MSH does not show any significant difference. **Panel B**: NPY and VGF positive cells (right) and their optical density (left) are reduced in the diabetic NTS. Note that also TH quantity shows a clear tendency to decrease, although the difference between control and diabetic groups is not statistically significant.
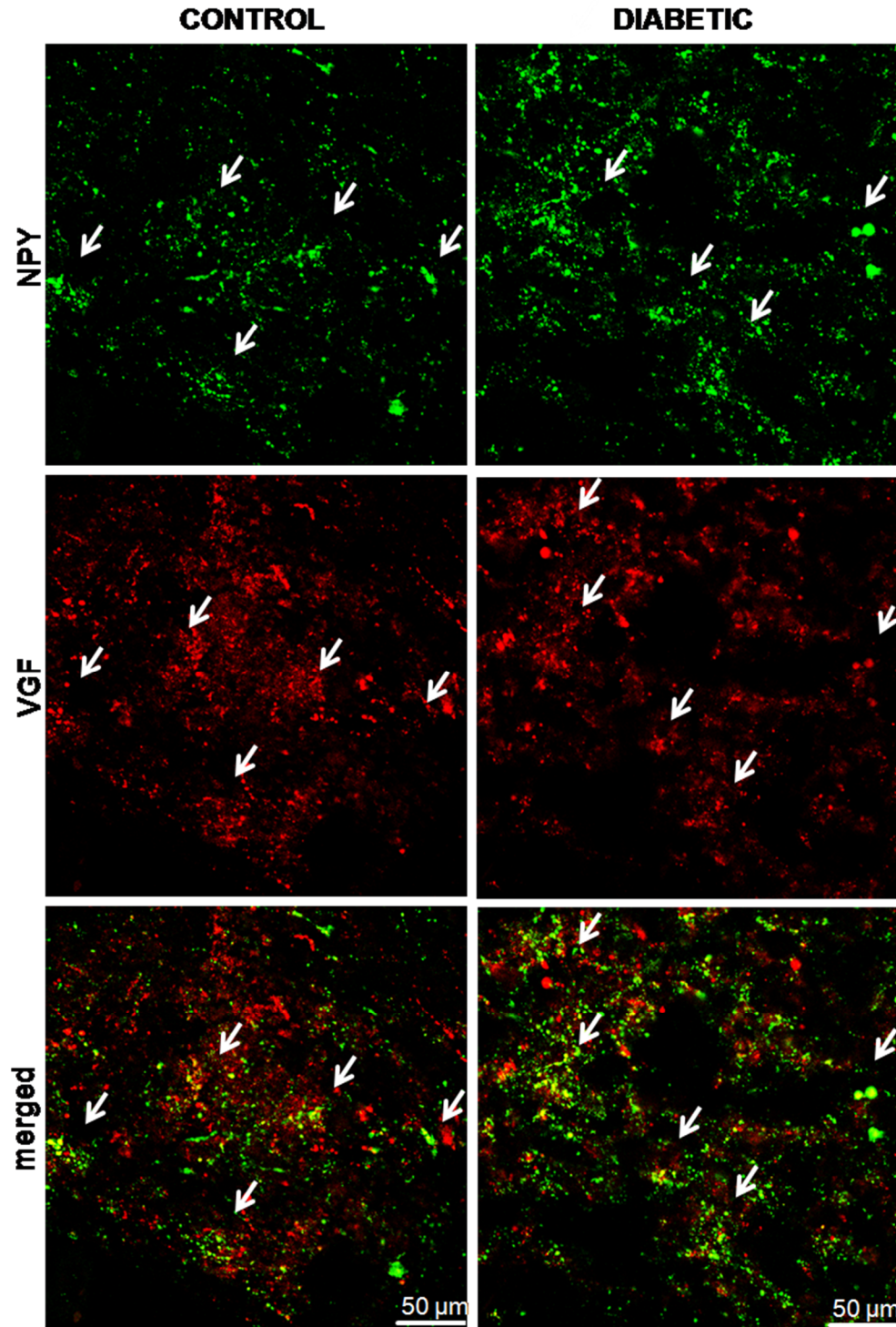
FIGURE 2.11: *NPY and VGF co-localizes in the human ARC of control and diabetic subjects.*
Confocal laser scanning image of the ventromedial ARC: NPY and VGF are visualized in green-Cy2 and red-Cy3, respectively. The white arrows indicate yellow co-localizing cellular elements. Scale bar = 50μm.
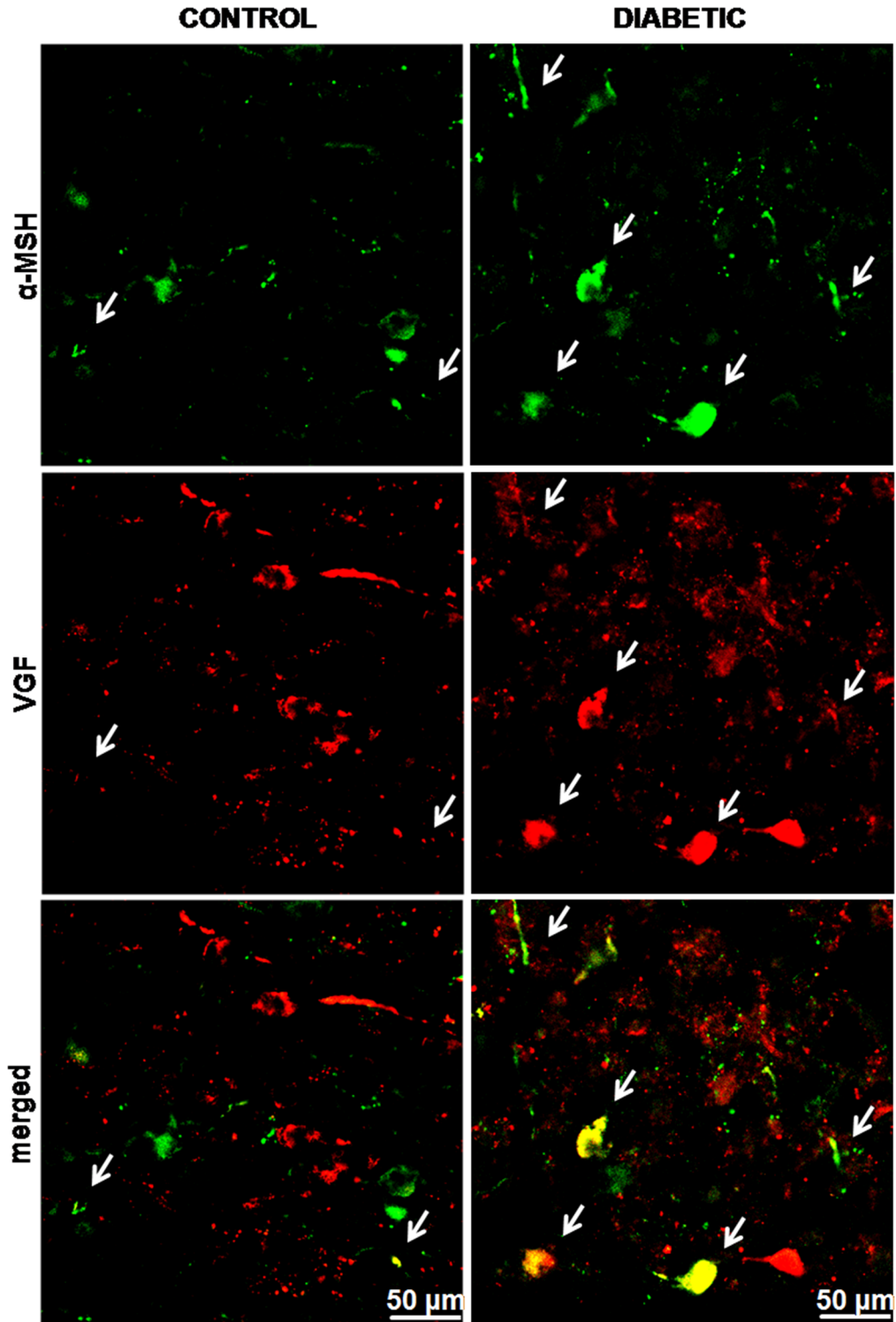
FIGURE 2.12: *α-MSH and VGF co-localizes in human non-diabetic and diabetic ARC.*
Confocal image of the ventrolateral ARC: α-MSH and VGF are visualized in green-Cy2 and red-Cy3, respectively. The white arrows indicate yellow co-localizing cellular elements. Note that co-localization is appreciably increased in the diabetic ARC. Scale bar = 50µm.

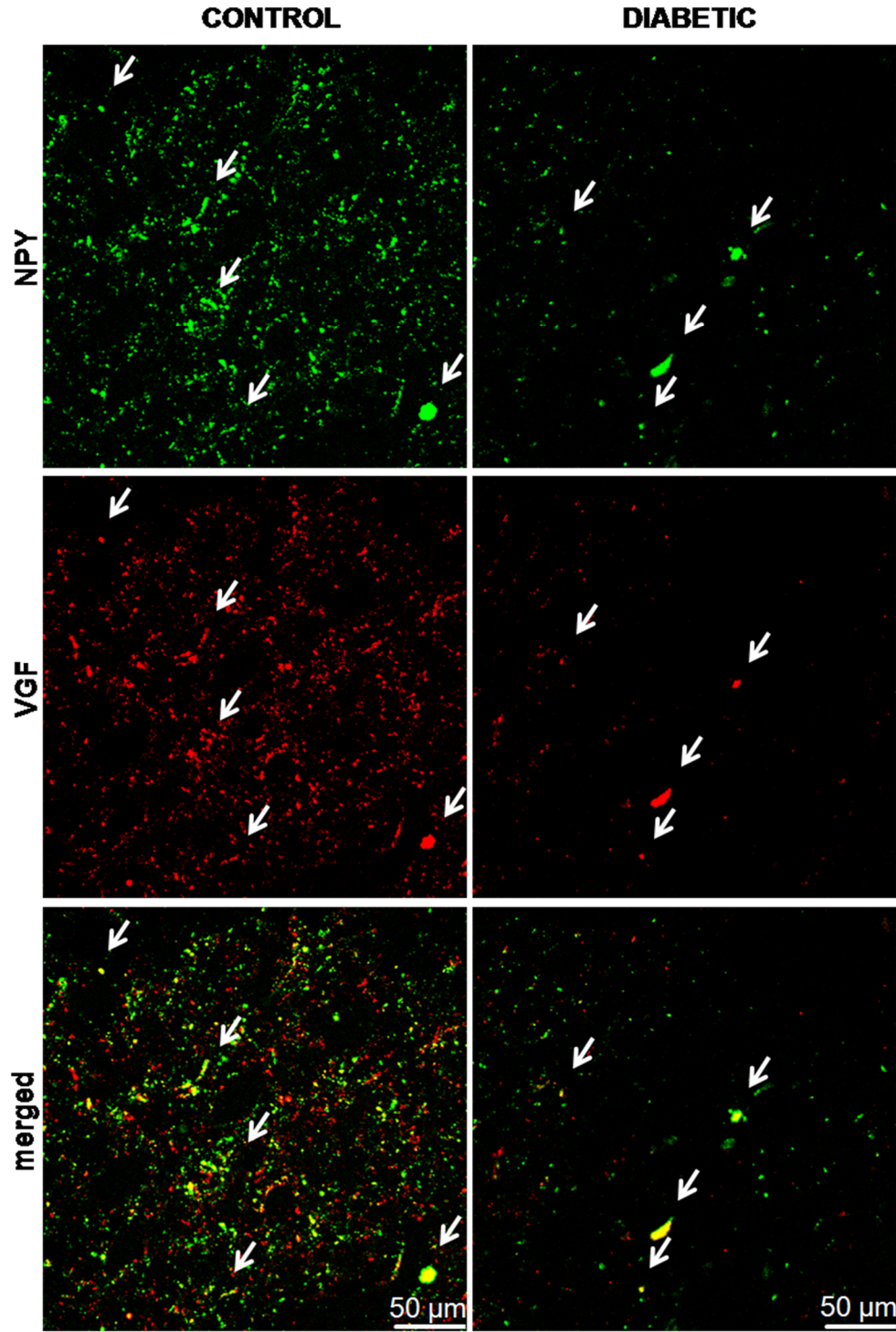**FIGURE 2.13:** *NPY and VGF co-localizes in the human NTS of control and diabetic subjects.*
Confocal image of the NTS at level III: NPY and VGF are visualized in green-Cy2 and red-Cy3, respectively. The white arrows indicate yellow co-localizing cellular elements. Note that diabetic NTS show the decrease in both NPY and VGF staining already observed with DAB-peroxyde staining (Figures 3 and 9). Scale bar = 50μm.

Chapter 3

A role for VGF in the hypothalamic Arcuate and Paraventricular nuclei in the control of energy homeostasis

INTRODUCTION

The Suprachiasmatic Nucleus (SCN) controls the phase of body physiology, mainly by imposing activity-resting cycles that are transmitted by time organized autonomic and hormonal changes [*Buijs & Kalsbeek, 2001; Dibner et al, 2010*]. Several studies indicated that in order to execute a correct temporal organization of these behavioral and physiological functions the SCN needs to integrate the physiological state of the body [*Hastings et al, 1997; Yannielli & Harrington, 2004*]. Several areas in the hypothalamus, forebrain and hindbrain up to the Raphe nuclei provide the SCN with "non-photic" information. Up till now very little is known about the functional meaning of this input, with exception of the input arising from the Intergeniculare Leaflet (IGL) Dorsal Raphe (DR) and Arcuate nucleus (ARC). While IGL and DR provide the SCN with information about activity [*Janik & Mrososvski, 1994, Kuroda et al, 1997*] the ARC is proposed to provide the SCN with metabolic information [*Yi et al, 2006*].

AIM & HYPOTHESIS

On the basis of previous studies that demonstrated that phase advances induced by time and caloric feeding restriction are appreciably decreased in IGL-lesioned rats (*Challet et al, 1996*) and NPY

projections from the ARC to the SCN, we aim to investigate whether either the ARC or the IGL may provide metabolic related information to the SCN. We hypothesize that NPY immunoreactivity might be increased in the SCN after food deprivation, and the ARC might contribute to this up-regulation.

MATERIALS & METHODS

Food availability experiments (immunohistochemistry)

Male Wistar rats, weighing 250-300g, were housed in a 12:12 light-dark cycle (light-on at 7:00 am) with free access to food and water, during one week previous to the beginning of the experimental procedures. Experiments were approved by the committee for ethical evaluation at the Universidad Nacional Autónoma de México, in strict accordance with the Mexican norms for animal handling, Norma Oficial Mexicana NOM-062-ZOO-1999.

The first day of the experiment, rats were randomly assigned to one of the following groups: 5 were fed *ad libitum* (CTR group); 5 were fasted for 48 hours (FST group) starting at ZT10; 5 were fasted for 48 hours starting at ZT7; then refed for 3 hours. All Animals were sacrificed at ZT10 of the third day of the experiment by intracardial perfusion with 4% paraformaldheyde (Sigma –Aldrich Corp., San Luis, MO, USA) in phosphate buffer (0.01M, ph7.6) preceded by deep anesthesia with an overdose of sodium pentobarbital (Sedalpharma, Pet's Pharma, Mexico; 50mg/kg). Brains were dissected, post-fixed by immersion in 4% paraformaldheyde for 24h and cryoprotected in Phosphate Buffer Saline (PBS, 0.01M, ph7.6) containing 30% sucrose and 0.04% NaN_3 until sectioning. The hypothalami were cut in sections of 40 µm, each third section was used for immunohistochemical procedures. Sections of the SCN and the IGL were incubated with either rabbit-NPY [*Buijs et al, 1989*] or rabbit-c-Fos (Calbiochem, EMD Biosciences, INC. La Jolla, CA, USA antibodies). NPY and c-Fos antibodies diluted in Triphosphate Buffer Saline (TBS, 0.01M, ph7.6) added with 0.5% Triton X-100 (Sigma –Aldrich) and 0.25 % gelatin (Merck KGaA, Damstadt, Germany) 1:4000 and 1:10000,

respectively. Sections were incubated at room temperature for 1h and then at 4°C overnight. After rinsing, sections were incubated in biotinylated donkey-antirabbit secondary antibody (Jackson Immunoresearch, West Grove, PO, USA; 1:400) for 1.5h and then in an avidin-biotin complex (Vector, Burlingame, CA, USA, 1:500) solution. The final reaction was performed with a solution of 0.025% 3,3'-diaminobenzidine (DAB) and 0.01% H_2O_2 100 (Sigma–Aldrich) in TBS, for 10 minutes. For c-Fos staining, 10% $NiNH_4SO_4$ was also added to this solution. Sections were mounted on gelatinized slides, dried, dehydrated with graded solutions of ethanol, soaked in xylene, and finally coverslipped in Entellan embedding agent (Merck).

Food availability experiments (in situ hybridization)

This study was carried out identical as in the previous protocol, 12 male Wistar rats were randomly divided in 3 groups: the control group was fed *ad libitum* for all the time of the experiments (CTR); the fasted group was food-deprived for 48h (FST); and the 3-hours re-fed group was fasted for 48h and then re-fed for 3 hours (3h-RF). Brains were dissected and postfixed in 4% paraformaldehyde in PBS for 12h at 4 °C, and this was followed by cryoprotection in 30% diethyl pyrocarbonate-treated sucrose in PBS at 4 °C. Brains were frozen and sectioned with a cryostat (16 µm). Sections were dried at room temperature for 2 h before overnight incubation at 65 °C in hybridization buffer [1 × diethyl pyrocarbonate-treated 'salts' (200 mm NaCl, 5 mm EDTA, 10 mm Tris, pH 7.5, 5 mm $NaH_2PO_4.2H_2O$, 5 mm Na_2HPO_4); 50% deionized formamide; 1 × Denhardts (RNase/DNase-free; Invitrogen Corporation, Carlsbad, CA, USA); 10% dextran sulphate (Sigma–Aldrich)] containing 400 ng/mL digoxigenin-labelled RNA probes purified in Sephadex G-50 columns. Sense and antisense probes were generated by linearization or excision of plasmids with appropriate enzymes, and purified using QIAquick PCR Purification Kit (QIAGEN Inc., Valencia, CA, USA). Primers were synthesized by Sigma: sense 5´-TATCCCTGCTCGTGTGTTTG-3´; antisense 5´-AGGCAGACTGGTTTCACAGG-

77

3′.The hybridization solution consisted of 50% formamide, 2 × sodium phosphate, sodium chloride and EDTA (SSPE), 1 µg/µl bovine serum albumin (BSA), 1 µg/µl poly A, 2 µg/µl tRNA in diethyl pyrocarbonate (DEPC)-treated water). Following hybridization, sections were washed three times in wash solution (50% formamide, 1 × saline citrate, 0.1% Tween-20) at 65 °C and twice at room temperature in 1 × MABT (20 mM maleic acid, 30 mMNaCl, 0.1% Tween-20) before being incubated in blocking solution [1% blocking reagent (Roche Applied Science, Burgess Hill, UK)] and then overnight in alkaline phosphatase-conjugated anti-digoxigenin antibody (1: 1500; Roche). BM purple AP substrate precipitating (Roche) with 1 mM Levamisole (Roche) was used for colorimetric detection at 37 °C for 8–20 h. Sections were mounted with Glycerol (Sigma).

Lesion studies

The IGL of a group of 8 rats was ablated by mean of a bilateral electrolytic lesion. Before surgery, animals were anesthetized with a mix of Ketamine (Anesket, PiSA, Mexico, 6mg/Kg) and Xylazine (Procin, PiSA, Mexico; 2mg/Kg), and placed in a standard stereotaxic apparatus with the tooth bar set at -3.5 mm. The electrode was placed bilateral at coordinates: 45mm caudal to the bregma, 52mm lateral from the midline and 52mm deep from the brain surface. After 2 weeks of recovery from the surgery (during which food intake, body weight and locomotor activity were monitored), animals were fasted and sacrificed as in the food availability experiments, and the sections processed to evaluate NPY immunoreactivity in the SCN.

A group of 10 newborn rats was lesioned in the ARC by subcutaneous injections of 5mg/ml monosodium glutamate (MSG; Sigma –Aldrich) administered during the first ten days of life. Considering the birth-day as Post-Natal day 0 (PN=0), pups were injected with MSG 2mg/Kg on PN-1 and on PN-3, and with MSG 4mg/Kg at PN-5, PN-7 and PN-9 postnatal days. Animals were then housed in colony rooms at standard conditions, together with 4 vehicle (saline) injected control rats.

After three months, animals were fasted for 48-h, sacrificed and SCN sections processed for NPY previously indicated.

Tracing studies

Projections to and from the IGL

The antero and retrograde tracer Cholera Toxin B (CTB) 0.5% conjugated either with the Alexa Fluor-555or Alexa-488 fluorescent dyes (Molecular Probes, Eugene, OR, USA), was injected 0.01ul in the IGL of 10 rats with a microsyringe. The surgery methods and the coordinates of the injections were the same as reported for the IGL lesion. After 10 days of recovery, animals were sacrificed and sections of the IGL and SCN were incubated with rabbit NPY antibody followed by a secondary fluorescent antibody conjugated with Cy-2™ (Jackson Immunoresearch, West Grove, PO, USA).4 brains, in which the tracer was co-localized with NPY in the SCN, were considered to have received a correct injection. These brains were used to determine the presence of retrograde labeled cell bodies in the ARC and NTS as two main areas receiving metabolic information.

IGL innervation from the ARC and the NTS

The anterograde tracer Phaseolus Vulgaris (PhaL) (Vector Elite) was unilaterally injected in the ARC of 15 rats by iontophoresis. The injections were performed using a glass micro electrode with a tip of 20um. Alternate current of 6.8µA was allowed to pass for 10 minutes. The stereotaxic coordinates for the ARC injection were: 3.3mm caudal from the bregma; 1.0mm lateral from the midline; 9.8mm deep from the surface of the brain, with an inclination of 4º degrees and the teeth bar set at -3.4mm. After a week from the surgery, animals were perfused and the brains processed as in the previous experiment. A first DAB/peroxyde immunohistochemisty with a rabbit anti-PhaL antibody (1:1000; Vector Elite) was performed to test the accuracy of the injection. 6 brains from PhaL–injected animals

were considered to display the correct injection and used to analyze the projection from the ARC to the IGL.

After anesthesia, rats were placed in a David Kopf stereotact with the head fixed at 45°. The dura and arachnoid membranes were dissected to expose the dorsal surface of the medulla at the level of the area postrema. The rat's head was placed such that the micropipette aligned perpendicular to the medulla oblongata.Injections into the Nucleus Tractus Solitarius were made with 0.05µl, 1% Cholera toxin B (CTB) using a glass micropipette with a 20- to 40-µm tip diameter. Because, in contrast to CtB, fluorophore-labeled CTB cannot be applied by iontophoresis, we used pressure injection (10 mbar, 5 sec). Thus, fluorophore-conjugated CTB (with Alexa Fluor 555, Molecular Probes); CTB will be used in the text as the abbreviation of CTB-Alexa Fluor 555 for convenience. After 10 days of recovery, animals were sacrificed and precision of the injection confirmed by mean of an epifluorescence microscope. 5 of CTB- injected animals had received a correct injection. In order to visualize projections from the area of the NTS, IGL sections from these brains were incubated with rabbit CTB (Sigma–Aldrich Corp) and the staining developed with 0.025% DAB, 0.01% H_2O_2 and 10% $NiNH_4SO_4$ in TBS. To enhance the intensity of the staining in fibers, before being immersed in the last solution, sections were treated with a solution of biotynilated tyramine for 1 h, followed by another hour of incubation with the avidin-biotin complex. Since NPY is a marker for the IGL, a sheep NPY (1:8000; Chemicon International) immunostaining was performed to help to localize CTB-containing projections to the IGL.

Histochemical analysis

Digital pictures of $DAB/H_2O_2/NiNH_4SO_4$ and NPY mRNA stained sections were taken by using an Axioplan microscope (Zeiss, Jena, Germany) equipped with a digital color photocamera (Olympus DP25, Olympus, Japan).

To quantify NPY and c-Fos, 8 sections from each brain were analyzed bilaterally, and the number of NPY and c-Fos positive cells and the optical density of the NPY in the SCN and the IGL were quantified with the program ImageJ.

Sections stained with fluorescent dyes were analyzed with the LSM 5 Pascal confocal microscope and the LSM software (Zeiss, Jena, Germany).

Quantitative data are expressed as mean +/- the standard error from the mean (SEM). Results were analyzed with a one-way ANOVA followed by a Tukey multiple comparisons post hoc test. P-values of <0.05 were considered statistically significant.

RESULTS

Effect of food deprivation and re-feeding on NPY in the IGL

In the IGL both NPY-IR, indicated by integrated optical density, and the number of NPY-positive cells were increased after a period of 48-h of fasting with respect to control animals (for optical density: $F_{(2,9)=}$ 57.11, p<0.001; for NPY cells: $F_{(2,9)=}$75.44, p<0.001) (Figure. 3.1-A and B). After refeeding, the NPY optical density returned to basal levels, whereas the number of NPY positive cells showed a significant decrease in comparison to both control ($F_{(1,6)}$ =7.82, p<0.05) and fasted ($F_{(1,6)}$ =22.08, p<0.05) groups. In addition, IGL NPY mRNA was up-regulated by food deprivation ($F_{(1,4)}$ =11.08, p<0.05), demonstrating an enhanced activity of NPY neurons in the IGL under anabolic conditions similar as occurs in the ARC (Figure3.2-A and B).

The number of c-Fos positive cells in the IGL was also significantly increased by fasting and 3h-refeeding ($F_{(2,9)}$ = 88.92., p<0.001 from the control) (Figure 3.3-A and B), however no c-Fos could be detected in IGL NPY neurons indicating that the increase of activity is in another set of IGL neurons (Figure 3.3-A).

81

Effect of food deprivation and re-feeding on the SCN

NPY positive fibers were strongly increased in the vl-SCN of fasted rats in comparison to controls, this increase disappeared after refeeding ($F_{(2,9)=}$ 6.97, p=0.01) (Figure 3.4-A and B).

In the SCN, c-Fos expression was not affected by fasting, but it was increased by re-feeding and by IGL lesion followed by fasting ($F_{(3,10)=}$ 73.03, p<0.001) (Figure 3.5). Importantly, changes in c-Fos activations were particularly appreciable in the vl-SCN, where c-Fos immunoreactivity was enhanced by re-feeding in intact animals and by fasting in IGL-lesioned animals ($F_{(3,10)=}$ 11.16, p= 0.001).

NPY in the SCN arises from the IGL

In order to determine the origin of the NPY increase in the SCN in fasting rats, either the IGL or the ARC were lesioned and animals were food-deprived for 48-h. The comparison of NPY-IR in lesioned and fasted rats showed that NPY virtually disappeared in the SCN after the IGL-lesion, while after ARC lesion the NPY increase after the period of fasting is not affected ($F_{(2,7)=}$ 44.53, p<0.001) (Figure 3.6-A and B).

The neuronal tracer CTB applied in the IGL to determine the nature of these projections, demonstrated that IGL-projection to the vl-SCN contain NPY and the intensity of the NPY staining was notably enhanced by fasting (Figure 3.7 and 3.8).

The Nucleus Gracilis and NTS project to the IGL

Injection of the anterograde tracer PhaL into the ARC did not result in any occasion (n=5) in labeling of fibers in the IGL while with the same successful ARC injections clear innervation of e.g. PVN, DMH and PVT was visible. Injections into the NTS, however, revealed clear innervation of the IGL area (Figure 3.9-A). The injections of the anterograde and retrograde tracer CTB into the IGL revealed dense innervation of the SCN (Figure 3.7) confirming the accuracy of the injections into the IGL area,

showed few cell bodies within the NTS whereas most of the IGL projecting neurons were found in the Nucleus Gracilis (Figure 3.9-B).

DISCUSSION

The present study demonstrates that the metabolic condition induces important changes in the NPY expression in the IGL, coinciding with similar changes of the NPY projections of the IGL to the SCN. These changes revealed that the IGL is involved in the transmission of metabolic information to the SCN. In fasted animals lesioning of the IGL resulted in a significant increase of c-Fos in the SCN as compared to intact fasted animals demonstrating the inhibitory influence of the IGL to the SCN in fasting conditions. This inhibitory input became also visible when the animal, after fasting, was refed because also then c-Fos was increased, revealing a removal of the inhibitory input by refeeding. Together these observations show that in addition to the increased inhibitory IGL input during fasting, this negative metabolic condition also results in an increase of excitatory input to the SCN via other pathways. Consequently the present observations show that at least part of the non-photic input to the SCN, arising from the IGL contains information about the metabolic condition.

NPY is one of the most widely expressed neuropeptides in the brain [*Adrian et al, 1983; Gehlert et al, 1987, Chromwall & Zukiwska, 2004*], the vast majority of the reports relates to the NPY involvement in energy homeostasis, whereas only a minor part is focused on NPY in relation with the synchronization of the SCN or on other functions [*Soscia & Harrington, 2005; Harrington et al, 2007; Kim & Harrington, 2008*]. The present paper brings these observations together in the sense that here evidence is presented that the IGL transmits metabolic information to the SCN. However this observation does not exclude that the same neurons are also involved in facilitating arousal [*Harrington ME, 1997, Allen & Morin, 2006*].After all, a stronger inhibition of neuronal activity of the

SCN during the day period would in theory result in an animal that is more prone to show behavioral activity since an active SCN promotes inactivity.

The IGL as a relay for metabolic information to the Suprachiasmatic Nucleus

In 2006 Yi et. al. showed that the AgRP neurons of the ARC, which co-express NPY, project to the SCN. These cells are activated by ghrelin, a hormone released by the stomach in time of fasting, demonstrating a neuronal signal to the SCN driven by endocrine input to the ARC [*Yi et al, 2006*]. Our present results show that, it is not the ARC but the IGL which is the main source of NPY innervation in the SCN suggesting that there are two modalities by which NPY neurons may inform the SCN about the metabolic status, one mediated by the ARC possibly by AGRP as neurotransmitter rather than by NPY and another one, anatomically dominant, via the IGL and both inhibitory under fasting conditions.

Since the IGL area is characterized by a dense net of vascular capillaries with a thin endothelium in contact with neuronal elements [*Moore & Card, 1994*], it has been proposed that a modified blood brain barrier exists in this area [*Harrington ME, 1997*]. Although it is well known that the permeability of the blood brain barrier is increased at very low glucose levels [*Oztaş et al, 1985; Gulturk 2010*], in literature there is no information that confirms that blood borne signals might have access to the IGL through the vascular endothelium. In addition our present results do not show any significant direct input to the IGL from the ARC or NTS, which are known to receive respectively endocrine or neural feedback from the periphery about satiety, energy supply and fat depot [*Schwartz et al, 2000*]. This warrants the question from where the IGL could receive its metabolic information. The IGL may receive metabolic information in a more indirect way via the Lateral Parabrachial Nucleus (PBN) in the midbrain [*Horowitz et al, 2004*] or from the Lateral Hypothalamus (LH) [*Mintz et al, 2001*]. Clearly both PBN and LH are excellent candidates for relaying indirectly metabolic information to the IGL

84

[*Norgren R. 1976, Saper & Loewy 1980, Wu et al, 2009, Wu & Palminter 2011, Wu et al, 2012*]. In addition the LH is also in reciprocal connection with the ARC, and neuropeptides expressed in these nuclei and controlling metabolism compete for the control of energy balance [*Gao& Horvath, 2007*]. Recently, Pekala *et al.* showed that LH projections excite a subpopulation of orexin-sensitive IGL neurons, which include IGL NPY cells [*Pekala et al, 2011*]. Thus, the PBN-LH-IGL axis appears to be a good candidate for the translation of the metabolic input arising from the NTS and ARC into an adaptive circadian response. The other possibility would be the direct projection from the NTS and from the nucleus Gracilis.

IGL receives projections from the Nucleus Gracilis

Instead of confirming the expected connection based on the anterograde tracing with the NTS, the retrograde tracing from the IGL showed unexpectedly also and in majority retrogradely labeled neurons in the Nucleus Gracilis. The Nucleus Gracilis receives ascending fibers from the sensory layers of the dorsal horn that relay mainly visceral pain and inflammatory information as well as non-noxious stimuli such as the distension of abdominal viscera, temperature and baroreception [*Newman PP, 1974; Simon & Schramm, 1984; Berkley & Hubscher, 1995; Al-Chaer 1996*]. In spite of this information the role of the Gracilis in integrating this wide range of the viscerosensory input, also together with proprioceptive and muscular information, remains elusive [*El-Chaer et al, 1997*]. The present study shows that neurons of the Nucleus Gracilis are projecting to the IGL, whether they indeed transmit visceral sensory information to the IGL remains to be determined.There are two studies that support the IGL sensitivity to somatosensory stimulation. First, electrical stimulation of the rat tail enhances the response of the Geniculate Complex to light input and increases serotoninergic innervation [*Davidowa & Albrecht, 1992*]. Second, binding sites for the sensory neuropeptide Calcitonin Gene Related Peptide (CGRP) are expressed in the Geniculate Complex

[*Skofitsch & Jacobowitz, 1985*]. It has been proposed that visceral information to the IGL might represent an arousal stimulus that participates to the modulation of circadian rhythms [*Davidowa & Albrecht, 1992*]. The present results indicate that the metabolic condition might be a participating signal in this pathway. The fact that injections into the NTS provide innervation to the IGL might not only be explained by the presence of a few retrogradely neurons in the NTS that project to the IGL but also by the fact that the needle tract for the injection passes through the Gracilis and thus the leakage of CTB into the Gracilis might be responsible for the observed fibers. Hence the necessity to always demonstrate the presence of projections by the confirmation of cell bodies in the same area that gives rise to the projection.

Is food deprivation a non-photic stimulus?

According to literature, a non-photic stimulus induces phase changes in SCN activity when applied during the subjective day [*Mrosovsky 1988, Reebs & Mrosovsky 1989, Mead 1992, Maywood 1999, Yokota 2000, Maywood & Mrosovsky 2002*] and interferes with the effects of light pulses given during the subjective night [*Mrosovski & Salmon, 1987, Ralph & Mrosovski 1992, Mistelberger & Antle 1998*]. The effect of non-photic stimulation during the subjective day is mediated by NPY projection from the IGL, as demonstrated by a number of lesion and pharmacological studies performed over 20 years [*Johnson et al, 1988; Janik & Mrosovski, 1994; Wickland & Turek, 1994; Biello et al, 1994; Weber & Rea, 1997; Lall & Biello, 2002; Harrington & Schak, 2000*]. NPY antagonizes the retinal glutamatergic transmission, provoking a situation of conflict with light [*Yannielli & Harrington 2001; Lall & Biello, 2003; Yannielli et al, 2004*], suggesting an inhibitory role for NPY in the vl-SCN. According to the present set of data, together with the effect of time-caloric restriction of SCN activity [*Challet et al, 1996*], our results suggest that fasting provides a non-photic input to the SCN via the IGL in which the increased NPY activity may provide an increased inhibitory input to the IGL.

Re-feeding increases c-Fos in both the IGL and SCN

Consistently with a decrease in NPY-IR in the vl-SCN, we found an increase of c-Fos expression in the same area in re-fed animals in comparison to control and fasted groups. This demonstrates that in addition to fasting also refeeding is an important signal for the SCN arising from the IGL. Consequently both fasting and feeding signals may contribute as non-photic signals the IGL message to the SCN. A significant augmentation of c-Fos activity also occurs in the IGL of the same rats, although it does not involve the NPY neurons. This suggests that another population of IGL neurons, different from NPY cells, receives information about satiety and inhibits NPY activity. Such intra-IGL inhibitory circuitry has been demonstrated by Glass *et al* in 2010. They showed that activation of the GABA IGL interneurons results in the suppression of NPY neuronal activity [*Glass et al, 2010*].

The sequence of events that we described resembles the physiological changes that take place in the SCN during and after the dark-light transition, when an active well-fed animal turns into his rest phase. In fact, following light onset, the decrease of NPY levels in the SCN is accompanied by a progressive increase in c-Fos activation [*Earnest et al, 1990; Schwartz et al, 1994*]. Thus under normal conditions these two mechanisms may support each other keeping the animal at rest. The present data show that fasting interferes with the normal NPY cycle in the SCN, by advancing and increasing the magnitude of the physiological NPY levels at ZT10. The relief from this inhibitory effect on the SCN caused by re-feeding triggers the activation response as indicated by the c-Fos expressing cells. In this sense, it is very important to stress that an IGL lesion, which eliminates NPY containing fibers from the SCN causes a significant increase in the c-Fos activation of the vl-SCN in fasting conditions. The fact that ad libitum animals do not show a change in c-Fos after fasting indicates that in addition to the inhibitory input from the IGL also an activating input from other areas nullify this inhibition. This only becomes visible after IGL lesions. This confirms that indeed NPY has

an inhibitory control on the vl-SCN resulting in an activation of the SCN after refeeding when the NPYergic tone is decreased.

CONCLUSIONS

Here we show that the activity of the IGL-SCN axis is importantly changed by the metabolic conditions, hereby NPY and GABA have a prominent role in transmitting metabolic information from the IGL to the SCN. Consequently the present results demonstrate that the SCN does not depend directly and only on the ARC and NTS to get information about the metabolic status, also the IGL can directly transmit metabolic information to the light receiving part of the SCN. This information about the metabolic condition to the SCN may serve to prepare the individual better for a possible activity in the rest phase under fasting conditions or may ensure a rest under fed conditions.
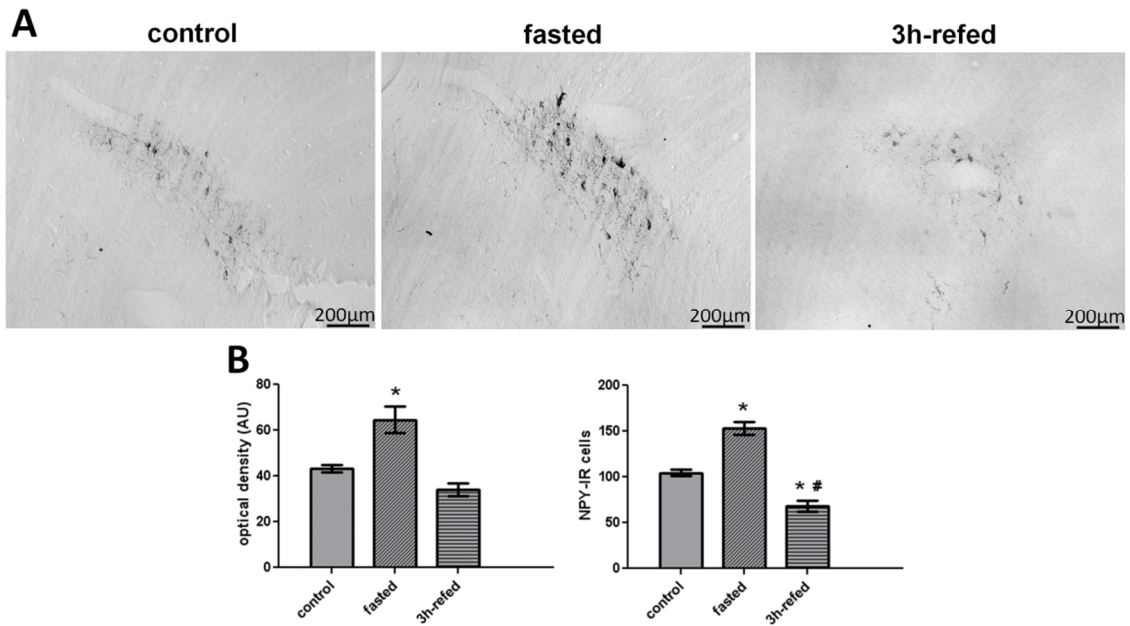
:

Figure 3.1: Comparison of NPY immunoreactivity (IR) in the IGL of free fed, fasted and refed rats.(A)
Photomicrographs of the IGL in the different conditions. Scale bar = 200 µm. **(B)** Quantification of NPY-IR as
integrate optical density (on the left) and number of positive cells.(on the right). Both optical density (p=0.04)
and number of NPY cells (p=0.035) are increased after 48h of fasting. The number of NPY positive cell is
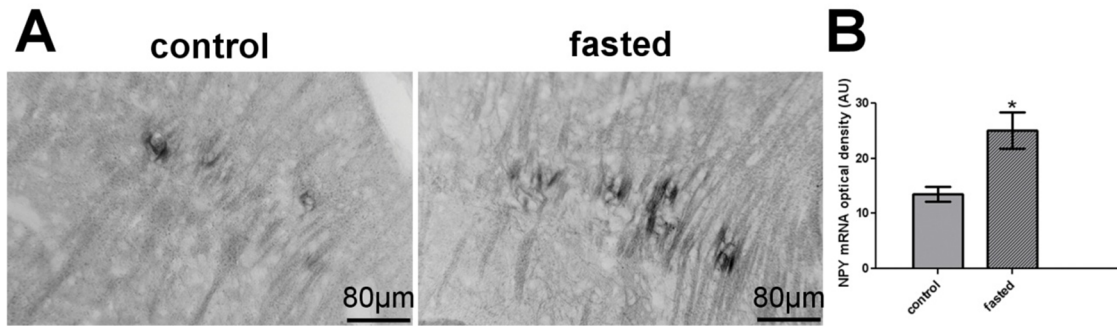significantly decreased by refeeding (p=0.046).

Figure 3.2: (A) Photomicrographs of the IGL of control and fasted rats (scale bar = 80 μm) and **(B) quantification of integrate optical density of NPY mRNA** showing that NPY expression is up-regulated by fasting (p=0.02).
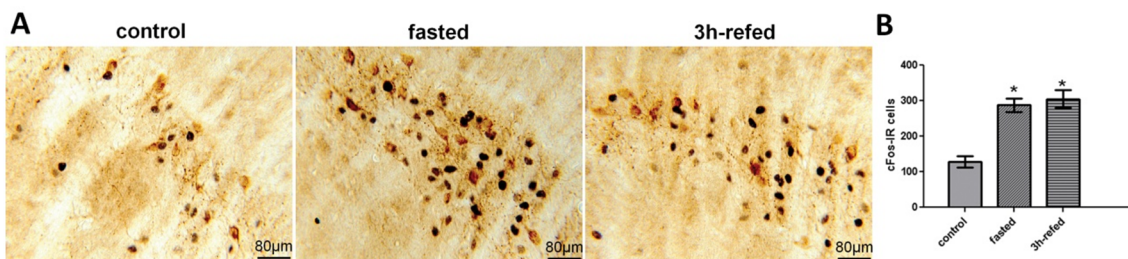

Figure 3.3: cFos (*black* nuclei), as NPY (*brown* cells), is increased in the IGL of fasted rats, as indicated by **(A)** photomicrographs of the IGL (scale bar = 80 μm) and **(B)** quantification of cFos-expressing cells (p=0.001).
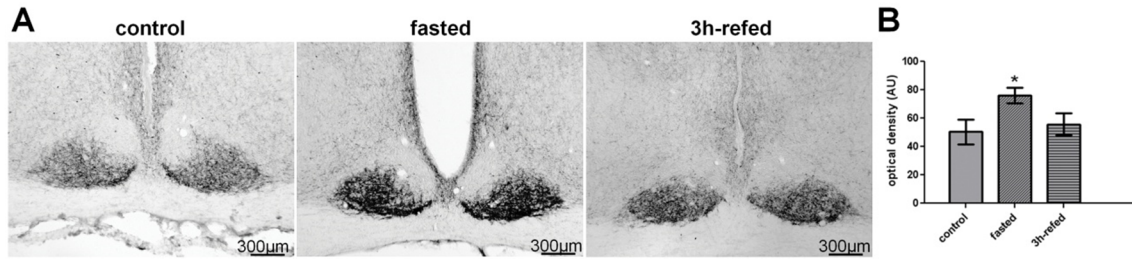
Figure 3.4: Comparison of NPY immunoreactivity (IR) in the SCN of free fed, fasted and refed rats. (A) Photomicrographs of the SCN in the different conditions. Scale bar = 300 µm. **(B)** Quantification of NPY-IR as integrate optical density showing that NPY-IR is increased after 48h of fasting (p=0.035).
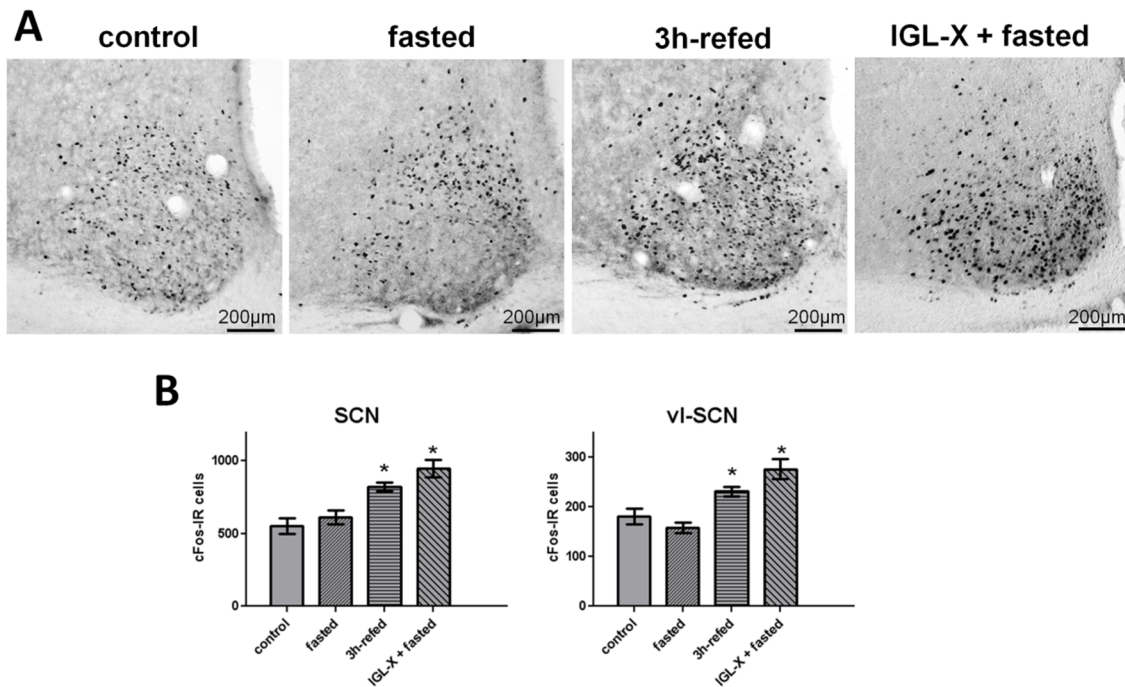

Figure 3.5: cFos activation in the SCN in response to food availability. (A) Photomicrographs of the SCN of free fed, fasted and refed rats. Scale bar = 200 µm. (B) Quantification of cFos-IR indicates that the number of positive cells is increased (p=0.026) by refeeding. Note that in the ventrolateral SCN (vl-SCN) cFos shows a slight tendency to decrease after a period of fasting and it is significantly increased by refeeding (p = 0.032).
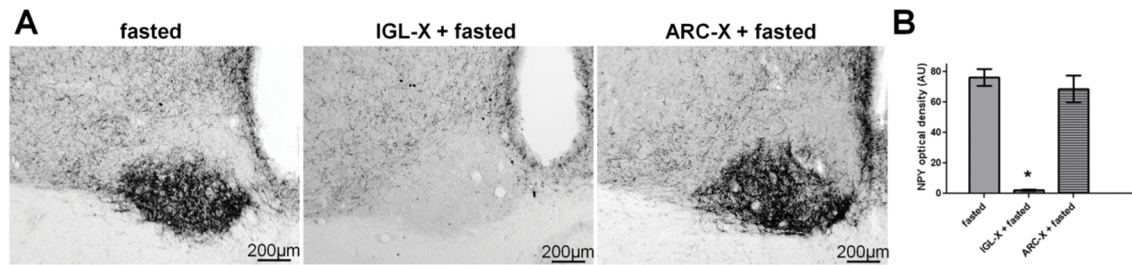
Figure 3.6: Effect of IGL and ARC lesion on fasting-induced NPY increase in the ventro-lateral SCN. **(A)** NPY-IR indicate that ablation of the IGL virtually eliminates NPY projections to the SCN, even after a period of fasting, whereas ARC lesion does not affect NPY response to food deprivation. Scale bar = 200 μm. **(B)** Quantification of NPY optical density showing the strong decrease of NPY-IR in fasted but IGL-lesioned rats (p= 0.0001).
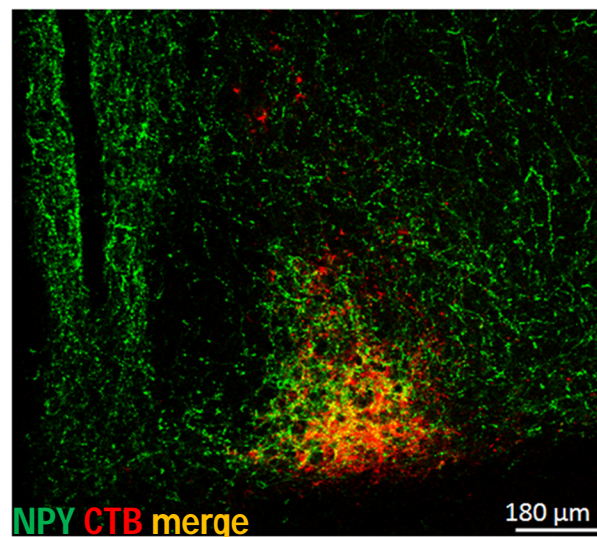

Figure 3.7: Confocal laser scanning image of CTB (*red*) containing IGL projections to the ventrolateral SCN, showing that they contain NPY (*green*). The co-localization between the tracer and NPY (*yellow*) attests the accuracy of CTB injection in the IGL. Scale bar = 200 μm.
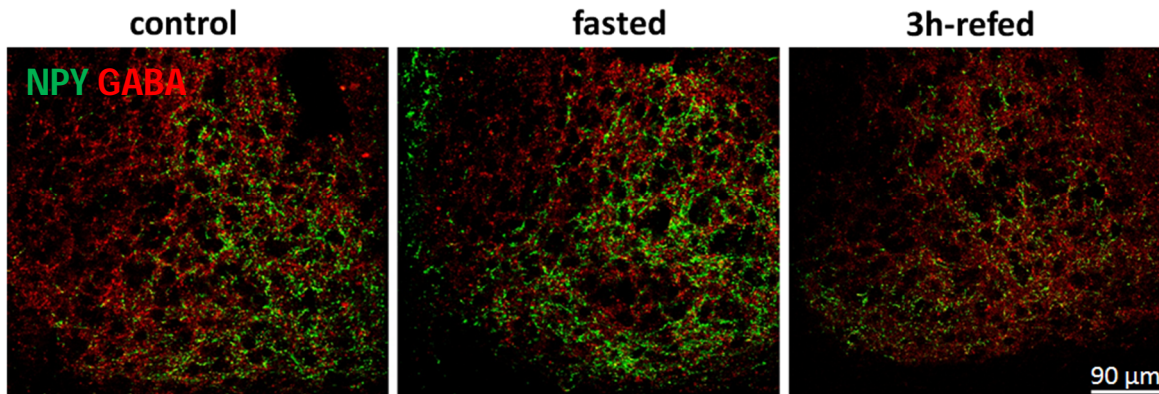
Figure 3.8: Confocal laser scanning image of SNC of control, fasted and refed animals, stained for NPY (*green*) and GAD-67 (GABA) (*red*), indicate that both NPY and GABA content in the ventrolateral SCN are affected by metabolic state. In particular, NPY is increased by fasting, whereas both NPY and GABA are decreased after re-feeding. Scale bar = 70 µm.
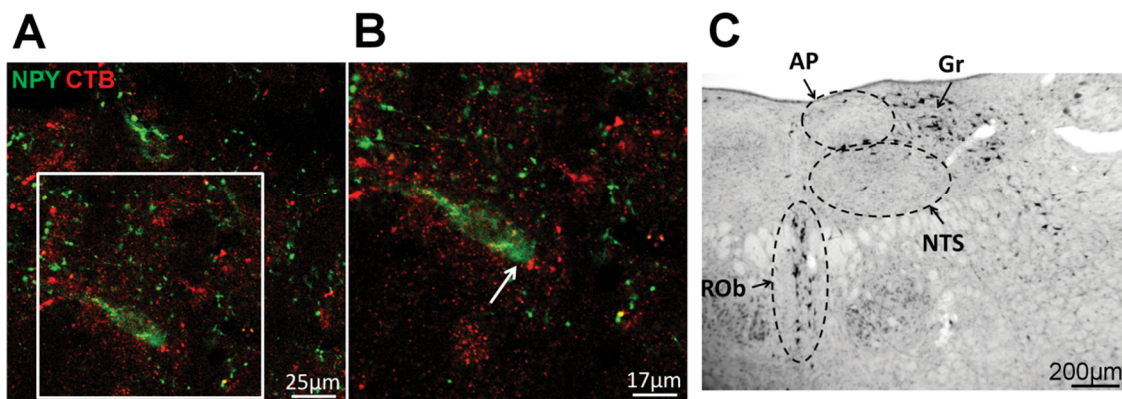
Figure 3.9: Morphological studies of the IGL-brainstem interconnections. (A) Anterograde tracing from the Dorsovagal Area showed CTB fibers (*red*) apposing on NPY neurons (*green*) of the IGL. Scale bar = 25 µm. **(B)** Reproduction at higher magnification of the area included in the white square of the panel A. Scale bar = 17 µm. **(C)** Retrograde tracing from the IGL showed high density of CTB – containing neurons in the Nucleus Gracilis (Gr) and in the Raphe Obscurus (ROb), instead of the expected Nucleus of the Tractus Solitarius (NTS) and Area Postrema (AP). Scale bar = 200 µm.

CONCLUDING REMARKS

In the past twenty years the ARC has been the subject of extensive investigations aimed to explore the initial step of the brain control of the body energy status, which is the sensing of neural and blood-borne metabolic cues, and then the mechanisms that translate peripheral information into endocrine, autonomic and behavioral adjustments. More recently, the ARC has been involved in studies that investigated multifactorial pathologies such as the metabolic syndrome, which in addition to overweight and related metabolic dysfunction is characterized by a high incidence of hypertension, sleep disorders and infertility.

With the present work we contribute to deepen the role that ARC neuropeptides have in conditions of both health and disease. The results obtained by the rat ARC (**Chapter 1**) unraveled the participation of the peptide VGF in the response of the two main categories of orexigenic (NPY) and anorexigenic (α-MSH) neurons to changing metabolic state and showed that ARC neurons expressing VGF project to pre-autonomic neurons of the PVN. Although many work has to be done to elucidate the VGF intracellular processing in the different cellular subtypes, the recent discovery of a receptor for the VGF-derived peptide TLQP-21 suggest the possibility of VGF as a postsynaptic neuromodulator of NPY and α-MSH activity. The **Chapter 2** shows that, especially where it concerns NPY and VGF neurons in the ARC, a significant increase in the number of neurons expressing these peptides can be found in the postmortem human diabetic brain. These changes, when extrapolated to experimental animal studies, suggest that the human ARC in the diabetic state is reflecting a catabolic state and is possibly unable to sense high circulating glucose levels. In addition the results show that the same neuronal phenotype in the NTS area responds quite differently to the diseased diabetic state. These observations suggest that the ARC functionality is especially affected by diabetes and that some of the alteration typical of this disease (for example: increased hepatic

glucose production) might be given to the ARC failure in detecting peripheral metabolic information, which in turn might be responsible of the inappropriate central response.

Despite the previous results support the central role of the ARC in central response in physiologic and pathologic conditions, the ARC is not the unique forebrain nucleus that is at the interface between the periphery and the hypothalamic homeostatic systems. In fact, lesion studies performed either in the ARC or in the thalamic IGL of fasted rats in attempt to demonstrate that the ARC provides metabolic information to the master circadian clock, attested that the NPY increment is dependent on IGL projections to the SCN (**Chapter 3**), thus casting some doubt as to the assumed "central role" of the ARC in the integration of all hypothalamic responses to nutrition. As a consequence, it appears more difficult now to relate the metabolic alterations observed in circadian desynchronization with an intra-hypothalamic conflict in ARC-SCN communication.

Finally, our results, especially those regarding the human diabetic subjects, suggest that indeed the ARC is essential for an appropriate central control of energy balance. Nevertheless, the molecular machinery of ARC neurons is partially understood, as it is demonstrated by the poor knowledge about VGF activity. In addition, while the ARC appear to be involved in the onset of many symptoms that involved different homeostatic systems, like metabolic dysfunction, hypertension, and infertility in the metabolic syndrome, this is not the case of the circadian system, which receives metabolic information from an extra-hypothalamic source.

REFERENCES

Adachi A, Shimizu N, Oomura Y, Kobáshi M. *Convergence of hepatoportal glucose-sensitive afferent signals to glucose-sensitive units within the nucleus of the solitary tract.* Neurosci Lett. 1984 46(2):215-8.

Ahrén B. *Autonomic regulation of islet hormone secretion--implications for health and disease.* Diabetologia. 2000 43(4):393-410.

Akabayashi A, Zaia CT, Silva I, Chae HJ, Leibowitz SF. *Neuropeptide Y in the arcuate nucleus is modulated by alterations in glucose utilization.* Brain Res. 1993 621(2):343-8.

Alder J, Thakker-Varia S, Bangasser DA, Kuroiwa M, Plummer MR, Shors TJ, Black, IB. *Brain-derived neurotrophic factor-induced gene expression reveals novel actions of VGF in hippocampal synaptic plasticity.* J Neurosci. 2003 23(34):10800-8.

Amir S. *Intra-ventromedial hypothalamic injection of glutamate stimulates brown adipose tissue thermogenesis in the rat.* Brain Res. 1990 511(2):341-4.

Anand BK, Chhina GS, Sharma KN, Dua S, Singh B. *Activity of single neurons in the hypothalamic feeding centers: effect of glucose.* Am J Physiol 1964 207: 1146–54.

Arita Y, Kihara S, Ouchi N, Takahashi M, Maeda K, Miyagawa J, Hotta K, Shimomura I, Nakamura T, Miyaoka K, Kuriyama H, Nishida M, Yamashita S, Okubo K, Matsubara K, Muraguchi M, Ohmoto Y, Funahashi T, Matsuzawa Y. *Paradoxical decrease of an adipose-specific protein, adiponectin, in obesity.* Biochem Biophys Res Commun. 1999 257(1):79-83.

Asakawa A, Inui A, Kaga T, Yuzuriha H, Nagata T, Ueno N, Makino S, Fujimiya M, Niijima A, Fujino MA, Kasuga M. *Ghrelin is an appetite-stimulatory signal from stomach with structural resemblance to motilin.* Gastroenterology. 2001 120(2):337-45.

Ashcroft FM, Harrison DE, Ashcroft SJ. *Glucose induces closure of single potassium channels in isolated rat pancreatic beta-cells.* Nature. 1984 312(5993):446-8.

Ashford ML, Boden PR, Treherne JM. *Glucose-induced excitation of hypothalamic neurons is mediated by ATP-sensitive K+ channels.* Pflugers Arch. 1990 415(4):479-83.

Balfour RH, Hansen AM, Trapp S. *Neuronal responses to transient hypoglycaemia in the dorsal vagal complex of the rat brainstem.* J Physiol 2006 570 (Pt 3): 469–84.

Balthasar N, Dalgaard LT, Lee CE, Yu J, Funahashi H, Williams T, Ferreira M., Tang V, McGovern RA, Kenny CD, Christiansen LM, Edelstein E, Choi B., Boss O, Aschkenasi C, Zhang CY, Mountjoy K, Kishi T, Elmquist JK, Lowell BB. *Divergence of melanocortin pathways in the control of food intake and energy expenditure.* Cell. 2005 123(3):493-505.

Bartness TJ, Bamshad M. *Innervation of mammalian white adipose tissue: implications for the regulation of total body fat.* Am J Physiol. 1998 275:R1399–411.

Bartolomucci A, La CG, Possenti R, Locatelli V, Rigamonti AE, Torsello A, Bresciani E, Bulgarelli I, Rizzi R, Pavone F, D'Amato FR, Severini C, Mignogna G, Giorgi A, Schinina ME, Elia G, Brancia C, Ferri GL, Conti R, Ciani B, Pascucci T, Dell'omo G, Muller EE, Levi A, Moles A. *TLQP-21, a VGF-derivedpeptide, increasesenergyexpenditure and preventstheearlyphase of diet-induced obesity.* ProcNatlAcadSci. USA. 2006 103:14584– 4589.

Baskin DG, Figlewicz Lattemann D, Seeley RJ, Woods SC, Porte Jr D, Schwartz MW. *Insulin and leptin: dual adiposity signals to the brain for the regulation of food intake and body weight.* Brain Res.1999 848:114–23.

Basu R, Basu A, Johnson CM, Schwenk WF, Rizza R. *Insulin dose-response curves for stimulation of splanchnic glucose uptake and suppression of endogenous glucose production differ in nondiabetic humans and are abnormal in people with type 2 diabetes.* Diabetes 2004 53(8): 2042–50.

Batterham RL, Cowley MA, Small CJ, Herzog H, Cohen MA, Dakin CL, Wren AM, Brynes AE, Low MJ, Ghatei MA, Cone RD, Bloom SR. *Gut hormone PYY(3-36) physiologically inhibits food intake.* Nature. 2002 418(6898):650-4.

Beck B. *Knock-out's and organisation of peptidergic feeding behavior mechanisms.* Neurosci Biobehav Rev. 2001 25:143–58.

Bellinger LL, Mendel VE, Bernardis LL, Castonguay TW. *Meal patterns of rats with dorsomedial hypothalamic nuclei lesions or sham operations.* Physiol Behav. 1986 36(4):693-8.

Bergen HT, Mizuno TM, Taylor J, Mobbs CV. *Hyperphagia and weight gain after gold-thioglucose: relation to hypothalamic neuropeptide Y and proopiomelanocortin.* Endocrinology. 1998 139:4483–4488.

Bernardis LL. *Food intake patterns from weaning to adulthood in male and female rats with hypothalamic lesions.* Experientia. 1963 19:541-3.

Berthoud HR. *The caudal brainstem and the control of food intake and energy balance.* In Handbook of Behavioral Neurobiology, ed. EM Stricker, SC Woods, 2004 pp. 195–240.

Bingham NC, Anderson KK, Reuter AL, Stallings NR, Parker KL. *Selective loss of leptin receptors in the ventromedial hypothalamic nucleus results in increased adiposity and a metabolic syndrome.* Endocrinology. 2008 149(5):2138-48.

Brancia C, Nicolussi P, Cappai P, La Corte G, Possenty R, et al. *Differential expression and seasonal modulation of VGF peptides in sheep pituitary.* J Endocrinol. 2005 186(1): 97–107.

Brightman MW, Broadwell RD. *The morphological approach to the study of normal and abnormal brain permeability.* Adv Exp Med Biol. 1976;69:41-54.

Brobeck JR. *Mechanism of the development of obesity in animals with hypothalamic lesions.* Physiol Rev 1946 26:541–559.

Brüning JC, Gautam D, Burks DJ, Gillette J, Schuber M, et al. *Role of brain insulin receptor in control of body weight and reproduction.* Science 2000 289(5487): 2122–5.

Buijs MR, Pool CW, Van Heerikhuize JJ, Sluiter AA, Van Der Sluis P, et al. *Antibodies to small transmitter molecules and peptides: production and application of antibodies to dopamine, serotonin, GABA, vasopressin, vasoactive intestinal peptide, neuropeptide Y, somatostatin and substance P.* Biomedical Research 1989 10: 213–221.

Buijs RM, Kalsbeek A. *Hypothalamic integration of central and peripheral clocks.* Nat Rev Neurosci. 2001 2(7):521-6.

Buijs RM, Kreier F. *The metabolic syndrome: a brain disease?* J Neuroendocrinol. 2006 18(9):715-6.

Buijs RM, la Fleur SE, Wortel J, Van Heyningen C, Zuiddam L, Mettenleiter TC, Kalsbeek A, Nagai K, Niijima A. *The suprachiasmatic nucleus balances sympathetic and parasympathetic output to peripheral organs through separate preautonomic neurons.* J Comp Neurol. 2003 464(1):36-48.

Canteras NS, Simerly RB, Swanson LW. *Organization of projections from the ventromedial nucleus of the hypothalamus: a Phaseolus vulgaris-leucoagglutinin study in the rat.* J Comp Neurol. 1994 348:41–79.
Carabaza A, Ciudad CJ, Baqué S, Guinovart JJ. *Glucose has to be phosphorylated to activate glycogen synthase, but not to inactivate glycogen phosphorylase in hepatocytes.* FEBS Lett. 1992 20;296(2):211-4.

Cechetto DF, Saper CB. *Neurochemical organization of the hypothalamic projection to the spinal cord in the rat.* J Comp Neurol. 1988 272(4):579-604.

Cechetto DF, Saper CB. *Role of the central cortex in autonomic function.* In: Loewy AD, Spyer KM, editors. Central regulation of autonomic functions. New York: Oxford University Press. 1990 pp 208–23.

Chou TC, Scammell TE, Gooley JJ, Gaus SE, Saper CB, Lu J. *Critical role of dorsomedial hypothalamic nucleus in a wide range of behavioral circadian rhythms.* J Neurosci. 2003 23(33):10691-702.

Ciofi P, Tramu G, Bloch B. *Comparative immunohistochemical study of the distribution of neuropeptide Y, growth hormone-releasing factor and the carboxyterminus of precursor protein GHRF in the human hypothalamic infundibular area.* Neuroendocrinology 1990 51(4): 429–36.

Cone RD. *Anatomy and regulation of the central melanocortin system. Nat Neurosci.* 2005 58:571–78.

Cone RD. *Studies on the physiological functions of the melanocortin system.* Endocr Rev. 2006 27(7): 736–49.

Cowley MA, Pronchuk N, Fan W, Dinulescu DM, Colmers WF, Cone RD. *Integration of NPY, AgRP, and melanocortin signals in the hypothalamic paraventricular nucleus: evidence of a cellular basis for the adipostat.* Neuron 1999 24(1):155-63.

Cowley MA, Smart JL, Rubinstein M, Cerdan MG, Diano S, et al. *Leptin activates anorexigenic POMC neurons through a neural network in the arcuate nucleus.* Nature 2001 411:480–8416.
Cummings DE, Purnell JQ, Frayo RS, Schmidova K, Wisse BE, Weigle DS. *A preprandial rise in plasma ghrelin levels suggests a role in meal initiation in humans.* Diabetes 2001 50:1714–19.

D'Alessio DA, Prigeon RL, Ensinck JW. *Enteral enhancement of glucose disposition by both insulin-dependent and insulin-independent processes. A physiological role of glucagon-like peptide I.* Diabetes. 1995 44(12):1433-7.

Dallaporta M, Himmi T, Perrin J, Orsini JC. *Solitary tract nucleus sensitivity to moderate changes in glucose level.* Neuroreport. 1999 20;10(12):2657-60.

Date Y, Murakami N, Toshinai K, Matsukura S, Niijima A, et al. *The role of the gastric afferent vagal nerve in ghrelin-induced feeding and growth hormone secretion in rats.* Gastroenterology 2002 123:1120–28.

Désy L, Pelletier G. *Immunohistochemical localization of alpha-melanocyte stimulating hormone (alpha-MSH) in the human hypothalamus.* Brain Res. 1978 154(2): 377–81.

Devenport LD, Balagura S. *Lateral hypothalamus: reevaluation of function in motivated feeding behavior.* Science. 1971 172(3984):744-6.

Dimicco JA, Zaretsky DV. *The dorsomedial hypothalamus: a new player in thermoregulation.* Am J Physiol Regul Integr Comp Physiol. 2007 292(1):R47-63.

Dudás B, Mihály A, Merchenthaler I. *Topography and associations of luteinizing hormone-releasing hormone and neuropeptide Y-immunoreactive neuronal systems in the human diencephalon.* J Comp Neurol. 2000 427(4): 593–603.

Edfalk S, Steneberg P, Edlund H. *Gpr40 is expressed in enteroendocrine cells and mediates free fatty acid stimulation of incretin secretion.* Diabetes. 2008 57(9):2280-7.

Elias CF, Aschkenasi C, Lee C, Kelly J, Ahima RS, Bjorbaek C, Flier JS, Saper CB, Elmquist JK. *Leptin differentially regulates NPY and POMC neurons projecting to the lateral hypothalamic area.* Neuron 1999 23:775–86.

Elmquist JK, Ahima RS, Elias CF, Flier JS, Saper CB. *Leptin activates distinct projections from the dorsomedial and ventromedial hypothalamic nuclei.* Proc Natl Acad Sci. USA 1998 95:741–6.

Feng J, Petersen CD, Coy DH, Jiang JK, Thomas CJ, Pollak MR, Wank SA. *Calcium-sensing receptor is a physiologic multimodal chemosensor regulating gastric G-cell growth and gastrin secretion.* Proc. Natl. Acad. Sci. U S A. 2010 12;107(41):17791-6.

Ferri GL, Noli B, Brancia C, D'Amato F, Cocco C. *VGF: An inducible gene product, precursor of a diverse array of neuro-endocrine peptides and tissue-specific disease biomarkers.* J. Chem. Neuroanat. 2011 42(4): 249–61.

Fioramonti X, Contié S, Song Z, Routh VH, Lorsignol A, et al. *Characterization of glucosensing neuron subpopulations in the arcuate nucleus: integration in neuropeptide Y and pro-opio melanocortin networks?* Diabetes 2007 56(5): 1219–27.

Froguel P, Boutin P. *Genetics of pathways regulating body weight in the development of obesity in humans.* Exp Biol Med (Maywood). 2001 226(11):991-6.

Fry M, Ferguson AV. *The sensory circumventricular organs: brain targets for circulating signals controlling ingestive behavior.* Physiol Behav. 2007 24;91(4):413-23.

Glaum SR, Hara M, Bindokas VP, Lee CC, Polonsky KS, Bell GI, Miller RJ. *Leptin, the obese gene product, rapidly modulates synaptic transmission in the hypothalamus.* Mol Pharmacol. 1996 50(2):230-5.

Goldstone AP, Unmehopa UA, Bloom SR, Swaab DF. *Hypothalamic NPY and agouti-related protein are increased in human illness but not in Prader-Willi syndrome and other obese subjects.* J Clin Endocrinol Metab. 2002 87(2): 927–37.

Goncharuk VD, Buijs RM, Swaab DF. *Corticotropin-releasing hormone neurons in hypertensive patients are activated in the hypothalamus but not in the brainstem.* J Comp Neurol. 2007 503(1): 148–68.

Hahm S, Mizuno TM, Wu TJ, Wisor JP, Priest CA, et al. *Targeted deletion of the Vgf gene indicates that the encoded secretory peptide precursor plays a novel role in the regulation of energy balance.* Neuron. 1999 23(3): 537–48.

Hahm S, Fekete C, Mizuno TM, Windsor J, Yan H, et al. *VGF is required for obesity induced by diet,gold thioglucose treatment, and agouti and is differentially regulated in pro-opiomelanocortin- and neuropeptide Y-containing arcuate neurons in response to fasting.* J Neurosci. 2002 22(16): 6929–38.

Hahn TM, Breininger JF, Baskin DG, Schwartz MW. *Coexpression of Agrp and NPY in fasting-activated hypothalamic neurons.* Nat Neurosci. 1998 1:271–272.

Halliday GM, Li YW, Joh TH, Cotton RG, Howe P, et al. *Distribution of monoamine-synthesizing neurons in the human medulla oblongata.* J Comp Neurol 1988 273(3): 301–17.

Halliday GM, Li YW, Oliver JR, Joh TH, Cotton R, et al. *The distribution of neuropeptide Y-like immunoreactive neurons in the human medulla oblongata.* Neuroscience 1988 26(1): 179–91.

Hass N, Schwarzenbacher K, Breer H. *T1R3 is expressed in brush cells and ghrelin-producing cells of murine stomach.* Cell Tissue Res. 2010 339(3):493-504

Holsen LM, Savage CR, Martin LE, Bruce AS, Lepping RJ, Ko E, Brooks WM, Butler MG, Zarcone JR, Goldstein JM. *Importance of reward and prefrontal circuitry in hunger and satiety: Prader-Willi syndrome vs simple obesity.* Int J Obes (Lond). 2012 36(5):638-47.

ter Horst GJ, Luiten PG. *The projections of the dorsomedial hypothalamic nucleus in the rat.* Brain Res Bull. 1986 16(2):231-48.

Hosoya Y, Sugiura Y, Okado N, Loewy AD, Knockouthno K. *Descending input from the hypothalamic paraventricular nucleus to sympathetic preganglionic neurons in the rat.* Exp Brain Res. 1991 85:10–20.

Ibrahim N, Bosch MA, Smart JL, Qiu J, Rubinstein M, Rønnekleiv OK, Low MJ, Kelly MJ. *Hypothalamic proopiomelanocortin neurons are glucose responsive and express K(ATP) channels.* Endocrinology. 2003 144(4):1331-40.

Janssen S, Laermans J, Iwakura H, Tack J, Depoortere I. *Sensing of fatty acids for octanoylation of ghrelin involves a gustatory G-protein.* PLoS One. 2012;7(6):e40168.

Janssen S, Depoortere I. *Nutrient sensing in the gut: new roads to therapeutics?* Trends Endocrinol Metab. 2013 24(2):92-100.

Jethwa PH, Warner A, Nilaweera KN, Brameld JM, Keyte JW, Carter WG, Bolton N, Bruggraber M, Morgan PJ, Barrett P, Ebling FJ. *VGF-derived peptide, TLQP-21, regulates food intake and body weight in Siberian hamsters.* Endocrinology. 2007 148: 4044– 4055.

Kalsbeek A, Strubbe JH. *Circadian control of insulin secretion is independent of the temporal distribution of feeding.* Physiol Behav. 1998 63(4):553-8.

Kalsbeek A, Foppen E, Schalij I, Van Heijningen C, van der Vliet J, Fliers E, Buijs RM. *Circadian control of the daily plasma glucose rhythm: an interplay of GABA and glutamate.* PLoS One. 2008 3(9):e3194.

Karaki S, Mitsui R, Hayashi H, Kato I, Sugiya H, Iwanaga T, Furness JB, Kuwahara A. *Short-chain fatty acid receptor, GPR43, is expressed by enteroendocrine cells and mucosal mast cells in rat intestine.* Cell Tissue Res. 2006 324(3):353-60.

Kitahama K, Jouvet A, Araneda S, Nagatsui I, et al. *Aromatic L-amino acid decarboxylase-immunoreactive structures in human midbrain, pons, and medulla.* J Chem Neuroanat 2009 38(2): 130–40.

Knutsson A: *Health disorders in shift workers.* Occup. Med.(Lond.). 2004 53(2):271-277.
Kojima M, Kangawa K. *Ghrelin: structure and function.* Physiol Rev. 2005 85(2):495-522.

Könner AC, Janoschek R, Plum L, Jordan SD, Rhoter E, et al. *Insulin action in AgRP-expressing neurons is required for suppression of hepatic glucose production.* Cell Metab. 2007 5(6): 438–49.

Kreier F, Kalsbeek A, Ruiter M, Yilmaz A, Romijn JA, Sauerwein HP, Fliers E, Buijs RM. *Central nervous determination of food storage--a daily switch from conservation to expenditure: implications for the metabolic syndrome.* Eur J Pharmacol. 2003 480(1-3):51-65.

Larsen PJ, Tang-Christensen M, Jessop DS. *Central administration of glucagon-like peptide-1 activates hypothalamic neuroendocrine neurons in the rat.* Endocrinology. 1997 138(10):4445-55.

Légrádi G, Lechan RM. *The arcuate nucleus is the major source for neuropeptide Y-innervation of thyrotropin-releasing hormone neurons in the hypothalamic paraventricular nucleus.* Endocrinology. 1998 139(7):3262-70.

Levi A, Eldridge JD, Paterson BM. *Molecular cloning of a gene sequence regulated by nerve growth factor.* Science. 1985 229: 393– 395.

Lin HV, Plum L, Ono H, Gutiérrez-Juárez R, Shanabrought M, et al. *Divergent regulation of energy expenditure and hepatic glucose production by insulin receptor in agouti-related protein and POMC neurons.* Diabetes 2010 59(2): 337–46.

Ludwig DS, Mountjoy KG, Tatro JB, Gillette JA, Frederich RC, Flier JS, Maratos-Flier E. *Melanin-concentrating hormone: a functional melanocortin antagonist in the hypothalamus.* Am J Physiol. 1998;274(4 Pt 1):E627-33.

Luiten PG, Horst GJ, Steffens AB. *The hypothalamus, intrinsic connections and outflow pathways to the endocrine system in relation to the control of feeding and metabolism.* Prog Neurobiol. 1987 28:1–54.

Maffei M, Halaas J, Ravussin E, Pratley RE, Lee GH, Zhang Y, Fei H, Kim S, Lallone R, Ranganathan S,et al. *Leptin levels in human and rodent: measurement of plasma leptin and ob RNA in obese and weight-reduced subjects.* Nat Med. 1995 1(11):1155-61.

Mahata SK, Mahata M, Hörtnag H, Fischer-Colbrie R, Steiner HJ, Dietze O, Winkler H. *Concomitant changes of messenger ribonucleic acid levels of secretogranin II, VGF, vasopressin and oxytocin in the paraventricular nucleus of rats after adrenalectomy and during lactation.* J Neuroendocrinol. 1993 5(3):323-30.

Marks JL, Waite K. *Some acute effects of intracerebroventricular neuropeptide Y on insulin secretion and glucose metabolism in the rat.* J. Neuroendocrinol. 1996 8(7): 507–13.

Matveyenko AV, Donovan CM. *Metabolic sensors mediate hypoglycemic detection at the portal vein.* Diabetes. 2006 55(5):1276-82.

Menéndez JA, McGregor IS, Healey PA, Atrens DM, Leibowitz SF. *Metabolic effects of neuropeptide Y injections into the paraventricular nucleus of the hypothalamus.* Brain Res 1990 516(1): 8–14

Mercer JG, Hoggard N, Williams LM, Lawrence CB, Hannah LT, Morgan PJ, Trayhurn P. *Coexpression of leptin receptor and preproneuropeptide Y mRNA in arcuate nucleus of mouse hypothalamus.* J Neuroendocrinol. 1996 8:733–5.

Minokoshi Y, Haque MS, Shimazu T. *Microinjection of leptin into the ventromedial hypothalamus increases glucose uptake in peripheral tissues in rats.* Diabetes. 1999 48(2):287-91.

Mokdad AH, Ford ES, Bowman BA, et al. *Prevalence of obesity, diabetes, and obesity-related health risk factors, 2001.* JAMA 2003 289:76–9.

Moriarty P, Dimaline R, Thompson DG, Dockray GJ. *Characterization of cholecystokininA and cholecystokininB receptors expressed by vagal afferent neurons.* Neuroscience 1997 79:905–13.

Morton GJ, Cummings DE, Baskin DG, Barsh GS, Schwartz MW. *Central nervous system control of food intake and body weight.* Nature. 2006 443(7109):289-95

Muroya S, Yada T, Shioda S, Takigawa M*. Glucose-sensitive neurons in the rat arcuate nucleus contain neuropeptide Y.* Neurosci Lett. 1999 264:113–6.

Obici S, Zhang BB, Karkanias G, Rossetti L. *Hypothalamic insulin signaling is required for inhibition of glucose production.* Nature Med. 2002 8:1376–1382.

Oomura Y, Ono T, Ooyama H, Wayner MJ. *Glucose and osmosensitive neurones of the rat hypothalamus.* Nature 1969 222(5190): 282–4.

Patterson LM, Zheng H, Berthoud HR. *Vagal afferents innervating the gastrointestinal tract and CCKA-receptor immunoreactivi*ty. Anat Rec. 2002 266:10–20.
Pearson J, Goldstein M, Markey K, Brandeis L. *Human brainstem catecholamine neuronal anatomy as indicated by immunocytochemistry with antibodies to tyrosine hydroxylase.* Neuroscience 1982 8(1): 3–32.

Pelletier G, Desy L, Kerkerian L, Cote J. *Immunocytochemical localization of neuropeptide Y (NPY) in the human hypothalamus.* Cell Tissue Res. 1984 238(1): 203–5

Peruzzo B, Pastor FE, Blasquez JL, Schöbitz K, Pelaez B, Amat P, Rodriguez EM. *A second look at the barriers of the medial basal hypothalamus.* Exp Brain Res. 2000 132(1):10-26.

Phillips RJ, Powley TL. *Tension and stretch receptors in gastrointestinal smooth muscle: re-evaluating vagal mechanoreceptor electrophysiology.* Brain Res Brain Res Rev. 2000 34(1-2):1-26.

Pilcher WH, Joseph SA, McDonald JV. *Immunocytochemical localization of pro-opiomelanocortin neurons in human brain areas subserving stimulation analgesia.* J Neurosurg. 1998 68(4): 621–9.

Pizzi WJ, Barnhar, JE. *Effects of monosodium glutamate on somatic development, obesity, and activity in the mouse.* Pharmacol. Biochem. Behav. 1976 5:551–557.

Pocai A, Morgan K, Buettner C, Gutierrez-Juarez R, Obici S, Rossetti L. *Central leptin acutely reverses diet-induced hepatic insulin resistance.* Diabetes 2005a 54:3182–3189.

Pocai A, Obici S, Schwartz GJ, Rossetti L. *A brain-liver circuit regulates glucose homeostasis.* Cell Metab. 2005b 1(1): 53–61.

Possenti R, Eldridge JD, Paterson BM, Grasso A, Levi A. *A protein induced by NGF in PC12 cells is stored in secretory vesicles and released through the regulated pathway.* EMBO J. 1989 8:2217–2223.

Prentice AM, Rayco-Solon P, Moore SE. *Insights from the developing world: thrifty genotypes and thrifty phenotypes.* Proc Nutr Soc. 2005 64(2):153-61.

Qu D, Ludwig DS, Gammeltoft S, Piper M, Pelleymounter MA, Cullen MJ, Mathes WF, Przypek R, Kanarek R, Maratos-Flier E. *A role for melanin-concentrating hormone in the central regulation of feeding behaviour.* Nature. 1996 380(6571):243-7.

Ravussin E, Bogardus C. *Energy balance and weight regulation: genetics versus environment.* Br J Nutr. 2000;83 Suppl 1:S17-20.

Ritter RC, Slusser PG, Stone S. *Glucoreceptors controlling feeding and blood glucose: location in the hindbrain.* Science 1981 213(4506): 451–2.

Robinson KT, Butler J. *Understanding the causal factors of obesity using the International Classification of Functioning, Disability and Health.* Disabil Rehabil. 2011 33(8):643-51.

Rossetti L, Massillon D, Barzilai N, Vuguin P, Chen W, et al. *Short term effects of leptin on hepatic gluconeogenesis and in vivo insulin action.* J. Biol. Chem. 1997 272(44): 27758–63.

Rozengurt E. Taste receptors in the gastrointestinal tract. I. *Bitter taste receptors and alpha-gustducin in the mammalian gut.* Am J Physiol Gastrointest Liver Physiol. 2006 291(2):G171-7.

Sakurai T, Amemiya A, Ishii M, Matsuzaki I, Chemelli RM, Tanaka H, Williams SC, Richardson JA, Kozlowski GP, Wilson S, Arch JR, Buckingham RE, Haynes AC, Carr SA, Annan RS, McNulty DE, Liu WS, Terrett JA, Elshourbagy NA, Bergsma DJ, Yanagisawa M. *Orexins and orexin receptors: a family of hypothalamic neuropeptides and G protein-coupled receptors that regulate feeding behavior.* Cell. 1998 92(4):573-85.

Saladin R, De Vos P, Guerre-Millo M, Leturque A, Girard J, Staels B, Auwerx J. *Transient increase in obese gene expression after food intake or insulin administration.* Nature. 1995 377(6549):527-9.

Salgado-Delgado R, Angeles-Castellanos M, Buijs RM, Escobar C. *Internal desynchronization in a model of night-work by forced activity in rats.* Neuroscience 2008 155(1): 297-307.

Salton SR, Fischberg DJ, Dong KW. *Structure of the gene encoding VGF, a nervous system-specific mRNA that is rapidly and selectively induced by nerve growth factor in PC12 cells.* Mol Cell Biol. 1991 11:2335– 2349.

Salton SR. *Neurotrophins, growth-factor-regulated genes and the control of energy balance.* Mt Sinai J Med. 2003 70(2):93-100.

Saper CB. *Hypothalamic connections with the cerebral cortex.* Prog Brain Res. 2000 126:39–48.

Scherer T, O'Hare J, Diggs-Andrews K, Schweiger M, Cheng B, Lindtner C, Zielinski E, Vempati P, Su K, Dighe S, Milsom T, Puchowicz M, Scheja L, Zechner R, Fisher SJ, Previs SF, Buettner C. *Brain insulin controls adipose tissue lipolysis and lipogenesis.* Cell Metab. 2011 Feb 2;13(2):183-94.

Smith GP, Jerome C, Norgren R. *Afferent axons in abdominal vagus mediate satiety effect of cholecystokinin in rats.* Am J Physiol. 1985 249:R638–41.

Snyder SE, Pintar JE, Salton SR. *Developmental expression of VGF mRNA in the prenatal and postnatal rat.J Comp Neurol.* 1998 394:64–90.

Snyder SE, Salton SR. *Expression of VGF mRNA in the adult rat central nervous system.* J Comp Neurol. 1998 394: 91–105.

Steinert RE, Gerspach AC, Gutmann H, Asarian L, Drewe J, Beglinger C. *The functional involvement of gut-expressed sweet taste receptors in glucose-stimulated secretion of glucagon-like peptide-1 (GLP-1) and peptide YY (PYY).* Clin Nutr. 2011 30(4):524-32.

Swaab DF. *The human hypothalamus: Basic and clinical aspects, Part I.* Handbook of Clinical Neurology. 2003 Vol. 79 p. (Series 3td, Vol.1).

Sukhov RR, Walker LC, Rance NE, Price DL, Young W. *Opioid precursor gene expression in the human hypothalamus.* J Comp Neurol. 1995 353(4): 604–22.

Taupenot L, Harper KL, O'Connor DT. *The chromogranin-secretogranin family.* N Engl J Med. 2003 348(12):1134-49

Thompson RH, Swanson LW. *Organization of inputs to the dorsomedial nucleus of the hypothalamus: a reexamination with Fluorogold and PHAL in the rat.* Brain Res Rev. 1998 27:89–118.

Thorens B, Larsen PJ. *Gut-derived signaling molecules and vagal afferents in the control of glucose and energy homeostasis.* Curr Opin Clin Nutr Metab Care. 2004 7(4):471-8.

Trani E, Ciotti T, Rinaldi AM, Canu N, Ferri GL, Levi A, Possenti R. *Tissue-specific processing of the neuroendocrine protein VGF.* J Neurochem. 1995 65:2441–2449.

Trani E, Giorgi A, Canu N, Amadoro G, Rinaldi AM, Halban PA, Ferri GL, Possenti R, Schinina ME, Levi A. *Isolation and characterization of VGF peptides in rat brain. Role of PC1/3 and PC2 in the maturation of VGF precursor.* J Neurochem. 2002 81:565–574.

Trayhurn P, Bing C. *Appetite and energy balance signals from adipocytes.* Philos Trans R Soc Lond B Biol Sci. 2006 361(1471):1237-49.

Tritos NA, Vicent D, Gillette J, Ludwig DS, Flier ES, Maratos-Flier E. *Functional interactions between melanin-concentrating hormone, neuropeptide Y, and anorectic neuropeptides in the rat hypothalamus.* Diabetes 1998 47:1687–92.

Van den Hoek AM, Voshol PJ, Karnekamp BN, Buijs RM, Romeijn J, et al. *Intracerebroventricular neuropeptide Y infusion precludes inhibition of glucose and VLDL production by insulin.* Diabetes 2004 53(10): 2529–34.

Van den Pol AN, Decavel C, Levi A, Paterson B. *Hypothalamic expression of a novel gene product, VGF: immunocytochemical analysis.* J Neurosci. 1998 9:4122–4137.
Van den Pol AN, Bina K, Decavel C, Ghosh P. *VGF expression in the brain.* J Comp Neurol. 1994 347:455–469.

Wang R, Liu X, Hentges ST, Dunn-Meynell AA, Levin E, et al. *The regulation of glucose-excited neurons in the hypothalamic arcuate nucleus by glucose and feeding-relevant peptides.* Diabetes 2004 53(8): 1959–65.

Watson E, Hahm S, Mizuno TM, Windsor J, Mongomery C, et al. *VGF ablation blocks the development of hyperinsulinemia and hyperglycemia in several mouse models of obesity.* Endocrinology 2005 146(12): 5151–63.

Watson E, Fargali S, Okamoto H, Sadahiro M, Gordon RE, Chakraborty T, Sleeman MW, Salton SR. *Analysis of knocknockoutut mice suggests a role for VGF in the control of fat storage and energy expenditure.* BMC Physiol. 2009 28:9-19.

Wells JC. *The evolution of human fatness and susceptibility to obesity: an ethological approach.* Biol Rev Camb Philos Soc. 2006 81(2):183-205.

White JD, Kershaw M. *Increased hypothalamic neuropeptide Y expression following food deprivation.* Mol Cell Neurosci 1990 1(1): 41–8.

Wisor JP, Takahashi JS. *Regulation of the vgf gene in the golden hamster suprachiasmatic nucleus by light and by the circadian clock.* J Comp Neurol. 1997 10;378(2):229-38.

Wu Q, Boyle MP, Palmiter RD. *Loss of GABAergic signaling by AgRP neurons to the parabrachial nucleus leads to starvation.* Cell. 2009 137(7):1225-34.

Wu Q, Palmiter RD. *GABAergic signaling by AgRP neurons prevents anorexia via a melanocortin-independent mechanism.* Eur J Pharmacol. 2011 660(1):21-7.